

HEAT STRESS INDUCES DOWNREGULATION OF HIPPOCAMPAL
SUPEROXIDE DISMUTASE-1; A POSSIBLE MECHANISM FOR
HEAT-RELATED NEURONAL CELL DEATH

Except where reference is made to the work of others, the work described in this dissertation is my own or was done in collaboration with my advisory committee. This dissertation does not include proprietary or classified information

Naglaa El-Orabi

Certificate of Approval:

James L. Sartin
Professor
Anatomy, Physiology and
Pharmacology

Dean D. Schwartz, Chair
Associate Professor
Anatomy, Physiology and
Pharmacology

Robert L. Judd
Associate Professor
Anatomy, Physiology and
Pharmacology

Elaine S. Coleman
Associate Professor
Anatomy, Physiology and
Pharmacology

Joe F. Pittman
Interim Dean
Graduate School

HEAT STRESS INDUCES DOWNREGULATION OF HIPPOCAMPAL
SUPEROXIDE DISMUTASE-1; A POSSIBLE MECHANISM FOR
HEAT-RELATED NEURONAL CELL DEATH

Naglaa El-Orabi

A Dissertation

Submitted to

the Graduate Faculty of

Auburn University

in Partial Fulfillment of the

Requirement for the

Degree of

Doctor of Philosophy

Auburn, Alabama
Dec. 15, 2006

HEAT STRESS INDUCES DOWNREGULATION OF HIPPOCAMPAL
SUPEROXIDE DISMUTASE-1; A POSSIBLE MECHANISM FOR
HEAT-RELATED NEURONAL CELL DEATH

Naglaa El-Orabi

Permission is granted to Auburn University to make copies of this dissertation, upon request of individuals or institutions and at their expense. The author reserves all publication rights.

Signature of Author

Date

VITA

Naglaa F. El-Orabi, Daughter of Amina M. Elsayed and Fathi M. El-Orabi, was born October 3, 1969, in Dakahlia, Egypt. She graduated from Zagazig University, Zagazig, Egypt with the degree of Bachelor of Pharmaceutical Sciences in June, 1991. She earned a Master's degree in Pharmacology from Zagazig University, Zagazig, Egypt, in September, 1997. In 1999 she received a governmental scholarship from Egypt to earn a doctoral degree from abroad. In the fall of 2001, she was accepted as a graduate student in the Department of Anatomy, Physiology and Pharmacology at Auburn University. She is married to Mohamed G. Hassan and has three children, Tasnim, Salsabeel and Omar.

DISSERTATION ABSTRACT

HEAT STRESS INDUCES DOWNREGULATION OF HIPPOCAMPAL
SUPEROXIDE DISMUTASE-1; A POSSIBLE MECHANISM FOR
HEAT-RELATED NEURONAL CELL DEATH

Nagla El-Orabi

Doctor of Philosophy, Dec. 15, 2006
(M.Sc., Zagazig University, Egypt 1997)
(B.S. Pharm., Zagazig University, Egypt, 1991)

176 Typed pages

Directed by Dean D. Schwartz

Exertional heat injury represents a major risk for people working or exercising in hot environments. Currently, no pharmacological therapies are available and little is known about the molecular response to heat stress in the brain. In the first part of this study, we examined gene expression changes associated with hyperthermia in the hippocampus of pigs. Twelve pigs were kept at either 70°F (Control) or 90 °F (heat-stressed) for 4, 8, 12 and 24 h. The pigs were monitored hourly for heart rate, respiratory rate and body temperature. At 4, 8, 12 and 24 h, the hippocampus was excised from 3 pigs in each group and total RNA was obtained for use in differential display PCR. A total of 31 differentially expressed cDNAs were isolated. Eight genes were chosen for further confirmation by real-time PCR analysis. Only slight increases in the expression of three different HSP genes were reported after heat stress at all sample times. DNA polymerase ϵ p12 gene expression was stimulated to 2.55 fold after

12 h while it was downregulated after both 4 and 8 h. Two genes encoding 26S proteasome subunits, PSMD10 and PSMB9 were also upregulated after heat stress at all sample times. Superoxide dismutase-1 gene was significantly inhibited after both 8 and 12 hours of heat stress to 0.39 and 0.45 fold respectively. Sodium channel voltage-gated β 1 subunit gene was inhibited after heat stress. This inhibition was only significant after 24 h. In conclusion, most of the hippocampal genes that have altered expression by heat stress are playing a role in cellular protection against hyperthermic insult and some altered genes may play a role in heat-related brain pathogenesis. More understanding about the heat-induced molecular changes in the brain could help in the development of effective therapeutic strategies for treatment of heat-related illness. In the second part of this study, we utilized immortalized hippocampal neuronal cells (HT-22) to investigate the effect of elevated heat (43°C/30 min) on both SOD-1 gene expression and translation as well as enzyme activity. The effect of heat stress on accumulation of ROS, cell number and induction of apoptosis were measured. Also, the effectiveness of pretreatment with the SOD mimetic EUK-134 to protect against heat-induced cell death was evaluated. We found that in HT-22 cells, heat stress decreased the SOD-1 mRNA, protein, and activity as well as cell viability. Apoptotic cell death is involved in heat-induced neuronal cell death with overproduction of ROS. All aspects of heat-induced cell death and apoptosis were abolished by pretreatment with EUK-134. Thus heat-induced downregulation of SOD-1 in HT-22 cells disturbed the cellular antioxidant defense mechanism leading to accumulation of ROS and cell death.

ACKNOWLEDGMENTS

I would like to express my sincere thanks and appreciation to my major advisor, Dr. Dean D. Schwartz for his continuous guidance, patience, understanding and support during the entire course of this study. My deepest thanks go to my committee members, Dr. James L. Sartin, Dr. Robert L. Judd and Dr. Elaine S. Coleman for helpful suggestions and support during this work. I would like to express my deep gratitude to Heather Gray-Edwards, Colin B. Rogers, and Terri Albrecht-Schmitt, for their assistance in the laboratory, their endless encouragement and support. I also thank Dr. Donald Lay and Dr. Heg-Wei Cheng at USDA Livestock Behavior Research Unit, Purdue University for performing the all work with pigs. My sincere thanks go to Dr. Yehia El Mogahzy, Professor of Statistics & Quality Engineering, Auburn University for his assistance in statistical analysis. I would like to express my deep appreciation and thanks to my parents for their encouragement, support and endless love. My special thanks and deep appreciation go to my husband for his patience, unwavering support, encouragement and sacrifices during these years. I wish to thank the Egyptian Cultural and Educational Bureau, the Office of Naval Research, Department of Anatomy, Physiology and Pharmacology and the Office of the Associate Dean for Research and Graduate studies for their support and giving me the opportunity to complete the degree.

Style manual or journal used: Neurosciences

Computer software used: Windows XP, Microsoft Word 2003, Microsoft Excel 2003,
Microsoft Picture It Express 7.0.

TABLE OF CONTENTS

LIST OF FIGURES.....	xii
LIST OF TABLES	xv
INTRODUCTION	1
Hypothesis and objective of this study.....	3
LITERATURE REVIEW.....	6
Heat stress.....	6
Heat-related illness.....	7
Heat shock proteins.....	11
Effect of heat stress on gene expression.....	16
Heat shock factors.....	22
Heat-induced oxidative stress.....	27
Mechanisms involved in heat-mediated accumulation of ROS.....	28
Antioxidant defense systems.....	30
Superoxide dismutases (SODs).....	32
Superoxide dismutase-1 (SOD-1).....	36
Superoxide dismutase mimetics.....	37
Statement of research objective.....	40
MATERIALS.....	44
METHODS.....	47

Experimental protocol 1.....	47
Animals.....	47
Induction of heat stress.....	47
RNA isolation from pig hippocampus.....	47
Analysis of gene expression.....	50
TA- cloning.....	52
Real-time RT-PCR analysis.....	57
Experimental protocol 2.....	60
Cell culture.....	60
Isolation of total RNA and cDNA synthesis from HT-22 cells.....	61
Measurement of SOD-1 gene expression by real-time RT-PCR.....	62
Measurement of SOD-1 protein expression by western blotting.....	63
Measurement of SOD-1 enzyme activity.....	65
Experimental protocol 3.....	67
Cell proliferation assay.....	67
Determination of intracellular reactive oxygen species (ROS) levels.....	68
Measurement of cytoplasmic cytochrome c.....	69
Analysis of DNA fragmentation.....	70
Experimental protocol 4.....	71
Drug treatment.....	71
Statistical analysis.....	72
RESULTS.....	74
Effect of heat stress on core body temperature, respiratory rate and heart rate of pigs...	74

Identification of total RNA quality and concentration.....	74
Differential display PCR and identification of differentially expressed bands.....	77
Sequences of isolated DNA fragments and BLAST search results on GenBank.....	86
Quantitative real-time PCR results on 12 hours heat stress.....	90
Effect of heat stress on time course of gene expression.....	94
Effect of heat stress on both SOD-1 mRNA and protein levels in HT-22 cells.....	100
Effect of heat stress on SOD-1 activity.....	105
Heat stress diminishes HT-22 cell viability over time.....	108
Effect of pretreatment with EUK-134 on heat-induced decrease in HT-22 cell viability.....	111
Effect of heat stress on intracellular ROS generations.....	114
Effect of pretreatment with 10 μ M EUK-134 on heat-induced ROS generation in HT-22 cells.....	116
Effect of heat stress on apoptotic cell death in HT-22 cells.....	118
DISCUSSION.....	125
SUMMARY.....	135
CONCLUSION.....	136
REFERENCES.....	137

LIST OF FIGURES

Figure 1: Genomic organization of the three known members of the human SOD enzyme family	34
Figure 2: Antioxidant pathway in scavenging of superoxide anion and its dismutation product, H ₂ O ₂ by SOD, catalase and glutathione peroxidase	35
Figure 3: Chemical structure of M40403 SOD mimetic.	41
Figure 4: Chemical structural characteristics of metalloporphyrin compounds.	42
Figure 5: Structures of salen-manganese complexes.	43
Figure 6: Insert sequence.	56
Figure 7: Chemical structure of KUK-134.	73
Figure 8: Effect of heat stress on respiratory rate.....	75
Figure 9: Effect of heat stress on heart rate.	76
Figure 10: RNA integrity gel.....	79
Figure 11: A representative autoradiograph of polyacrylamide sequencing gel displaying PCP fragments.....	81
Figure 12: Differentially expressed DNA fragments in pig hippocampus.....	83-84
Figure 13: A representative reamplification gel of isolated DNA fragments.	85
Figure 14: A representative EcoRI restriction digestion product on agarose gel.....	87
Figure 15A: Real-time PCR quantification graph for standard curve.	92
Figure 15B: Linear representation of real-time PCR standard curve.	92

Figure 16: Quantitative real-time PCR analysis of gene expression in pig hippocampus after heat stress for 12 hours compared with control.....	93
Figure 17 A: Quantitative real-time PCR analysis of gene expression in pig hippocampus after heat stress for 4, 8, 12, 24 hours compared with control.....	97
Figure 17 B: Quantitative real-time PCR analysis of gene expression in pig hippocampus after heat stress for 4, 8, 12, 24 hours compared with control	98
Figure 18: Phase contrast photograph of HT-22 cells.....	101
Figure 19: Effect of heat stress on SOD-1 mRNA expression in HT-22 cells.....	102
Figure 20: Effect of heat stress on SOD-1 protein level in HT022 cells.....	104
Figure 21: SOD-1 activity standard curve	106
Figure 22: Effect of heat stress on SOD-1 activity in HT-22 cells.	107
Figure 23: Cell proliferation assay calibration standard curve.....	109
Figure 24: Effect of heat stress on HT-22 cell proliferation.....	110
Figure 25: Effect of pretreatment of HT-22 cells with EUK-134 (10-100 μ M) on cell proliferation.....	112
Figure 26: Effect of pretreatment with EUK-134 (10 μ M) on heat-induced decrease in HT-22 cell proliferation	113
Figure 27: Effect of heat stress on ROS generation in HT-22 cells.....	115
Figure 28: Effect of pretreatment with EUK-134 (10 μ M) on heat-induced decrease in HT-22 cell proliferation	117

Figure 29: Effect of heat stress on cytochrome c release to the cytoplasm in HT-22 cells.....	120
Figure30: Effect of pretreatment with EUK-134 (10 μ M) on heat-induced cytochrome c release to the cytoplasm in HT-22 cells.....	121
Figure 31: Effect of heat stress on DNA fragmentation in HT-22 cells.....	123
Figure 32: Effect of pretreatment with EUK-134 (10 μ M) on heat-induced DNA fragmentation in HT-22 cells.....	124

LIST OF TABLES

Table 1: HSP families and cellular localization in eukaryotic cells	12
Table 2: Genes other than HSPs whose expression is affected by heat stress.	17 - 21
Table 3: Total RNA concentration in different experimental groups.....	80
Table 4: Differentially expressed DNA fragments on differential display gel.....	82
Table 5: Blast search results that matched the sequences of the isolated PCR fragments that appear to be differentially expressed after heat stress in pig hippocampi.....	88
Table 6: The genes chosen to verify their heat-induced differential expression by real-time PCR analysis.....	89
Table 7: Primers for all tested genes by real-time PCR.....	91

INTRODUCTION

The term “*Heat Stress*” usually indicates perceived discomfort and physiological strain associated with exposure to a hot environment during physical training or work for extended periods of times (*Bouchama, 2006 & Bouchama and Knochel, 2002*). Heat stress and associated hyperthermia can be presented as a spectrum of clinical symptoms ranging from weakness, headache, profuse sweating and malaise to the severe life-threatening complications such as hyperpyrexia, delirium, coma, multiple organ failure, endotoxemia and death (*Chia and Teo, 2003*). In recent years, heat-related diseases have been considered a serious social and medical problem (*Sharma, 2006a*); however, no pharmacological preventative or intervention is available for heat-provoked sickness. This is due mainly to the lack of understanding of the molecular and cellular mechanisms involved in the heat stress response (*Yan et al., 2006*). Heat stress has powerful effects in all biological systems, and the central nervous system appears to be more sensitive to heat than other body tissues (*Maroni et al., 2003*). Studies at the cellular level suggest that heat can directly produce nervous tissue injury and brain dysfunction, which have long-term behavioral, physiological and neuropathological consequences (*Sharma and Hoopes, 2003*).

The precise mechanisms of brain injury following hyperthermic insults are still unclear and many factors are responsible for the neuropathological changes seen in the central nervous system (*Sharma and Hoopes, 2003 & Le Grevès et al., 1997*). At the molecular level, exposure to different stressors (including heat stress) elicits activation of specific signaling pathways leading to a stimulus-specific program of gene expression related to different cellular functions such as cell growth, cell survival or cell death. In response to heat stress, the expression of the heat-shock proteins (HSPs) is enhanced in eukaryotic cells (*Sherman and Goldberg, 2001*). The HSPs are molecular chaperones that assist many cellular processes involving proteins, including folding, transport through membranes, degradation, escape from aggregation and reactivation of denatured proteins (*Borges and Ramos, 2005*). HSPs are also involved in cellular protection through anti-apoptotic actions (*Franklin et al, 2005*). HSPs play a central role in allowing cells to cope with changes in their environment and to survive in otherwise toxic conditions (*Garido et al, 2001*). Additionally, the expressions of gene families other than HSPs are affected by heat stress. These genes control such diverse cellular functions as membrane transport, cellular metabolism, signal transduction, cell proliferation and differentiation (*Sonna et al, 2002*).

Hyperthermia is also associated with the overproduction of reactive oxygen species (ROS) such as superoxide radicals ($O_2^{\cdot-}$), hydrogen peroxide (H_2O_2), and hydroxyl radicals ($\cdot OH$) in different cell types including neuronal cells (*Zhao et al., 2006; Pérez-Crespo et al., 2005; Zhang et al., 2003 & Zuo et al., 2000*). The accumulation of ROS is caused by either enhancement of ROS production and/or suppression of ROS destruction mechanisms (*Satoh et al., 2004*). An imbalance of the equilibrium between ROS

generation and elimination by antioxidant defense systems can lead to the accumulation of free radicals and an increased risk of oxidative stress. Neuronal cells are at a particularly high risk of damage by heat-induced oxidative stress due to their high oxygen turnover, low levels of antioxidant defense enzymes and high polyunsaturated fatty acid content, which are potential substrates for oxidative stress-induced lipid peroxidation (*Huber et al., 2006; Behl et al., 1997 & Behl, 1997*).

Hypothesis and objective of this study:

The first part of the present study was designed to use mRNA Differential Display PCR to identify novel genes associated with heat stress in the brains of pigs as a model of human heat stress. This technology allows direct side-by-side comparison of the mRNAs in brains from control and heat-stressed pigs. It also enables the recovery of sequence information and the development of probes to isolate cDNA and genomic DNA for further molecular and functional characterizations and does not suffer from the limitation of species-specific probes. Therefore, the hypothesis to be tested in this section is that Differential Display PCR will identify genes in the pig brain not previously known to be part of the cellular response to acute heat stress.

The hippocampus was chosen as a representative brain region. It is involved in integrating information arriving from different sensory organs and associated areas and is essential for memory storage and retrieval, learning, motivation and emotion (*Fountoulakis et al., 2005*). The hippocampus is very sensitive to many types of neurological insults. It is a primary target for neuronal injury in many stressful

conditions such as trauma, ischemia and various stressors (McEwen, 2005) including heat stress (Maroni et al., 2003). Many neurodegenerative disorders including Alzheimer's disease (AD), amyotrophic lateral sclerosis (ALS) and Parkinson's disease (PD) have hippocampal involvement (Behl et al., 1997). Hippocampal cells also express glucocorticoid receptors (GRs), and are a principal target site for glucocorticoids secreted during stress. Under certain conditions, glucocorticoids exacerbate the sensitivity of hippocampal tissues to pathological insults such as seizures, hypoxia-ischemia, oxidative stressors and exposure to various neurotoxins (Behl et al., 1997). Whole body hyperthermia has also been reported to cause profound edema, and cell and tissue injury in the hippocampus of rats (Sharma et al., 2006a) and leads to upregulation of both constitutive and inducible isoforms of nitric oxide synthase (cNOS and iNOS), heme oxygenase-2 (Alm et al., 2000; Sharma et al., 2000), HSP70 (Maroni et al., 2003), HSP27 and HSP32 (Bechtold and Brown, 2003). Hyperthermia has also been reported to cause phosphorylation and activation of PKB and members of the MAPK family as well as to stimulate the activation of transcription factors like HSF and MEF2 (Maroni et al., 2003).

As an outcome of the first part of this proposed investigation, we expect to identify novel genes that are involved in the molecular response of the brain to heat stress.

In the second part of this investigation, an immortalized mouse hippocampal cell line (HT-22) was chosen as an *in vitro* model for hippocampal neuronal tissue. HT-22 cells were derived from HT4 cells which were immortalized from primary mouse hippocampal neurons by retroviral transduction of temperature-sensitive Simian Virus 40 large T antigen gene (Morimoto and Koshland, 1990). HT-22 cells have been suggested to be a

good model for the study of oxidative toxicity (*Lewerenz et al., 2006*). Excitatory amino acids like glutamate cause cell toxicity in HT-22 cells via a mechanism that involves glutathione depletion and the accumulation of ROS (*Chen et al., 2005*). This accumulation of ROS plays a pivotal role in heat-induced neuronal cells degeneration (*Sreedhar et al., 2002*).

Results derived from differential display RT-PCR in the first part of this study suggests that heat stress induced a decrease in the expression of the Cu/Zn superoxide dismutase (SOD-1) gene in pig hippocampus. Downregulation in hippocampal SOD-1 expression has been reported in response to other oxidative stress-related disorders such as cerebral ischemia, kainate-induced seizures, traumatic brain injury and glutamate-induced oxidative stress (*Peluffo et al., 2005*). Furthermore, preliminary experiments in our lab suggested that heat stress decreases SOD-1 production and cell number in HT-22 neuronal cells. Therefore, we hypothesized that the heat-induced decrease in SOD-1 gene expression was responsible for the accumulation of ROS and neuronal cell death associated with heat stress in hippocampal neuronal cells. We utilized HT-22 cells in this part of the study to investigate the effect of heat stress on SOD-1 and the relationship between downregulation of SOD-1 and heat-induced cell death. Lastly, we investigated the effectiveness of treatment with a synthetic SOD-mimetic drug, EUK-134, on the protection of HT-22 cells from the deleterious effects of heat-induced oxidative stress.

LITERATURE REVIEW

Heat stress:

The term “**Heat Stress**” usually denotes perceived discomfort and physiological strain associated with exposure to hot environment (air temperature > 32°C) due to physical exercise or daily work for long periods (*Bouchama, 2006*). The human body maintains a fairly constant internal temperature, even though it is exposed to constant changes in environmental temperature. To keep the internal body temperature within safe limits, endogenous mechanisms of heat loss and heat production are employed to maintain body temperature within a narrow range. The removal of excess heat is accomplished primarily through varying the rate and amount of blood circulation through the skin and release of fluid onto the skin by sweat glands. Pulmonary ventilation can also contribute to the regulation of body temperature. These automatic responses usually occur when blood temperature exceeds 37°C (98.6°F) (*Mortola, 2005*). The rise in core body temperature above the hypothalamic set point (37°C) is known as hyperthermia. Hyperthermia is caused by an impairment of heat-dissipating mechanisms in response to either external exposure to high environmental temperatures, or internal factors (metabolic heat production, drugs or disease) (*Kamijo and Nose, 2006*). Heat stress appears to be a disorder of the thermal information processing system that is chiefly regulated in the hypothalamus (*Rusyniak and Sprague, 2006 & Cuddy, 2004*). Heat stress and associated hyperthermia can present as a spectrum of symptoms, ranging from the sense of feeling

unwell (headache and malaise) to the most harsh form of heat related injuries (heat stroke), leading to death (*Chia and Teo, 2003*). The prognosis of heat-related illness is directly related to the degree of hyperthermia and its duration (*Hadad et al., 2004*). Findings indicate that in USA approximately 400 people die each year from excessive heat exposure and from 1979-2002, a total of 8,966 heat-related deaths were reported in the United States (*CDC, 2005*). Outdoor laborers compose the largest percentage of patients with heat-related illnesses (*Glazer, 2005*). Significant morbidity and mortality have resulted from heat-related illness associated with diverse activities such as military training, athletes exercising during warm weather, mining activities and fire fighting (*Seto et al., 2005; Chou et al., 2003; Khosla and Guntupalli, 1999 & Simon, 1993*). Heat stress-related mortality is among the main impacts of climatic extremes on human society (*Kysely, 2004*) and it represents at least 7% of wilderness-related deaths (*Lugo-Amador et al., 2004*).

Heat-related illness:

Based on clinical and epidemiological experiences, heat-related illness can be classified into the following categories.

1- Heat cramps:

Heat cramps, the least severe heat-related illness, is characterized by extreme dehydration, painful muscle spasm and hyponatremia. Core body temperature may or may not be elevated. Heat cramps occur mostly among those who sweat profusely in heat as a result of fluid and electrolyte imbalance following strenuous exercise performed in

a hot environment. Treatment consists of rest, administration of oral balanced electrolyte solutions or intravenous normal saline (*Stofan et al., 2005 & Wexler, 2002*).

2-Heat syncope:

Heat syncope refers to sudden loss of consciousness especially in persons who are poorly acclimatized to hot weather. Consciousness returns promptly with assumption of a recumbent posture. Heat syncope results from volume depletion, circulatory instability due to peripheral vasodilatation, and decreased vasomotor tone and occurs most commonly in elderly and poorly acclimatized individuals (*Lugo-Amador et al., 2004*).

3-Heat exhaustion:

Heat exhaustion is the most common heat-related illness and is characterized by salt and water depletion, fatigue, weakness, lethargy, severe headache, intense thirst, anxiety, dizziness, fainting, profuse sweating and hyponatremia (*Marto, 2005*). There is mild to moderate hyperthermia with core body temperature exceeding 37°C but usually remaining below 40°C. Heat exhaustion patients usually experience orthostatic syncope. The cause of heat exhaustion appears to be fluid and electrolyte imbalance caused by loss of a large amount of fluid with excessive loss of salt due to increase perspiration in response to intense heat (*Lugo-Amador et al., 2004*).

4-Heat stroke:

Heat stroke is the most severe form of heat-induced complications. It is a serious and potentially life-threatening condition (*Bazille et al., 2005 & Yeo, 2004*). Heat stroke is the third leading cause of death in athletes and exercising individuals (*Coris et al., 2006 & Coris et al., 2004*). The two major diagnostic findings of heat stroke are the presence of a core body temperature $\geq 40^{\circ}\text{C}$ and central nervous system dysfunction manifesting as

seizures, delirium, or coma accompanied by multi organ dysfunction (*Bouchama and Knochel, 2002*). It is thought that heat stroke is a continuum of heat exhaustion and that the neurological symptoms associated with heat stroke may be present in heat exhaustion, albeit to a lesser degree (*Chia and Teo, 2003*). Heat stroke can be categorized further into two types depending on the cause. Classic heat stroke is caused by exposure to high environmental temperature and humidity and usually occurs in the very young, elderly persons or individuals with chronic illness such as dementia, schizophrenia, cardiac conditions and obstructive pulmonary disease (*Sucholeiki, 2005, Lugo-Amador et al., 2004 & Hermesh et al., 2000*). Exertional heat stroke occurs as a result of strenuous exercise and primarily affects poorly acclimatized individuals and is characterized by rapid onset (*Yan et al., 2006 & Glazer, 2005*). Classical and exertional heat strokes are not distinct clinical entities. Rather, they represent two ends of a spectrum of circumstances under which heatstroke occurs. Anyone, young or old, can develop heat stroke if subjected to a sufficiently prolonged and intense heat stress. Exercise increases the production of metabolic heat, predisposing persons of all ages to the development of heat stroke (*Bouchama and Knochel, 2002*).

Heat stress has potent biological effects in all systems with the brain being more susceptible to heat stress than other body tissues (*Maroni et al., 2003 & Vogel et al., 1997*). Studies at the cellular level suggest that heat can directly induce nervous tissue injury and brain dysfunction, which have long-term behavioral, physiological and neuropathological consequences. The severity of the injury depends on the level and duration of heat stress (*Sharma, 2006a & Sharma and Hoopes, 2003*). The exact mechanisms of brain damage following hyperthermic insults remain unclear with no

single factor responsible for all the neuropathological changes seen in the central nervous system (*LeGrevès et al., 1997*). In fact, it is most likely due to a combination of many factors and neurochemicals exerting a synergistic influence on the CNS (*Sharma and Hoopes, 2003*). Hyperthermia is associated with cerebral ischemia (*Lin, 1997*), cerebral edema, hemorrhage and infarction (*Drobatz and Macintire, 1996*). The release of factors such as dopamine, serotonin, glutamate and cytokines (IL-1 β , IL-6, TNF- α) has been associated with hyperthermia (*Lin, 1997*). Other factors contributing to the hyperthermic-induced injury include generation of free radicals, increased production of reactive oxygen species (ROS) and alterations in cellular metabolism. Heat-associated generation of free radicals, oxidative stress and increased lipid peroxidation will induce direct membrane damage of the nerve cells, glial cells and the endothelial cells (*Chiueh, 1994*). Breakdown of the blood brain barrier (BBB) will result in extravasation of serum proteins leading to formation of vasogenic edema (*Sharma, 2000b*).

At the molecular level, changes in gene expression are an integral part of the cellular response to heat stress (*Kinoshita et al., 2001*). Heat stress triggers alterations in gene expression patterns and in the activity of expressed proteins, resulting in changes in cellular functions such as differentiation, proliferation, survival and adaptation and programmed cell death (apoptosis) (*Mager and De Kruijff, 1995*). The most characterized cellular response to heat stress is the induction of a group of genes coding for heat shock proteins (HSPs) (*Sherman and Goldberg, 2001*).

Heat shock proteins:

Heat shock proteins (HSPs), so named because their expression can be induced in cells upon thermal stress, are an essential part of the universal heat stress response. They are known to play diverse roles such as molecular chaperones and/or proteases that assist many cellular processes involving proteins (*Verbeke et al., 2001*). HSPs display important functions in folding, unfolding, assembly, disassembly and transport of multistructured protein complexes, refolding of denatured proteins, degradation of misfolded, aggregated and damaged proteins, as well as in the activation of enzymes and receptors (*Kampinga, 2006b; Scheibel and Buchner, 2006, Sorensen et al., 2005 & Borges and Ramos, 2005*). HSPs also participate in the regulation of immune function (*Kelly, 2005*) and cellular protection through anti-apoptotic actions (*Franklin et al., 2005*) and have a role in DNA damage repair (*Kampinga, 2006a; Pandita, 2005 & Pandita et al., 2004*). They play a central role in allowing cells to adapt to gradual changes in their environment and to survive in otherwise lethal conditions (*Garrido et al., 2001*). This may be achieved either via an active ATP-dependent mechanism or via a passive ATP-independent mechanism (*Lee and Tsai, 2005*). The major heat shock proteins are arranged into families of different molecular weights (**Table 1**) (*Borges and Ramos, 2005 & Verbeke et al., 2001*).

1-HSP100 family:

The HSP100 family is the newest member of the HSP group. They are universally conserved and are required for thermo-tolerance and may provide interchangeable function with HSP70 proteins. These proteins have two ATP-binding sites required for

Family	HSP	Localization
sHSPs	HSP27	Cytoplasm / nucleus
	HSP28	Cytoplasm / nucleus
	HSP25	Cytoplasm
	α -B-crystallin	Cytoplasm
	Ubiquitin	Cytoplasm
	HSP10	Mitochondria
HSP30	HSP32 (HO-1)	Cytoplasm / nucleus
HSP40	HSP40	Cytoplasm / nucleus
	HSP47	Endoplasmic reticulum
	Hdj 1	Cytoplasm / nucleus
	Hdj 2	Cytoplasm / nucleus
HSP60	HSP56	Cytoplasm
	HSP60	Mitochondria
	HSP65	Cytoplasm/nucleus
HSP70	HSP70/HSP72	Cytoplasm/ nucleus
	HSP73/HSC70	Cytoplasm / nucleus
	mitHSP70	Mitochondria
	Grp75	Mitochondria
	Grp 78 (BiP)	Endoplasmic reticulum
HSP90	HSP90 α / β	Cytoplasm / nucleus
	HSP83	Cytoplasm / nucleus
	Grp94	Endoplasmic reticulum
	Trap1	Mitochondria
HSP100	HSP100	Cytoplasm / nucleus
	HSP104	Cytoplasm
	HSP110	Cytoplasm / nucleus

Table 1: HSP families and cellular localization in eukaryotic cells. Modified from: *Borges, J and Ramos, C, 2005. Protein Pept Let; 12: 257-261* and *Verbeke, P et al., 2001. Cell Biol Int; 25: 845-857.*

function to prevent aggregation of proteins. To date their function includes chaperoning activity much like HSP70 (*Nishimura and Sharp, 2005*).

2- HSP90 family:

The HSP90 family of proteins is an abundant molecular chaperone (~ 1% of total cytosolic protein) that is highly conserved from prokaryote to eukaryotes. They are essential for cell growth and are involved in the folding and conformational regulation of numerous client proteins. HSP90s have defined protein substrates that are implicated in the cellular signaling network as protein kinases, transcription factors, and steroid hormone receptors (*Terasawa et al., 2005*). HSP90 binds to these proteins and suppresses their function (*Picard, 2002*). A number of associated proteins have been identified with HSP90, some of which are part of the glucocorticoid receptor complex. HSP90 also interacts with HSP70 and its co-chaperone HSP40. Together, these proteins comprise a major portion of the glucocorticoid receptor complex which transports the glucocorticoid receptor to the nucleus, dissociates from the receptor, thus allowing receptor binding to DNA. HSP90s also play a role in cell cycle and proliferation (*Wegele et al., 2004*).

3- HSP70 family:

The HSP70 family contains known chaperones that assist in a wide range of folding processes, including the folding and assembly of newly synthesized proteins, refolding of misfolded and aggregated proteins, membrane translocation of organelles and secretory proteins, and control of the activity of regulatory proteins. HSP70s thus have housekeeping functions in the cell in that they are built-in components of folding and signal transduction pathways, and quality control functions in which they proofread the structure of proteins and repair misfolded conformers (*Mayer and Bukau, 2005*). The best

characterized of these proteins is HSP70, which is highly inducible. HSP70 also autoregulates its own synthesis by interacting with heat shock factor-1. HSP70 is also known to chaperone unfolded or mutant protein to the ubiquitin–proteasome system for degradation. As noted for HSP90, HSP70 and HSP40 are obligate proteins of the glucocorticoid receptor complex. Within the HSP70 family is the constitutively active heat shock cognate 70 protein (Hsc70). Hsc70 is not inducible to the same extent as HSP70, although it likely serves the same function as HSP70 during stressful conditions. Hsc70 plays a role in membrane trafficking and lysosomal degradation. The function of these proteins relate to their chaperone activity and ability to refold or fold peptides (*Bukau et al., 2006 & Mosser and Morimoto, 2004*). In addition, within the endoplasmic reticulum, chaperones such as glucose-regulated protein 78 (GRP78) may be required for proper post-translational modification of proteins processed in the endoplasmic reticulum. Together with HSP70, these chaperones are responsible for the proper folding of newly synthesized peptides (*Nishimura and Sharp, 2005*).

4- HSP60 family:

HSP60 has primarily been reported to be a mitochondrial protein. Together with HSP10, it is suggested that they bind, unfold and refold peptides to active proteins after import into the mitochondria. They appear to also be capable of dissolving protein aggregates. A significant amount of HSP60 is also present in the extra-mitochondrial cytosol of many cells (*Gupta and Knowlton, 2005*). HSP56 is one member of this family that is stress inducible in the cytoplasm. HSP56 binds the steroid hormone receptor complex and has rotamase function (peptidyl-prolyl cis-trans isomerase) that plays a role in protein folding and activation (*Minowada and Welch, 1995*). Another member of this

family, HSP65, has anti-tumorigenic action, and is constitutively synthesized in the cytoplasm and plays a role in the folding of actin and tubulin (*Jolly and Morimoto, 2000*).

5-HSP 40 family:

HSP40s represent a large protein family that functions to specify the cellular action of HSP70 chaperone proteins. HSP40 proteins are inducible proteins that regulate the complex formation between HSP70 and polypeptides by 3 mechanisms. First, HSP40 proteins have evolved to contain unique classes of polypeptide-binding domains that bind and deliver specific clients to HSP70. Second, HSP40 proteins stabilize HSP70-polypeptide complexes by driving the conversion of HSP70 from its ATP-containing form to the ADP-containing form. Third, specialized members of the HSP40 family are localized to different sites within the same cellular compartment. Interaction of HSP70 with differentially localized HSP40s enables different HSP70-HSP40 pairs to bind unique clients at these sites (*Fan et al., 2003*).

6- HSP 30 family:

The HSP30 family contains HSPs that are enzymes, such as heme oxygenase. Heme oxygenase is an inducible protein that is synthesized during oxidative stress and heat stress. It degrades heme proteins to produce carbon monoxide, ferrous ion, and biliverdin. Biliverdin is converted into bilirubin by biliverdin reductase. The downstream products of the activity of heme oxygenase (bilirubin and carbon monoxide) may be important in protection from oxidative injury and signal transduction (*Nishimura and Sharp, 2005*).

7- Small HSP (smHSP) family:

Small HSPs include Hsp27 in humans (Hsp25 in rodents) and the alpha crystallins, along with some newly discovered but less characterized small HSPs. Many of these

proteins are constitutively synthesized in the cytoplasm such as Hsp27 and alpha B-crystallin. Although these proteins are present in oligomeric forms (9-24 mer) in the cell, a major function is their chaperone activity, regulation of cytoskeleton and the prevention of protein aggregates especially in the nervous system and heart. These proteins may also be involved in thermotolerance and in oxidative tolerance by the induction of anti-oxidative enzymes in the cytoplasm (*Latchman, 2005*). They also have a role in resistance to UV and inflammatory stresses. Ubiquitin is a small heat shock protein that is associated with Hsp70 and proteasome-mediated protein degradation (*Nishimura and Sharp, 2005*).

Effects of heat stress on gene expression:

Thermal stress leads to an alteration in expression of a substantial number of genes other than HSPs (*Sonna et al., 2002*). These genes are involved in a variety of cellular functions such as gene transcription, cell cycle regulation (*Dinh et al., 2001*), DNA repair, protein repair (*Kültz, 2003*), antioxidant and metabolic activity (*Zhang et al., 2002*) and apoptosis (*Jin, et al., 2006 & Zhao et al., 2006*). **Table 2** lists genes other than HSPs whose expression is reported to be affected by heat in different mammalian tissues and cells (*Sonna et al., 2002*).

Functional class	Gene	Change	Species/ Tissue	Exposure model	Reported timing of change	Proposed mechanism/Comments
Acute phase reactant	- C-reactive protein(CRP)	Up	Mouse liver	Intact animal	Recovery period	- HSF-1 binding to HSE in the promoter.
	- Orm 1 (orsomucoid 1, acid glycoprotein 1, AGP-1)	Up	Mouse liver	Intact animal	Recovery period	- Increased expression of specific isoforms of transcription factors C/EBP α and C/EBP β .
	- Orm 2 (orsomucoid 2, AGP-2)	Up	Mouse liver	Intact animal	Recovery period	- Same as for Orm 1.
Apoptosis inhibitor	- Bcl-2	Down	Human leukemia cells HL60	Cell culture	Recovery period	
Blood proteins	- Albumin	Up	Mouse liver	Intact animal	Recovery period	- HSF-1 binding to HSE in the promoter.
Cell adhesion	- ICAM-1	Down	Rat pancreas	Intact animal	Recovery period	- I κ B α sequestration of NF- κ B.
Cell cycle	- p53	Up	Human glioblastoma A-172 cells; human colorectal carcinoma cells RKO.C; human fibroblasts	Cell culture	Recovery period	
	- p21 (WAF-1)	Up	Human glioblastoma A-172 cells; human colorectal carcinoma cells RKO.C; human fibroblasts	Cell culture	Recovery period	- May involve p53 activation.
Cell activation marker	- ED-1	Down	Rat brain macrophages/ microglia	Intact animal	Recovery period	- I κ B α sequestration of NF- κ B.
Cell differentiation	- mcl-1	Up	Human embryonal carcinoma MCR-G3 cells	Cell culture	Recovery period	
Cell differentiation marker	- Cytokeratin 8	Up	Human embryonal carcinoma MCR-G3 cells	Cell culture	Recovery period	
	- Hcg	Up	Human embryonal carcinoma MCR-G3 cells	Cell culture	Recovery period	
Coagulation	- β -Fibrinogen	Down	Rat liver	Intact animal	Recovery period	- Transcriptional effect, mediator unkn.

Table 2: Genes other than HSPs whose expression is affected by heat stress. Modified from *Sonna, L et al, 2002. J Appl Physio; 192: 1725-1742.*

Functional class	Gene	Change	Species/ Tissue	Exposure model	Reported timing of change	Proposed mechanism/Comments
Cytokine	- Interleukin-1 β	Down	Mouse pretoneal macrophages; human astrocytes U-373; human monocytes THP-1	Cell culture	Both	- HSF-1 binding to HSE in the promoter.
	- Interleukin-6	Up	Human intestinal epithelial cells (Caco-2); mouse jejunal mucosa	Cell culture (Caco-2 cells); intact animals	Recovery period	
	- Interleukin- 8	Down	Human airway epithelial cells (BEAS-2B) and alveolar pneumocytes (A549)	Cell culture	Recovery period	- I κ B α sequestration of NF- κ B.
	- Osteopontin	Down	Human peripheral blood mononuclear cells	Cell culture	Recovery period	
	- RANTES	Down	Human alveolar pneumocytes (A549)	Cell culture	Recovery period	- I κ B α sequestration of NF- κ B.
	- TNF- α	Down	Mouse macrophage Raw 264.7; mouse pretoneal macrophages; human mononuclear cells, human astrocytes U-373; mouse kupffer cells; mouse liver slices; rat pancreas; human airway epithelial cells (BEAS-2B); human alveolar pneumocytes (A549)	Cell culture; tissue bath (mouse liver); intact animal (rat pancreas)	Both	- Termination of TNF- α transcription? increased degradation of TNF- α mRNA, I κ B α sequestration of NF- κ B. The TNF- α promoter does not contain a HSE. In the mouse model, in vivo heat exposure led to transient increases in plasma TNF- α suggesting dissociation between gene expression and secretion.
Cytoskeleton	- Glial fibrillary acidic protein	Up	Rat brain	Intact animal	During heat exposure	
Growth factor	- basic fibroblast growth factor	Up	Human breast carcinoma MCF-7/ADR	Cell culture	During heat exposure	- Activation of AP-1.
	- Vascular endothelial growth factor(VEGF)	Up	Mouse SCC VII tumors	Intact animal	Recovery period	- Unclear whether hyperthermia or ischemia accounts for the observed upregulation.
	- Transforming growth factor β (TGF- β)	Up	Rat heart, cultured rat cardiac fibroblasts, rat model of pancreatitis	Cell culture; intact animal	Recovery period	- In hearts from rats exposed to heat stress, the response is biphasic (initial decrease followed by subsequent increase) and localizes to the myocytes.
		Down	Rat neonatal cardiomyocytes	Cell culture	Recovery period	

Table 2: continued.

Functional class	Gene	Change	Species/ Tissue	Exposure model	Reported timing of change	Proposed mechanism/Comments
Heavy metal binding	- Metallothionein	Down	Rat liver; human HeLa cells	Intact animal; cell culture	Both	- In HeLa cells, mRNA levels had returned to baseline at the first recovery time point examined (3 hours after heat shock).
Membrane transporter	- MDR1 (ATP binding cassette transporter) - MRP1 (ATP binding cassette transporter)	Up	Human colon carcinoma cell lines HCT15 and HCT116	Cell culture	Recovery period	- YB-1 translocation to the nucleus.
		Up	Human colon carcinoma cell lines HCT15 and HCT116	Cell culture	Recovery period	- YB-1 translocation to the nucleus.
Proteases	- Protease HTR-A2	Up	Human neuroblastoma SHSY5Y cells	Cell culture	During heat exposure	
Protease inhibitor	- Amyloid precursor proteins	Variable	Human fetal astrocytes CC2565	Cell culture	Recovery period	- Affects splicing of the gene rather than expression, as there was an increase in APP-751, no change in APP-695 and a decrease in APP-770 (splice variants of the same gene).
Receptor	- M ₁ muscarinic receptor - NMDA receptor Subunits NMDAR1, NMDAR2A, and NMDAR2B - Bradykinin receptor B ₁ - T-cell receptor ζ-chain	Up	Reporter assays in rat glial cells CCL-107 and mouse neuroblastoma cells CCL-147	Cell culture	Recovery period	- HSF-1 binding to HSE in the promoter.
		Down	Rat hippocampus	Intact animal	During heat stress	
		Up	Rat aorta and heart; rat aorta smooth muscle cells	Intact animal; cell culture	Recovery period	- Activation of p38 and p42/p44 kinases
		Down	Human T lymphocytes	Cell culture	Recovery period	- Activation of transcription factor Elf-1.
Redox control	- MnSOD	Up	Rat myocardium and rat cardiomyocytes	Intact animal; cell culture	Recovery period	- In intact animals, MnSOD enzymatic activity showed a biphasic increase; the early phase (seen immediately after heating) was not accompanied by increased expression of MnSOD protein..
		Down	Mouse lung epithelium MLE-15 cells	Cell culture	Recovery period	

Table 2: continued.

Functional class	Gene	Change	Species/ Tissue	Exposure model	Reported timing of change	Proposed mechanism/Comments
Ribosomal RNA	- Ribosomal RNA	Down	Mouse lymphosarcoma P-1798 cells	Cell culture	Recovery period	- Decreased expression of the p72 subunit of transcription factor E1BF/Ku.
Signal transduction	- Annexin I (lipocortin)	Up	Human lung A549 and HeLa cells	Cell culture	Recovery period	- HSF-1 binding to HSE in the promoter.
	- cNOS	Up	Rat hippocampus	Intact animal	During heat exposure	
	- DUSP1(CL-100)	Up	Human skin fibroblasts EK4	Cell culture	Recovery period	
	- DUSP5	Up	Human skin fibroblasts EK4	Cell culture	Recovery period	
Transcription factor	- iNOS	Up	Rat brain	Intact animal	During heat exposure	
		Down	Rat pulmonary artery smooth muscle cells; rat hepatocytes; human hepatocytes (AKN-1); mouse lung epithelium (MLE-15); rat and human pancreatic islets; rat astrocytes; rat brain macrophages/ microglia	Cell culture; tissue bath (pancreatic islets); intact animal (rat brain) macrophages/ microglia	Recovery period	- I κ B α sequestration of NF- κ -B.
	- Rad (Ras associated with diabetes)	Up	Human PBMCs	Cell culture	Recovery period	
	- Ran (Ras-related nuclear protein)	Down	Human leukemia cells HL60	Cell culture	Recovery period	
	- C/EBP- α (CCAAT-enhancer binding protein α)	Down	Mouse liver	Intact animal	Recovery period	- Heat stress affects both the level of mRNA expression and the relative expression of different protein isoforms of this gene.
	- C/EBP- β (CCAAT-enhancer binding protein β)	Up	Mouse liver	Intact animal	Recovery period	- HSF-1 binding to HSE in the promoter, heat stress also affects the relative expression of different protein isoforms of this gene.
	- <i>c-fos</i>	Up	Human HeLa cells; mouse NIH/3T3 cells; human Hyon (pre-B) cells; pre-T cells (DND-41) and thymocytes	Cell culture	Both	- Post-transcriptional mechanism; the <i>c-fos</i> promoter does not have a HSE.
		Down	Chinese hamster ovary K-1 fibroblasts	Cell culture	During heat exposure	- HSF-1 mediated inhibition of the Ras mediated increase in <i>c-fos</i> , by a mechanism that does not involve HSF-1 binding to the <i>fos</i> promoter.
	- <i>erg-1</i> (early growth response-1)	Up	Mouse NIH/3T3 cells	Cell culture	During heat exposure	- p38- and JNK-mediated phosphorylation of elk-1.

Table 2: continued.

Functional class	Gene	Change	Species/ Tissue	Exposure model	Reported timing of change	Proposed mechanism/Comments
Transcription factor inhibitor	- <i>c-jun</i>	Up	Human HeLa cells; mouse NIH3T3 cells; human Hyon (pre-B) cells; pre-T cells (DND-41), B cells (Daudi), T cells (PEER); thymocytes	Cell culture	Both	- Enhanced cytoplasmic degradation of <i>c-myc</i> mRNA. - Leads to decreased RNA polymerase I-directed transcription. - HSF-1 binding to HSE in the promoter.
	- <i>c-myc</i>	Down	Human leukemia cells HL60; HeLa cells; human B cell lines BJAB and BJAB-6A; human Hyon (pre-B) cells; pre-T cells (DND-41), B cells (Daudi), T cells (PEER); thymocytes	Cell culture	Both	
	- E1-BF (enhancer-1 binding factor), subunit p72	Down	Mouse lymphosarcoma P-1798 cells	Cell culture	During heat exposure	
	- IκBα	Up	Human lung carcinoma A549 cells; human bronchial epithelial BEAS-2B cells; rat brain macrophages/ microglia; mouse jejunal mucosa	Cell culture; intact animal (rat brain macrophages/ microglia, mouse jejunal mucosa)	Recovery period	
	- Integrin beta-4 binding protein (ITGB4BP; eIF6; p27-BBP)	Down	Human pancreatic carcinoma cells FG2 and immortalized human keratinocytes HaCaT	Cell culture	Recovery period	
Unknown	- Hypothetical protein T1-227H (GenBank #D50525)	Up	Human leukemia cells HL60	Cell culture	Recovery period	- IκBα sequestration of NF-κ-B.
Untranslated RNA	- B1 and B2 short interspersed elements (SINE) RNase; (Alu repeats)	Up	Mouse liver, spleen, kidney, testis; human HeLa cells, mouse NIH/3T3 and rabbit skin fibroblast RAB-9 cells	Intact animal; cell culture	Recovery period	

Table 2: continued.

In all eukaryotes, the heat shock response involves the activation of evolutionary conserved protein, heat shock transcription factor (HSF) which is necessary for turning on the expression of HSP genes that encode heat shock proteins (*Shamovsky and Gershon, 2004*).

Heat Shock factors:

Heat shock factors (HSFs) are transcription factors that regulate HSP expression through interaction with a specific DNA sequence, heat shock element (HSE), in the promoter region of susceptible genes (*Hahn et al., 2006 & Pirkkala et al., 2001*). The mammalian genome encodes three homologues of HSF: HSF1, HSF2 and HSF4 (*Trinklein et al., 2004a*). A fourth HSF, HSF3, is present only in avian species (*Pirkkala et al., 2001*). The HSF proteins bear five domains; an amino terminal DNA-binding domain, an adjacent coiled-coil trimerization domain, a central regulatory domain, a second coiled-coil domain, and a transcriptional activation domain at the carboxyl-terminal heptad repeat (*Vujanac et al., 2005*). The structures of the DNA-binding and trimerization domains are highly conserved among all characterized HSFs (*Ahn et al., 2001 & Morimoto et al., 1997*).

1-Heat Shock Factor-1 (HSF1):

HSF1 is believed to be the HSF isoform responsible for regulating the heat-induced transcriptional response in mammalian cells (*Ahn et al., 2005 & Batulan et al., 2005*). The heat-shock transcription factor HSF1 is a low abundance protein that is synthesized as a repressed monomer capable of rapid and maximal conversion to DNA-binding homotrimers upon heat stress. Under normal conditions, HSF1 exists as a monomer

localized to the cytoplasm and forms heterocomplexes with regulatory heat shock proteins like HSP70 and HSP90 and the co-chaperon Hdj1, which interferes with HSF1 transactivation. It is generally accepted that accumulation of non-native proteins caused by heat stress is a proximal signal for HSF1 activation. As a result of competition with non-native proteins for chaperones that prefer non-native proteins to HSF1, HSF1 is relieved and activated through oligomerization to a trimetric state. HSF1 translocates into the nucleus, where it is hyperphosphorylated at serine residues and binds to heat shock element (HSE) located upstream of HSP genes resulting in rapid and efficient induction of heat shock genes (*Morrison et al., 2006 & Park, et al., 2005*). The nature of the protein kinase involved in HSF1 activation is still not clear. Some studies have demonstrated a role for protein kinase A in HSF1 activation (*Sonna et al., 2002*). Others have suggested a role for Protein kinase C in HSF1 activation (*Holmberg et al., 1997*). In addition, other studies suggest a role for phosphatidylinositol-3 kinase and the downstream protein kinase B (*Bijur and Jope, 2000*). The response to heat shock is rapid; activation of HSF1 and binding to HSE are detected within minutes after temperature elevation (*Mager and De Kruijff, 1995*). Other studies suggest an alternative mechanism involving three auxiliary factors in the regulation of heat shock response by activation of the HSF1. These auxiliary factors include an inhibitor protein (HSF-I) that forms a complex with monomeric HSF-1 in the cytoplasm and prevent its trimerization under normal conditions and the two promoting factors, elongation factor -1 α (EF-1 α) and a large non coding RNA (HSR). The latter two factors are physically associated with HSF1 and aid in the trimerization and binding to HSE as a result of exposure to elevated temperature (*Shamovsky and Gershon, 2004*).

Heat shock element (HSE): Heat shock element is a stretch of DNA located upstream in the promoter region of susceptible genes. It contains simple sequential copies (adjacent and inverse) of the consensus pentanucleotide sequence 5'-nGAAn-3'. The HSE found in mammalian cells contains three alternately-oriented 5-bp units (nGAAnnTTCnnGAAn) that represents a complete binding site for the homotrimeric HSF-1 molecule (*Tonkiss and Claderwood, 2005 & Santoro, 2000*).

2- Heat shock factor 2 (HSF2):

HSF2 is primarily involved in controlling development and differentiation-specific gene expression. It is activated in response to distinct developmental cues or differentiation stimuli (*Santoro, 2000 & Trinklein et al., 2004b*). HSF2 has also been proposed to be responsible for the specific HSP expression observed during the developmental process (*Pirkkala et al., 2001*). Upon stimulation it is converted from an inert dimer to an active trimer. Its activation requires a longer time period than that of HSF1 (16-24 hours). HSF2 also remains in the trimeric activated state for a longer time period than HSF1 (48-72 hours) (*Santoro, 2000*). HSF2 can co-operate with HSF1 in the activation of HSP promoters and increase stress-induced HSP transcription (*Batulan et al., 2003*).

3- Heat shock factor 3 (HSF3):

HSF3 is an avian-specific HSF. Like HSF1, HSF3 is a stress-responsive transcription factor (*Nakai, 1999*). HSF3 is found as an inert dimer; and shares many characteristics with HSF1, such as negative regulation by HSPs, and activation to a homotrimeric state, and sequence-specific binding to HSE. HSF3 is a stress-responsive transcription factor. The threshold temperatures required to activate HSF1 and HSF3 are different. HSF1 is

activated upon mild heat shock, whereas co-activation of HSF1 and HSF3 occurs after severe heat shock and the kinetics of activation exhibits a delayed response compared to HSF1. HSF3 appears to be an important co-regulator of HSF1, enhancing the cellular ability to tightly regulate the heat shock response (*Pirkkala et al., 2001 & Santoro, 2000*).

4-Heat shock factor 4 (HSF4):

HSF4 is a novel member of the HSF family. HSF4 lacks the carboxyl-terminal portion of the protein necessary for suppression of HSF trimer formation. It has been shown to constitutively bind to DNA, but is unable to activate transcription. It is suggested that HSF4 acts as a negative regulator of the heat shock response, repressing the expression of HSP genes (*Pirkkala et al., 2001; Santoro, 2000 & Tanabe et al., 1999*).

Recently it was demonstrated that several transcriptional systems other than HSFs are also affected by heat shock and implicated in gene differential expression after heat stress (*Park, et al., 2005; Trinklein et al., 2004a & Sonna et al., 2002*). At least three different methods have been identified through which heat stress specifically affects these systems.

(a) Heat stress changes the expression level of transcription factors:

Heat stress can change the expression of transcription factor itself in both mRNA and protein levels. A variety of mechanisms may be included in this heat-induced modified expression of transcription factors. For example, the heat-induced stimulation of the activator protein-1(AP-1) system is related to an increase in expression of the mRNA and protein of its two major components (*c-jun* and *c-fos*) (*Zhang et al., 2004 & Sonna et al., 2002*). Another example is *c-myc* transcription factor that is down-regulated by the effect

of enhanced degradation of cytoplasmic mRNA (*Sonna et al, 2002; Balcer-Kubiczek et al, 2000 & Wennborg et al, 1995*).

(b) Heat stress changes the activity of transcription factors:

Heat stress can modify the activity of transcription factors other than HSF1. Heat stress may alter the activity of the transcription factor by changing the DNA binding activity. For example, heat stress enhances the DNA binding and so transcription activity of the tumor suppressor p53 system (*Ohnishi et al, 1996*). Another example is the heat-induced diminution in the transcription activity of Oct-1 and CREB systems by decreasing their DNA binding. Heat stress can also change transcription factor activity through modification of their phosphorylation state. For example, heat stress stimulates the activity of transcription factors *elk-1* and *c-jun* component of AP-1 by stimulation of p38- and JNK-mediated phosphorylation (*Sonna et al, 2002, Lim et al., 1998 & Adler et al., 1995*).

(c) Heat stress changes the cellular location of transcription factors:

Heat stress can affect transcription activity by changing the cellular distribution of many transcription factors other than HSF1. This has been shown to activate transcription in some experimental systems. For example, heat stress produces translocation of Y-box transcription factor 1 from the cytoplasm to the nucleus, resulting in increased expression of multidrug resistance transporters MDR-1 and MRP-1 (*Stein et al., 2001*). Conversely, heat shock can also inhibit transcription by preventing translocation of the transcription factor to the nucleus. The best studied example of this is inhibition of translocation of nuclear factor- κ B (NF- κ B) translocation to the nucleus (*Pespeni et al., 2005; Gius et al., 2004 & DeMeester et al., 2001*). This inhibition is thought to be mediated by

an effect on I κ B α , a protein that sequesters NF- κ B in the cytoplasm. Heat shock inhibits the activation of I κ B kinase (IKK) activity leading to a decrease in phosphorylation and subsequent ubiquitination of I κ B α . The net effect is an inhibition of I κ B α degradation that prevents NF- κ B translocation to the nucleus by holding it in an inactive bound state in the cytoplasm (*Shanley et al., 2000 & Yoo et al., 2000*). Additionally heat stress has been shown to increase I κ B α mRNA expression (*Malago et al., 2002 & Pritts et al., 2000*).

The heat shock response is a rapid, complex, highly regulated process that involves coordinated control of multiple signal transduction pathways. Several components of the signaling pathway leading to the heat shock response are also stimulated by environmental stresses (*Pirkkala et al., 2001*) such as exposure to hypoxia-reperfusion, heavy metal toxicosis, and viral infections, all of which appear to perturb cellular redox status (*Gius et al., 2004*). Taken together, these data suggest that heat stress, perhaps through alteration in cellular metabolism, produces a condition of oxidative stress similar to that seen with other forms of cellular stresses (*Matsuzuka et al., 2005; Pèrez-Crespo et al., 2005; Lord-Fontaine and Averill-Bates, 2002; Gius et al., 2004 & Sreedhar et al., 2002*).

Heat-induced oxidative stress:

Oxidative stress is a condition characterized by elevation in cellular steady-state concentration of reactive oxygen species (ROS) due to an imbalance between the production of ROS and the anti-oxidant defense systems (*Rojas et al., 2006; Suntres and Lui, 2006a; Suntres and Lui, 2006b Jallali et al., 2005 & Emerit et al., 2004*). Reactive oxygen species are generated as byproducts of various oxygen consumption metabolic

pathways in different cellular compartments. There are multiple mechanisms or processes by which cells and tissues protect themselves against ROS; however, under certain circumstances, these protective mechanisms can be either overwhelmed or inefficient in handling ROS resulting in accumulation of these ROS and oxidative stress (Cook, et al., 2004). The accumulated ROS reacts with lipids, proteins and DNA leading to lipid peroxidation, alteration of protein structure and enzymatic activities, and DNA damage. The damage imparted in various macromolecules by reaction with ROS can initiate an apoptotic program of cell death or lead to cell death by necrosis (Zhao et al., 2006; Galli et al., 2005a; Galli et al., 2005b; Osorio et al., 2003 & Decraene et al., 2004). Heat stress has been reported to enhance numerous forms of ROS including superoxide anion ($O_2^{\cdot-}$), hydrogen peroxide (H_2O_2), hydroxyl radical ($\cdot OH$), nitric oxide ($\cdot NO$), and peroxynitrite ($OONO^-$) in various cell types (Zhao et al., 2006; Pérez-Crespo et al., 2005 & Arnaud et al., 2002).

Mechanisms involved in heat-mediated accumulation of ROS:

A number of biochemical and physiological events associated with hyperthermia can potentially promote ROS formation (Flanagan et al., 1998). The mitochondrial electron transport chain (ETC) has been recognized as a major cellular generator of ROS formed as a side product of oxidative phosphorylation (Morisson et al., 2005; Zou et al., 2000 & Flanagan et al., 1998). Mitochondrial ETC, mainly at the level of complexes I and III, produce basal levels of ROS via univalent leakage of one electron to oxygen during normal metabolism (Petrosillo et al., 2006). When oxygen accepts an electron the superoxide anion ($O_2^{\cdot-}$) is formed as a by-product from this incomplete reduction of

molecular oxygen. Under physiological O₂ level, 1-2% of the O₂ consumed is converted to O₂^{•-} (Emerit *et al.*, 2004). This can increase dramatically under stress conditions in which the mitochondrial metabolic activity increases or mitochondrial damage occurs. Heat stress has been shown to increase ATP utilization and the flux of oxygen through the mitochondrial ETC and induce a temperature-dependent uncoupling of the mitochondrial ETC oxidative phosphorylation proteins leading to increased O₂^{•-} formation (Morrison *et al.*, 2005; Becker, 2004; Zou *et al.*, 2000; Tsong and Su, 1999 & Flanagan *et al.*, 1998). The initial product of the electron transport chain (ETC) is O₂^{•-}, which is quickly transformed into H₂O₂ by the enzyme mitochondrial superoxide dismutase (SOD-2). H₂O₂ can be reduced to water by catalase or glutathione peroxidase or can be converted into [•]OH in the presence of reduced transition metals (reduced copper or iron) (Camello-Almaraz *et al.*, 2006 & Boveris *et al.*, 2006).

The enzymatic activity of such enzymes as xanthine oxidase, NADPH oxidase, cyclooxygenase, phospholipase A₂ and nitric oxide synthase could be another source of ROS generation associated with heat stress. Hyperthermia stimulates the conversion of xanthine dehydrogenase to xanthine oxidase. Xanthine oxidase is the enzyme that catalyzes the oxidation of hypoxanthine to xanthine and H₂O₂ and can further catalyze the oxidation of xanthine to uric acid and H₂O₂. Superoxide anion is also generated as a secondary product during these reactions (Zou *et al.*, 2000; Flanagan *et al.*, 1998 & De Keulenaer *et al.*, 1998).

Membrane-associated NADPH oxidase plays a role as a source of heat-related ROS production. NADPH oxidase activity is enhanced by the effect of heat. NADPH oxidase generates O₂^{•-} by transferring electrons from NADPH inside the cell across the

membrane and coupling these to molecular oxygen. (Zou *et al.*, 2000 & Munzel *et al.*, 1999).

Activation of phospholipase A₂ appears to be a necessary step in the increase of ROS generation by different types of cells during exposure to elevated temperature. The activation of phospholipase results in the generation of arachidonic acid from available membrane substrates. ROS are then generated as by-products from oxidative metabolism of arachidonic acid through the cyclooxygenase pathway (Droge, 2001; Zou *et al.*, 2000; Xiao *et al.*, 1999 & Nethery *et al.*, 1999).

Another potential source of the heat-induced increase in ROS generation is the influence of heat on $\cdot\text{NO}$ production. Two isoforms of nitric oxide synthase (NOS) have been demonstrated to be stimulated by the effect of elevated temperature; neuronal isoform (nNOS) and inducible isoform (iNOS) (Alm *et al.*, 2000 & Venturini *et al.*, 1999). As a result of NOS enhancement, increase in $\cdot\text{NO}$ production occurs. Because $\cdot\text{NO}$ is known to react rapidly with $\text{O}_2^{\cdot-}$, peroxynitrite (OONO^-) can be produced as result of heat stress (Zhao *et al.*, 2006 & Zou *et al.*, 2000).

Cells can be protected from oxidative stress and oxidative damage by primary and secondary defense systems. The primary mechanisms include direct scavenging of ROS by antioxidants that include enzymatic and non-enzymatic compounds. The secondary system includes different mechanisms of repairing oxidative damage (Lee *et al.*, 2005).

Antioxidant defense systems:

A number of antioxidant systems exist in aerobic organisms that function to counteract the cellular production of ROS. These endogenous antioxidant pathways

include a network of compartmentalized enzymes that are distributed within the cytoplasm and among various organelles. In eukaryotic organisms, antioxidant enzymes such as superoxide dismutase (SOD), catalase (CAT), glutathione-S-transferase (GST) and different forms of peroxidases like glutathione peroxidase (GPX), peroxiredoxins (PRX) and thioredoxin peroxidase (TRX) work in a complex series of integrated reactions to convert ROS to more stable molecules such as water and O_2 . Besides these primary antioxidant enzymes, a large number of secondary enzymes act in concert with small molecular-weight antioxidants to provide necessary cofactors for primary antioxidant enzyme functions. Small molecular weight antioxidants like glutathione, NADPH, thioredoxin, vitamins E and C, and trace metals such as selenium also function as direct scavengers of ROS. These enzymatic and non-enzymatic antioxidant systems promote normal cell function by maintaining a delicate intracellular redox balance and by reducing or preventing cellular damage caused by ROS (*Kregel and Zhang, 2006 & Willcox et al., 2004*). The SOD/CAT/GPX catalytic triad is quite ubiquitous and has been found in virtually all prokaryotic and eukaryotic aerobic organisms. Superoxide dismutase catalyzes the dismutation of the superoxide anion ($O_2^{\cdot-}$) to produce hydrogen peroxide (H_2O_2). Although it recycles the superoxide anion free radical, SOD is more of a pro-oxidant since it converts a rather short-lived and confined molecule ($O_2^{\cdot-}$) into a quite stable and invasive one, H_2O_2 . To efficiently recycle hydrogen peroxide, catalase and glutathione peroxidase transform H_2O_2 into H_2O , although under different conditions. Catalase uses H_2O_2 as a substrate and functions when H_2O_2 concentration is above physiological levels such as can occur in oxidative bursts characteristic of stress responses. Glutathione peroxidases use different substrates in addition to H_2O_2 , and

function even at low concentrations of H₂O₂. Therefore, GPX activity represents the first protective response for small adjustments in H₂O₂ concentrations under normal physiological conditions. In addition, beside H₂O₂, GPX can also metabolize organic peroxidized molecules. Neither catalase nor peroxiredoxin have this function (*Drevet, 2006*).

Superoxide dismutases (SODs):

The superoxide dismutases (SODs) are the front-line intracellular defense against ROS particularly superoxide anion radicals (*Cook et al., 2004*). SODs are metalloenzymes that have been isolated and characterized from a wide variety of organisms. One class consists of SODs with Cu(II) plus Zn(II) at the active site (Cu/ZnSOD), another with Mn(III) (MnSOD), a third with Fe(III) (FeSOD), and a fourth with Ni(II/III) (NiSOD). Cu/ZnSODs are generally found in the cytosol and extracellular fluid of eukaryotic cells, and in some prokaryotes whereas MnSODs are found in prokaryotes and in mitochondria. FeSODs are generally found in prokaryotes, in algae and in some higher plant chloroplasts and NiSODs have been found in *Streptomyces* (*Scandalios, 2005*).

In mammals, three distinct isoforms of SOD have been identified and each is encoded by distinct genes. Two isoforms of SOD have Cu and Zn in their catalytic center and are localized to either intracellular cytoplasmic compartments (Cu/Zn-SOD or SOD-1) or to extracellular elements (EC-SOD or SOD-3). SOD-1 is a homodimer with molecular mass of about 32,000 Da and has been found in the cytoplasm, nuclear compartments, and lysosomes of mammalian cells. The SOD-1 gene is localized to human chromosome 21 (region 21q22). SOD-3 is the most recently discovered and least characterized member of

the SOD family. The enzyme exists as a homotetramer of molecular weight 135,000 Da. It is glycosylated and exhibits high affinity for sulfated polysaccharides like heparin. SOD-3 was first detected in human plasma, lymph, ascites, cerebrospinal fluids, and extracellular matrix. It shows some sequence homology to SOD-1 (**Figure 1**) and is secreted by cells into the extracellular space. The SOD-3 gene is localized to human chromosome 4 (region 4p-q21). A third isoform of SODs has manganese (Mn) as a cofactor and is localized to mitochondria of aerobic cells (Mn-SOD or SOD-2)]. It exists as a homotetramer with a molecular weight of about 86,000-88,000 Da. Besides its role as superoxide dismutase, SOD-2 also plays a major role in promoting cellular differentiation and tumorigenesis as well as protection against hyperoxia-induced pulmonary toxicity. SOD-2 has no significant amino acid sequence homology with either SOD-1 or SOD-3. The SOD-2 gene is localized to human chromosome 6 (region 6q25) (*Xiong et al., 2005; Zelko et al., 2002; Fridovich, 1997 & Fridovich, 1995*). Figure 2 shows the genomic organization of the three SOD isozymes. The SODs catalyze the dismutation of the superoxide anion ($O_2^{\cdot-}$) to produce hydrogen peroxide (H_2O_2) (**Figure 2**). Although it recycles the superoxide anion free radical, one can consider SOD more as a pro-oxidant since it converts a rather short-lived and confined molecule ($O_2^{\cdot-}$) into a quite stable and invasive one, H_2O_2 . Moreover, taking into account the Fenton/ Haberweiss coupled reactions, H_2O_2 accumulation if not efficiently recycled, will lead to the appearance of the highly reactive hydroxyl radical ($\cdot OH$) (**Figure 2**). Hydroxyl radical is a highly reactive to cellular components such as lipids in membranes, proteins, carbohydrates as well as nucleic acids ultimately leading to cell death. The formed hydrogen peroxide is well recycled by another two enzymes, catalase and

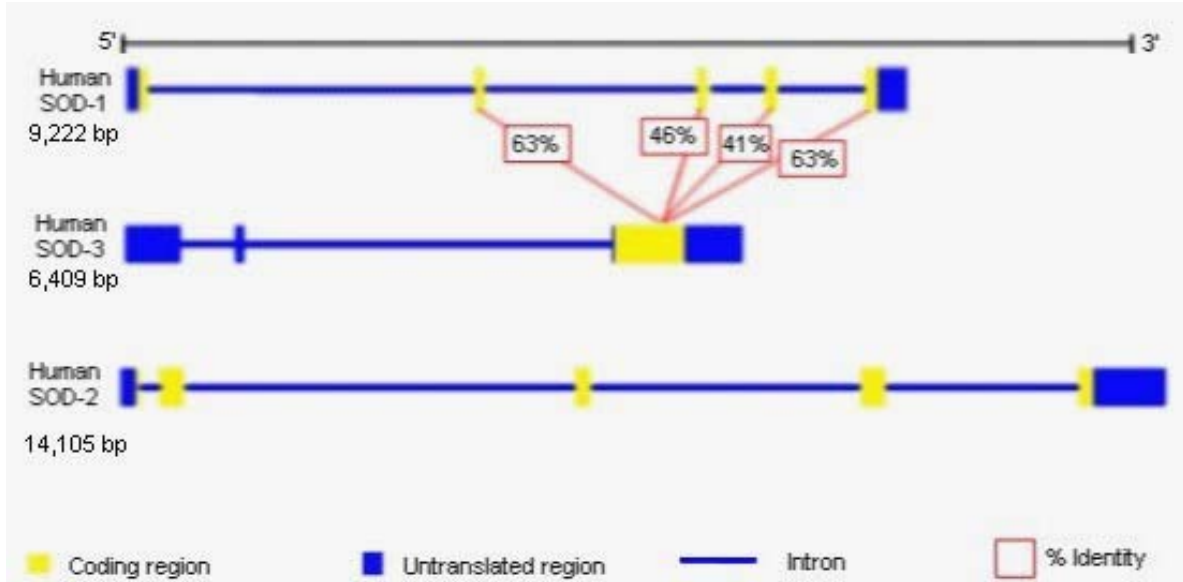


Figure 1: Genomic organization of the three known members of the human SOD enzyme family. SOD3 was placed in the middle in order to demonstrate areas of amino acid sequence homology between SOD1 and SOD3. SOD2 has no significant amino acid sequence homology with either SOD1 or SOD3. Modified from: *Zelko I et al, 2002. Free Radical Biology and Medicine; 33 (3): 337-34*, NCBI Entrez Gene Database at (<http://www.ncbi.nlm.nih.gov/entrez/query.fcgi?db=gene>) and from Genecards web site at (<http://www.genecards.org/cgi-bin>).

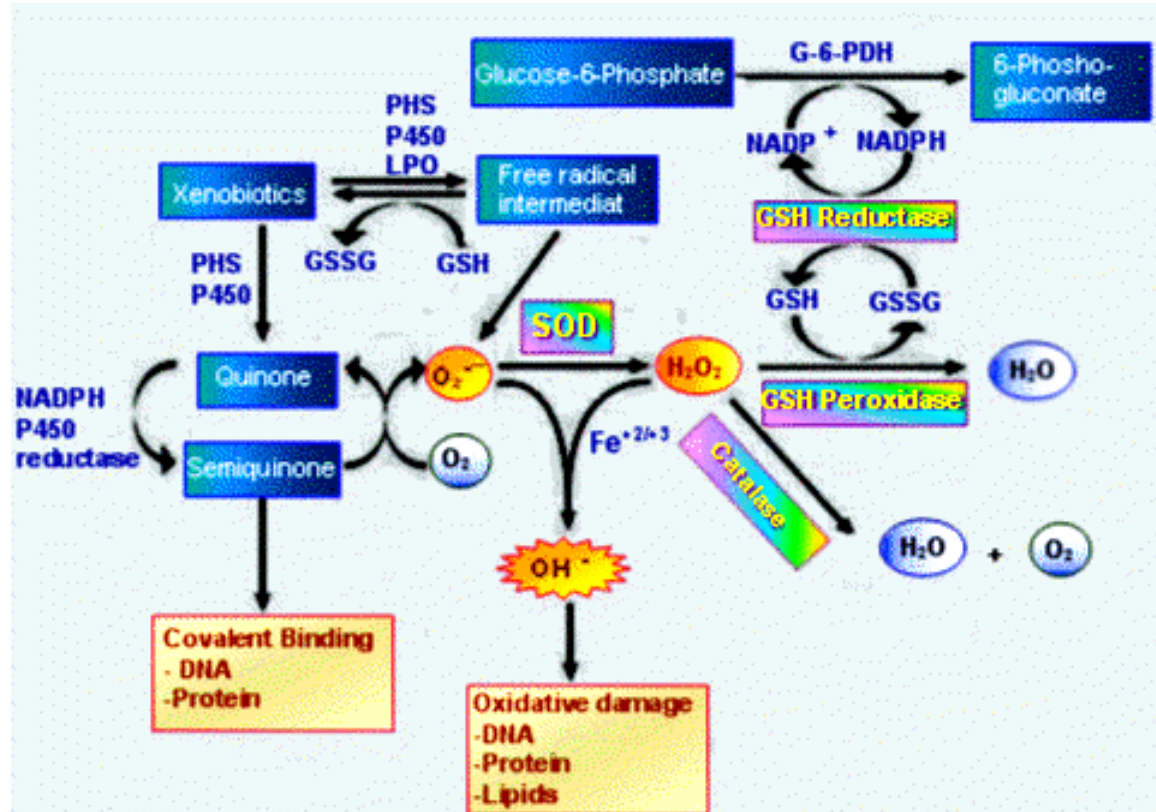


Figure 2: Antioxidant pathway in scavenging of Superoxide anion and its dismutation product, H_2O_2 , by SOD, catalase and glutathione peroxidase. Modified from: Sigma-Aldrich web page pathway slide of oxidative stress (<http://www.sigmaaldrich.com/>).

glutathione peroxidase, that convert H_2O_2 into H_2O and O_2 (Drevet, 2006; Kinnula and Crapo, 2003 & Takahashi, 2000). The superoxide radical and/or SODs have been implicated in a broad range of human pathologic conditions including diabetes, cancer, inflammatory diseases, atherosclerosis, pulmonary fibrosis, diseases of ischemia and reperfusion injuries, neurodegenerative diseases and aging (McCord and Edeas, 2005 & Thannickal and Fanburg, 2000).

Superoxide dismutase-1 (SOD-1):

SOD-1 is the main superoxide dismutase that displays approximately 90% of the cellular SOD activity (Busuttill et al., 2005 & Noor et al., 2002). It was originally localized to the cytosol, nucleus and lysosomes of cells. However, recent evidence suggests that a substantial amount of Cu/Zn SOD is located in the intermembrane space of mitochondria (Xiong et al., 2005 & Higgins et al., 2002). The gene encoding SOD-1 is located in chromosome 21 (locus 21q22.1) in humans (Shin et al., 2006 & Kinnula and Crapo, 2003). The activity of SOD-1 is inhibited by cyanides (Takahashi et al., 2000). It exists as a homodimer linked by a disulphide bond with an individual subunit molecular weight of 16,000 Da. Each monomer contains one Cu^{2+} which is essential for enzymatic activity and one Zn^{2+} which is essential for protein stability (Carroll et al, 2006, Johnson and Giulivi, 2005 & Miller, 2004). Cu/Zn SOD is expressed in all brain areas (Halliwell, 2001). Altered expression and/or mutation of SOD-1 expression or SOD-1 activity are related to several degenerative neurological disorders and CNS diseases such as familial and sporadic amyotrophic lateral sclerosis (ALS), Parkinson's disease (PD), Alzheimer's disease (AD), Down's syndrome, Wilson disease, prion disease and Dengue fever

(Kitzberger *et al.*, 2005 & Noor *et al.*, 2002). The activity and the expression of SOD-1 are altered in response to many stressful conditions like heat stress in different tissues and cell types. Heat stress decreases SOD-1 activity in brain tissue (Lushchak and Bagnyukova, 2006, Niu *et al.*, 2003 & Yang *et al.*, 2002), and liver tissue (Morrison *et al.*, 2005 & Zhang *et al.*, 2003). SOD-1 mRNA and/or protein levels show different responses as a result of heat stress; heat induces stimulation in SOD-1 mRNA and/or protein level in HL60 human leukemia cells (Blacer-Kubiczek *et al.*, 2000), human HepG2 hepatoma cells (Yoo *et al.*, 1999) and cortical neurons (Meloni *et al.*, 2005), while it downregulates mRNA level in rat liver cells (Zhang *et al.*, 2002).

Superoxide dismutase mimetics:

Several classes of synthetic SOD mimetics have recently been developed and are reported to possess significant antioxidant capacity. These small molecular weight compounds distribute easily to tissues, potentially reaching high concentrations in intracellular domains and avoiding the limited stability and permeability along with problems of antigenicity that is a concern with native antioxidants enzyme therapy. SOD mimetics were successfully used to ameliorate oxidative stress-induced cellular damage and apoptosis in different cell types and tissues associated with different pathologic conditions such as type I diabetes (Olcott *et al.*, 2004), type II diabetes (Kowluru and Abbas, 2003), chronic obstructive pulmonary disease (Rahman and Kilty, 2006), viral infection (Malassgne *et al.*, 2001), ischemia-reperfusion (Li *et al.*, 2005), UV-irradiation (Decraene *et al.*, 2004), saturosporine-induced neurotoxicity (Pong *et al.*, 2001), heat stress (Zhang *et al.*, 2006, Zhang *et al.*, 2004 & Gill *et al.*, 2003), heavy metal-induced

toxicity (*Yang et al., 2005*), and models of neurodegenerative disorders including amyotrophic lateral sclerosis (ALS) (*Jung et al., 2001*); Parkinson's disease (PD) (*Peng et al., 2005*); Alzheimer's disease (AD) (*Anderson et al., 2001*). The three classes of metal-containing SOD mimetics include the manganese-macrocyclic ligand complexes, manganese porphyrin complexes, and salen-manganese compounds (*Kinnula and Crapo, 2003; Doctorow et al., 2002 & Fridovich, 1995*).

The macrocyclic class of SOD mimetics binds Mn in a five-ring structure so that the metal is available for single electron transfers. An important property of these SOD mimetics is that they catalytically remove superoxide anion at a high rate without interacting with other ROS. A prototypic macrocyclic SOD mimetic, M40403 (see chemical structure in **Figure 3**), has been suggested to have marked protective effects in inflammatory states of several organs and septic shock by suppressing superoxide generation. Also, it is protective in ischemia-reperfusion injury and improves endothelial function in cardiovascular disorders associated with elevated vascular oxidative stress (*Jiang et al., 2003; Kinnula and Crapo, 2003 & Salvemini et al., 2001*).

The manganese porphyrin class of antioxidant SOD mimetics exhibit strong antioxidant properties, including scavenging of superoxide, H₂O₂, peroxynitrite, and lipid peroxy. They exhibit definite, but low, catalase-like activity that has been attributed to their extensive conjugated ring system and reversible one-electron oxidations. Their capacity to scavenge peroxynitrite apparently involves the formation of an oxo-Mn (IV) complex that can be reduced to the Mn(III) by endogenous antioxidants. The metalloporphyrin antioxidant compound contains a wide variety of compounds like Mn(III) meso-tet-rakis (4-benzoic acid) porphyrin (Mn-TBAP) and MnTE-2-PyP

(chemical structure in **Figure 4**). Manganic porphyrins have been shown to protect against lung injury in animal models of enhanced oxidative stress, to protect against liver failure, zymosan-induced shock, cardiomyopathy, excitotoxic injuries and neurological manifestations (*Patel, 2003; Kinnula and Crapo, 2003; Ross et al., 2002 & Szabo et al., 1996*).

The salen-manganese class of SOD mimetics shares a five-ring structure containing Mn^{3+} (salen= N, N'-bis-(salicylideneamino) ethane). The prototype of these compounds is EUK-8, which expresses both SOD and catalase- like activities (*Baudry et al., 1993*). Newer versions include EUK-134 and EUK-189 with the newer salen compounds reported to exhibit higher catalase activity (chemical structure in **Figure 5**). These enzymatic activities give these compounds the ability to inactivate superoxide radical and its dismutation product, H_2O_2 , thereby preventing hydroxyl radical formation. They also catalyze the breakdown of numerous NO products to more benign species, limiting the formation of the nitrogen oxides, peroxyxynitrite, nitrogen dioxide and nitrite (*Doctrow et al., 2002 & Sharpe et al., 2002*). These compounds have been shown to be neuroprotective in several neurological disorders resulting from oxidative stress, including those for inflammatory immune disease, ischemia, epilepsy, stroke, Alzheimer disease, Parkinson's disease, multiple sclerosis and ALS (*Peng et al., 2005 & Decraene et al., 2004*). EUKs also significantly increase the mean and maximum lifespan in *C. elegans*; have been shown to ameliorate acute heat-induced oxidative damage in the liver; and they prolong the survival of MnSOD knockout mice (*Zhang et al., 2006 & Zhang et al., 2004*). The salen antioxidant compounds also have protective effects against oxidative stress-related injuries in lung, kidney, skeletal muscles, pancreas and heart

(*McDonald et al., 2003 & Bianca et al., 2002*). They also inhibit spontaneous type I diabetes and aid in prolonging survival of islets allograft in mice (*Olcott et al., 2004*). The EUK compounds have been shown to be protective antidote to cadmium toxicity (*Yang et al., 2005*).

Statement of research objective:

From the above literature review, we summarize that heat stress alters the gene expression pattern in mammalian cells. In brain cells, little is known about the change in gene expression in response to heat stress. The mechanism of brain tissue injuries after heat stress is not known in all its details. In this study we will utilize mRNA differential display PCR to identify novel genes in pig hippocampus that are involved in the molecular response of the brain to heat stress. In this study we will also focus on the effect of heat stress on Superoxide dismutase-1 in hippocampal neuronal cells and investigate the relationship between this enzyme and the heat-induced neuronal cell death.

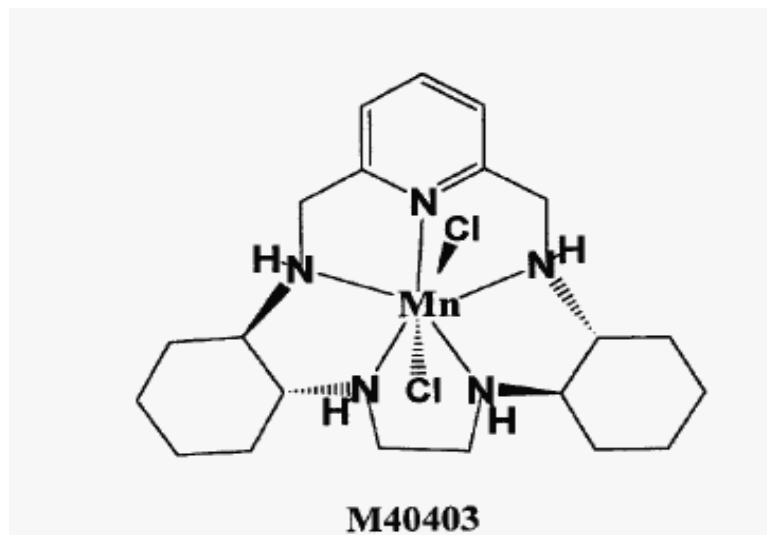
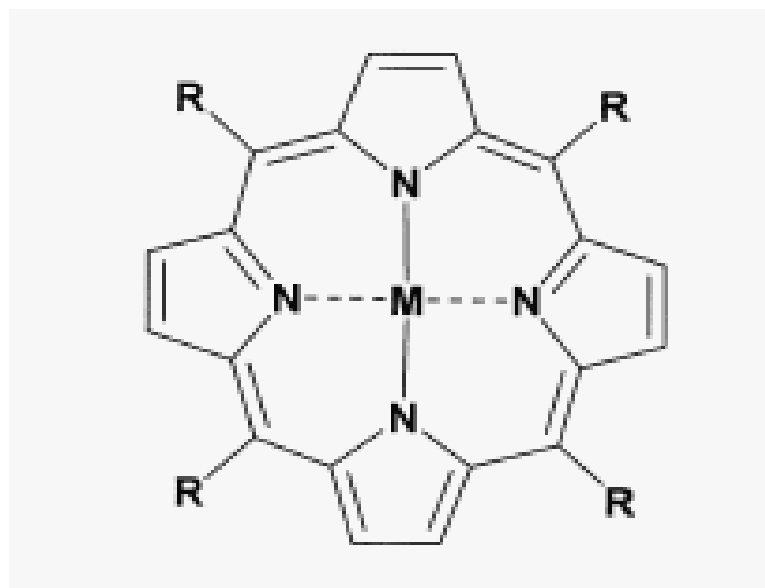
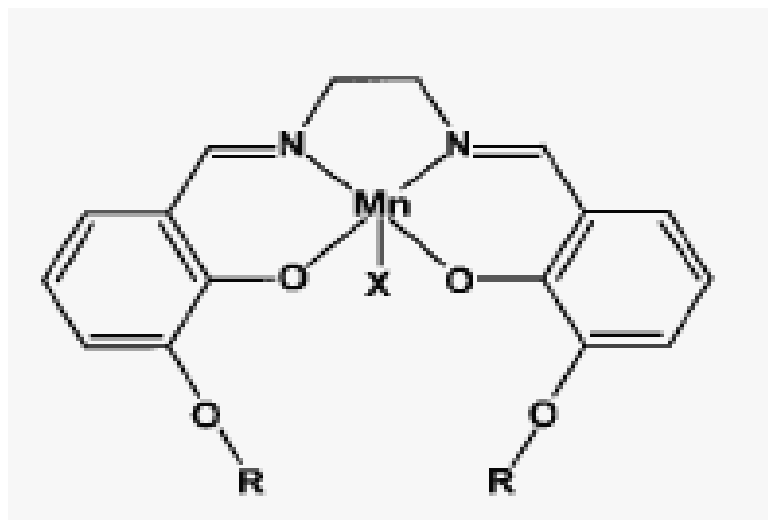


Figure 3: Chemical structure of M40403 SOD mimetic. Modified from: *Salvemini D, 2001. British Journal of Pharmacology; 132: 815-827.*



<u>R</u>	<u>M</u>	<u>Name</u>
	Mn ³⁺	MnTE-2-PyP
	Mn ³⁺	Mn-TBAP

Figure 4: Chemical structural characteristics of metalloporphyrin compounds. Modified from: *Ross A et al, 2002. Free Radical Biology & Medicine; 12: 1657–1669,*



Compound	R	X
EUK-8	H	Cl
EUK-134	OMe	Cl
EUK-189	OEt	OAc

Figure 5: Structures of salen-manganese complexes. Substituents are as indicated in the table. OMe, methoxy (CH₃O); OEt, ethoxy (CH₃CH₂O); OAc, acetoxy (CH₃COO). Modified from: Doctrow S, 2002. *J. Med. Chem.*; 45:4549-4558.

MATERIALS

Animals: Pigs were obtained and maintained in USDA-ARS Livestock Behavior Research Unit, Purdue University (West Lafayette, IN).

Cells: Immortalized mouse hippocampal neuronal cell line (HT-22) was a kind gift from Dr. David Schubert, The Salk Institute for Biological Studies, La Jolla, CA.

Cell culturing reagents: Dulbecco's minimal essential medium (DMEM), fetal calf serum, antibiotic/antimycotic reagent, phosphate-buffered saline, and Hank's balanced salt solution (HBSS) were purchased from Invitrogen Corp. (Carlsbad, CA). T-25 and T75 tissue culture flasks, 10 cm and 2 cm tissue culture dishes, culture slides, 12-well plates and 96-well plates were purchased from B.D. Falcon Co. (Franklin Lakes, NJ). Tubes (15 and 50 ml conical tubes) were purchased from Corning Inc. (Corning, NY).

Nucleic acids reagents: Trizol reagent, blue juice gel loading buffer, One Shot TA cloning kit, and LB agar medium were purchased from Invitrogen Corp. (Carlsbad, CA). RNeasy mini kit, RNeasy midi kit and DNeasy tissue kit were purchased from Qiagen Inc. (Valencia, CA). Message-clean kit and RNA image kit were purchased from GenHunter Corp. (Nashville, TN). Taq polymerase and 10 X Taq polymerase buffer were purchased from Eppendorf Inc. (Westbury, NY). The iQ SYBER supermix for real-time PCR detection, iScript cDNA synthesis kit, 96-well PCR plates and optical tapes were purchased from Bio-Rad Laboratories (Hercules, CA). Polyacrylamide gel,

agarose gel, RNALater tissue collection solution, NothernMax denaturing gel buffer, NothernMax MOPS gel running buffer, formaldehyde sample loading dye, RNase-free water and nuclease-free water were purchased from Ambion Inc. (Austin, TX). Radiolabelled γ -[³²P] dATP was purchased from ICN Biomedical Inc. (Irvine, CA). Minipreps DNA plasmid purification system, EcoRI and restriction enzyme buffer were purchased from Promega Corp. (Madison, WI). All purpose Hi Lo DNA molecular weight ladder was purchased from Bionexus Inc. (Oakland, CA). Tris-Acetate-EDTA (TAE) buffer, Tris-EDTA (TE) buffer, Tris-Borate-EDTA (TBE) buffer, razor blades and chloroform were purchased from Fisher Scientific (Pittsburgh, PA). Biomax X-ray film was purchased from Kodak Corp. (Rochester, NY). 3M HPLC papers were purchased from Whatman Inc. (Clifton, NJ). Thin-walled PCR tubes, 1.5 ml and 2ml centrifuge tubes were purchased from LabScientific Inc. (Livingston, NJ). The YT medium and 10 cm Petri dishes were purchased from Becton Dickson Co. (Franklin Lakes, NJ).

Western blotting reagents: DC protein assay kit, Laemmli sample buffer, Tris-Glycine-SDS buffer, β -mercaptoethanol, prestained SDS-PAGE standard broad range molecular weight marker and 12% SDS-PAGE ready gels were purchased from Bio-Rad Laboratories (Hercules, CA). ECL plus Western blotting detection kit and nitrocellulose membranes were purchased from Amersham Biosciences (United Kingdom). Rabbit anti-mouse anti SOD-1 polyclonal antibody, goat anti-rabbit IgG HRP-coupled antibody, mouse anti-cytochrome c monoclonal antibody, rabbit anti β -tubulin polyclonal antibody, goat anti-rabbit IgG HRP-coupled antibody and goat anti-mouse IgG HRP- coupled antibody were purchased from Stressgen Bioreagents (Victoria Canada).

Both purified Superoxide dismutase-1 and purified cytochrome c were purchased from Sigma-Aldrich Corp. (St. Louis, MO).

EUK-134 [manganese 3-methoxy *N, N'*-bis (salicylidene) ethylenediamine chloride], and superoxide dismutase activity kit were purchased from Cayman chemicals (Ann Arbor, MI).

The CyQUANT Cell Proliferation Assay Kit and Image-iT live green ROS detection kit were purchased from Molecular Probes Inc. (Eugene, OR).

Unless otherwise stated, all chemicals used in this work were obtained from the Sigma-Aldrich Corp. (St. Louis, MO).

METHODS

1- Experimental protocol 1: Effect of heat stress on novel gene expression in pig hippocampus

1.1- Animals :

All work with animals was performed at USDA-ARS Livestock Behavior Research Unit, Purdue University (West Lafayette, IN) under the direction of Dr. Donald Lay.

1.2- Induction of heat stress:

Twenty four pigs (100 lbs each) were acclimated for 48 hours and then moved to pens and maintained at either 70 °F (Control groups) or 90 °F (heat-stressed groups) for 4, 8, 12 or 24 hours. The pigs were monitored for heart rate, respiration, and core body temperature. At the end of each time point, 3 pigs in each group were euthanized using pentobarbital sodium (50 mg/Kg) and the hippocampuses were excised and rapidly stored in RNALater and kept at -20°C until further processing. The experiment was repeated twice.

1.3-RNA isolation from pig hippocampus:

1.3.1- Tissue homogenization: Each frozen hippocampus sample was weighed and minced. Trizol reagent was added to each minced hippocampus in 15 ml centrifuge tubes in ratio of 1ml Trizol per 100 mg of tissue. Tissues were homogenized in Trizol reagent using a Tissuemiser tissue homogenizer (Fisher Scientific, Pittsburgh, PA), for 45 seconds at medium speed on ice until the sample was uniformly homogenized.

1.3.2- Phase separation: The homogenized samples were incubated for 5 min at room temperature, and then chloroform was added to each sample in a ratio of 0.2 ml per 1 ml Trizol reagent. Each tube was capped securely and shaken vigorously by hand for 15 seconds and incubated for 5 minutes at room temperature. Samples were centrifuged at 12,000 x g for 15 minutes at 4°C. Following centrifugation, the mixture was separated into three distinct layers; a lower red organic phase, an interphase and a colorless upper aqueous phase that contains the extracted RNA. The aqueous phases were transferred into fresh 15 ml tubes.

1.3.3- Isolation of total RNA using RNeasy midi kit: Total RNA was extracted from the above solution using the RNeasy midi kit (Qiagen). In brief, an equal volume of 70% ethanol was added to each sample and shaken vigorously for 10 seconds. Samples were transferred to RNeasy midi columns placed in 15 ml tubes. Samples were centrifuged at 5,000 x g for 5 minutes at room temperature and the flow-through was discarded. RNA samples on the column silica membranes were washed with 4 ml RNeasy RW1 buffer and then 2X with 2.5 ml RNeasy RPE buffer. Buffer solutions were removed by centrifugation for 5 minutes at 5,000 x g and the flow-through was discarded. The RNeasy columns were then transferred to new 15 ml tubes. Total RNA was eluted from each sample by pipetting 150 µl RNase-free water directly to the silica-gel membrane and incubated for 1 minute at room temperature followed by centrifugation at 5,000 x g for 3 minutes. RNA samples were stored at -80°C until further processing.

1.3.4- RNA qualitative assessment: The purity of the isolated RNA samples was determined by denaturing-formaldehyde agarose gel electrophoresis (*Mattheus et al., 2003*). 1.2 % agarose gel was prepared in NothernMax denaturing gel buffer

(1X MOPS buffer; 50% formamide; 6% formaldehyde). 5 μ l from each RNA sample were mixed with 15 μ l formaldehyde sample loading dye (1X denaturing gel running buffer; 50% glycerol; 1 mM EDTA, pH 8.0; 0.25% bromophenol blue; 0.25% xylene cyanol) and incubated at 65°C for 15 minutes. Samples were then collected by centrifugation and kept on ice for 5 minutes. 20 μ l of sample/dye mixture were loaded into each well of the gel. Suitable quantity of 1X NothernMax MOPS gel running buffer (0.02 M morpholinopropanesulfonic acid, pH 7.0; 8 mM sodium acetate; 1 mM EDTA) was added over the gel and electrophoresed at 60 volts for 2 hour. The gel was then stained with ethidium bromide solution in RNase-free water (0.5 μ g/ml) for 30 minutes. Ethidium bromide solution was removed and the gel was de-stained in RNase-free water for 10 minutes. The gel was photographed under UV illumination on a Flour-S imager (Bio-Rad). The integrity of each RNA sample was determine using the 28S and 18S ribosomal RNA bands which should be distinct from the background and the 28S band twice as bright as the 18S band.

1.3.5- RNA quantitative analysis: The concentrations of the isolated RNA samples were determined spectrophotometrically. Two dilutions of RNA samples (1:50, 1:100) were prepared in 1X TE buffer (10 mM Tris-HCl, pH 7.5; 1 mM EDTA). The optical density of RNA solutions at both 260 nm and 280 nm were assessed by UV spectroscopy using SmartSpec plus spectrophotometer (Bio-Rad). An absorbance at 260 (A_{260}) of 1 is equivalent to 40 μ g/ml RNA. The concentration of RNA in μ g/ml is therefore calculated by multiplying the A_{260} x dilution factor x 40. The ratio of A_{260} to A_{280} values is another measure of RNA purity, and should fall in the range of 1.7 to 2.1. All RNA samples were stored at -80 °C until further analysis.

1.4- Analysis of gene expression:

Messenger RNA differential display PCR (DD-PCR) was performed using the RNImage kit as described by *Liang et al., 1994*.

1.4.1- Reverse transcription and cDNA synthesis: Total RNA was reverse transcribed using three different one-base anchored primers (H-T₁₁M, where M=G, C or A) and reverse transcriptase (RT) to produce cDNA. The reverse transcription reaction mixture contained 9.4 µl RNase-free H₂O, 4.0 µl 5X reverse transcriptase buffer, 1.6 µl 250 µM dNTPs, 2 µl 2 µM H-T₁₁M anchored primer, 2.0 µl total RNA (0.1 µg/µl) and 1 µl MMLV reverse transcriptase (final volume is 20 µl). The reaction conditions were 65°C for 5 min, 37°C for 10 min, and then the thermocycler was paused to add 1 µl MMLV reverse transcriptase to each reaction mixture. Incubation was continued at 37°C for 50 min, 75°C for 5 min and final hold at 4°C.

1.4.2- Amplification of resulting cDNAs by polymerase chain reaction: The resulting cDNAs were amplified by polymerase chain reaction (PCR) using a combination of one of three 3' oligo dT anchored primers (H-T₁₁M) and one of 80 arbitrary 5' primers (HAPx, x= 1-80). A total of 240 primer pairs were used in this experiment. The DD-PCR was carried out in a total volume 20 µl containing: 11.1 µl nuclease-free water, 2 µl 10X Taq buffer, 1.6 µl 25 µM dNTPs, 2 µl HAPx, 2 µl H-T₁₁M, 1 µl cDNA, 0.1 µl γ-[³²P] dATP and 0.2 µl Taq polymerase. The thermal cycling conditions were adjusted for 40 repeats of a three-step cycle; 30 sec at 94°C, 2 min at 50°C and 30 sec at 72°C followed by one-step cycle at 72°C for 5 min and final hold at 4°C.

1.4.3- Resolution of amplified cDNAs by gel electrophoresis: The amplified cDNAs were separated on a 6% denaturing polyacrylamide gel prepared in 1X TBE buffer (89 mM Tris, pH 8.3; 89 mM Boric acid; 2 mM EDTA) and electrophoresed at 1600 volt for 3.5 hours. The polyacrylamide DNA sequencing gel was blotted onto a sheet of 3M HPLC paper and dried under vacuum at 80°C for 1 h on a gel dryer (Bio-Rad). The blotted gel was exposed to BioMax X-ray Kodak film for 24 - 48 hours at -80°C. The film was developed and analyzed visually for differentially expressed bands between the control and heat stressed groups. The differentially expressed bands were cut from the gel according to the pattern on the film. The autoradiogram was oriented with the gel and the band of interest was located by punching through the film with a clean needle at the four corners of the band. Each located band was cut out with a clean razor blade.

1.4.4- Extraction of cDNAs from the gel: PCR products were extracted from the dried gel and blotting paper by soaking in 100 µl nuclease-free water for 10 minutes. The samples were then incubated for 1 hour in a 37°C water bath and centrifuged for 2 minutes at 12,000 x g. The supernatant was removed and placed in fresh tube and the DNA was precipitated by adding 10 µl 3 M sodium acetate, 5 µl glycogen and 450 µl 100% ethanol and stored at -80°C overnight. Precipitated DNA was collected by centrifugation at 14,000 x g for 2 minutes at 4°C. The supernatant was removed and the DNA pellet was rinsed with 85% ethanol, centrifuged at 14,000 x g for 2 minute and the ethanol was aspirated. Residual ethanol was air-dried. The DNA pellet was dissolved in 10 µl nuclease-free water.

1.4.5- Reamplification of the isolated cDNAs probes: Isolated cDNAs were reamplified by PCR using the original primer pair from the DD-PCR. The reamplification PCR was carried out in a total volume of 40 μ l containing: 20.4 μ l nuclease-free water, 4 μ l 10X Taq buffer, 3.2 μ l 250 μ M dNTPs, 4 μ l HAPx, 4 μ l H-T₁₁M, 4 μ l cDNA and 0.4 μ l Taq polymerase. The thermal cycling conditions were adjusted for 40 repeats of a three-step cycle; 30 sec at 94°C, 2 min at 40°C and 30 sec at 72°C followed by a one-step cycle at 72°C for 5 min and final hold at 4°C. The reamplified cDNAs were resolved on 1.2% agarose gel to detect their purity and size. The agarose gel was prepared in 1X TAE buffer (40 mM Tris, pH 8.5; 20 mM acetic acid; 1 mM EDTA). 10 μ l from each DNA sample was mixed with 1 μ l 10X blue juice gels loading buffer (10 mM Tris-HCl (pH 7.5); 10 mM EDTA; 65% (w/v) sucrose; 0.3% (w/v) bromophenol blue) and loaded to the gel wells. Suitable quantity of 1X TAE buffer was added over the gel and electrophoresed at 100 volts for 1 hour. The gel was then stained with ethidium bromide solution in nuclease-free water (0.5 μ g/ml) for 10 minutes. Ethidium bromide solution was removed and the gel was de-stained in nuclease-free water for 10 minutes then the gel was photographed under UV illumination on a Flour-S imager.

1.5- TA-cloning:

The reamplified DNA fragments were cloned directly into linearized plasmid vector and transformed to *E. Coli* cells using One Shot TA cloning Kit (Invitrogen).

1.5.1-Ligation of reamplified DNA to linearized plasmid: Freshly reamplified DNA fragments were ligated to linearized plasmid vector PCRII at 14°C overnight in 10 μ l reaction containing 1 μ l T4 DNA ligase (4 units/ μ l), 2 μ l PCRII linearized plasmid vector

(25 ng/ μ l), 1 μ l 10X ligation buffer (60 mM Tris HCl, pH 7.5; 60 mM MgCl₂; 50 mM NaCl; 70 mM β -mercaptoethanol; 1 mM ATP; 20 mM dithiothreitol; 10 mM spermidine and 1 mg/ ml BSA), 2 μ l freshly reamplified DNA and 4 μ l nuclease-free water.

1.5.2-Transformation of ligated DNA to INV α F' *E. Coli* competent cells: Two microliters of ligation mix was mixed with 50 μ l INV α F' *E. Coli* competent cells and incubated for 30 minutes on ice. The bacterial-plasmid mixture was heat shocked by placing the mixture in a 42°C water bath for 30 seconds without shaking and then removed and incubated on ice for 10 minutes. The transformed bacterial mixture was pooled in a tube containing 250 μ l of SOC media (2% tryptone; 0.5% yeast extract; 10 mM NaCl; 2.5 mM KCl; 10 mM MgSO₄ ; 10 mM Mg₂Cl and 20 mM glucose) and incubated for 1 hour at 37°C on an orbital shaker at 225 rpm.

1.5.3-Plating of recombinant *E. Coli* cells: The recombinant *E. Coli* cells in SOC medium were plated on LB agar plates containing 100 μ g/ml ampicillin, 1.6 mg X-Gal and incubated at 37°C for 12-18 hours for blue/white screening. Five white colonies were picked and each colony was transferred to sterile tubes containing 5 ml YT broth containing 100 μ g/ml ampicillin. The tubes were incubated at 37°C for 12-18 hours with shaking at 225 rpm.

1.5.4-Plasmid isolation: Plasmids containing the DNA fragments were isolated from bacterial cells using the Wizard Plus Minipreps plasmid DNA purification system (Promega). Three ml from bacterial suspension was transferred to new centrifuge tubes and the remaining bacterial suspension in YT broth was stored at -80°C. The bacterial suspensions were centrifuged at 10,000 x g for 5 minutes at room temperature to collect

the cells and the supernatant was discarded. Bacterial cells pellets were resuspended in 250 μ l resuspension solution by soft pipetting and the bacterial cell suspensions were mixed well with 250 μ l cell lysis solution and 10 μ l alkaline protease solution. After incubation for 5 minutes at room temperature, the solutions were mixed with 350 μ l Wizard plus SV neutralizing solution and centrifuged at 14,000 x g for 10 minutes. The clear cell lysates were transferred to spin columns placed into 2 ml collection tubes and centrifuged at 14,000 x g for 1 minute and the flow-through was discarded. The column membranes were washed 2X with 750 μ l column wash solution and centrifuged at 14,000 x g for 2 minutes. The columns were transferred to new sterile 1.5 ml microcentrifuge tubes and the plasmid DNA was eluted from each sample by pipetting 100 μ l nuclease-free water to the column and allowing the columns to stand for 1 minute at room temperature and centrifugation at 14,000 x g for 1 minutes. Plasmid DNA samples were quantified to determine their concentrations by UV spectrophotometric analysis. The plasmid DNA samples were diluted 1:50 in nuclease-free water, and the absorbance at 260 nm was measured using a SmartSpec plus spectrophotometer (Bio-Rad). An absorbance at 260 (A_{260}) of 1 is equivalent to 50 μ g/ml DNA. The concentration of plasmid DNA in μ g/ ml is therefore calculated by multiplying the A_{260} x dilution factor x 50. Plasmid DNA samples were stored at -20°C.

1.5.5-Determination of the presence of insert: The presence of our PCR inserts was confirmed by EcoRI restriction digestion analysis. The linearized plasmid vector has two EcoRI restriction enzyme recognition sites on its sequence. DNA sequences were inserted between these two EcoRI recognition sites. The EcoRI restriction digestion was used to digest the ligated DNA insert. In brief, the restriction digestion reaction was carried out in

a total volume of 20 μl containing 10 μl EcoRI (10 U/ μl), 2 μl restriction enzyme buffer H, 0.2 μl acetylated bovine serum albumin (10 $\mu\text{g}/\mu\text{l}$), 1 μl plasmid DNA solution (adjusted at 1 $\mu\text{g}/\mu\text{l}$), and 16.3 μl nuclease-free water. The restriction reaction digestion mix was incubated in a 37°C water bath for 4 hours. The restriction digestion products were resolved on 1.2% agarose gel stained with ethidium bromide and photographed under UV illumination on a Fluor-S imager. The gels were analyzed visually for the correct size product based on our reamplification of isolated cDNA probes (section 1.4.5).

Plasmid concentrations were adjusted to 200 ng/ μl in nuclease-free water and sequenced at The Auburn University Genomic and Sequencing Laboratory using the T7 promoter and M13 reverse priming sites. An example of insert sequences is shown in **Figure 6**.

The sequences received from The Auburn University Genomic and Sequencing Laboratory including our insert surrounded by the cloning vector sequences were analyzed using Vector NTI 10.1.1 software (Invitrogen Corp.). A BLAST search was performed on the sequence between the two EcoRI sites to compare the resulting DNA sequences to any known sequences in GenBank (the NIH genetic sequence database). The database for NCBI GenBank is available on line at www.ncbi.nih.gov/Genbank. The expectation value is a parameter of BLAST search that defined as the number of times this match would be expected to occur by chance in a search of the entire database. An expect value of 10.0 is the default value of statistical significance (*Karlin and Altschul, 1990*). The lower the expectation value the greater the similarity between the input sequence and the match.

		AvaI ~~~~~		PstI ~~~~~	
1	CNGGGCTCTG	ATGCATGCTC	GAGCGGCCGC	CAGTGTGATG	GATATCTGCA
	GNCCCAGAC	TACGTACGAG	CTCGCCGGCG	GTCACACTAC	CTATAGACGT
	PstI				
	~				
	EcoRI				
	~~~~~				
51	<u>GAATTC</u> GGTN	TTNNNNTTTT	TTTNGGNAAA	AGCTGTAATT	TGGCTTAATT
	<u>CTTAAG</u> CCAN	AAANNNAAAA	AAANCCNTTT	TCGACATTAA	ACCGAATTAA
101	CACTGTTTCC	TGCCCATGAT	AGNCTGTAAG	AAGCAGCTCA	TGATTTAGGG
	GTGACAAAGG	ACGGGTACTA	TCNGACATTG	TTCGTCGAGT	ACTAAATCCC
151	GCTAGCAGTG	TACAGGAAAA	CTGGAAACAG	AATTTTGACA	AATGTAAATG
	CGATCGTCAC	ATGTCCTTTT	GACCTTTGTC	TTAAAAGTGT	TTACATTTAC
201	TTTGCAGGGA	GATGAAGCTA	ATATTTTCTC	AATCCGCATG	TCCCAGTAAT
	AAACGTCCCT	CTACTTCGAT	TATAAAAAGAG	TTAGGCGTAC	AGGGTCATTA
				HindIII	
				~	
251	CAAAAAGAAG	TGGACCCTTT	AGTTCTTATT	ATGAATATGT	GGCCAGAGAA
	GTTTTTCTTC	ACCTGGGAAA	TCAAGAATAA	TACTTATACA	CCGGTCTCTT
	HindIII	<b>EcoRI</b>			BamHI
	~~~~~	~~~~~			~~~~~
301	<u>AGCTTAAGCC</u>	<u>GAATTC</u> CAGC	ACACTGGCCG	CCGTACTAG	TGGATCCGAG
	<u>TCGAATTCGG</u>	<u>CTTAAG</u> GTGC	TGTGACCGCC	GGCAATGATC	ACCTAGGCTC
		HindIII			
	~~~~~	~~~~~			
351	CTCGGTACCA	AGCTTGATGC	ATAGCTGAG	TATTCTATAG	TGTCACCTAA
	GAGCCATGGT	TCGAACTACG	TATCGAACTC	ATAAGATATC	ACAGTGGATT
401	ATAGCTTGGC	GTAATCATGG	TCATAGCTGT	TTCTGTGTG	AAATTGTTAT
	TATCGAACCG	CATTAGTACC	AGTATCGACA	AAGGACACAC	TTTAAACAATA
451	CCGCTCACAA	TTCCACACAA	CATACGAGCC	GGAAGCATAA	AGTGTAAGC
	GCGAGTGTT	AAGGTGTGTT	GTATGCTCGG	CCTTCGTATT	TCACATTTCC
501	CTGGGGTGCC	TAATGAGTGA	GCTAACTCAC	ATTAATTGCG	TTGCGCTCAC
	GACCCACGG	ATTACTCACT	CGATTGAGTG	TAATTAACGC	AACGCGAGTG
551	TGCCCGCTTT	CCAGTCGGGA	AACCTGTCGT	GCCAGCTGCA	TTAATGAATC
	ACGGGCGAAA	GGTCAGCCCT	TTGGACAGCA	CGGTCGACGT	AATTACTTAG
601	GGCCAACGCG	CGGGGAGAGG	CGGTTTGCCT	ATTGGGCGCT	CTTCCGCTTC
	CCGGTTGCGC	GCCCCCTCTC	GCCAAACGCA	TAACCCGCGA	GAAGGCGAAG
651	CTCGCTCACT	GACTCGCTGC	GCTCGGTCGT	TCGGCTGCGG	CGAGCGGTAT
	GAGCGAGTGA	CTGAGCGACG	CGAGCCAGCA	AGCCGACGCC	GCTCGCCATA
701	CAGCTCACTC	AAAGGCGGTA	ATACGGTTAT	CCACAGAATC	AGGGGATAAC
	GTGAGTGAG	TTTCCGCCAT	TATGCCAATA	GGTGTCTTAG	TCCCCTATTG
751	GCAGGAAAGA	ACATGTGAGC	AAAANG		
	CGTCCTTTCT	TGTACACTCG	TTTTNC		

**Figure 6: Insert sequence.** The sequence of insert DNA fragment NAVHI-22T7-D09 as it came back from sequencing laboratory. The underlined sequences represent two EcoRI restriction enzyme recognition sites that the DNA fragment was inserted between. The highlighted sequence is our insert that we look for its similarity with any known sequence in NCBI GenBank.

Once the similar sequences were decided then these resulting sequences were further determined in the fragments corresponding to sequences in the 3' open reading frame of genes. The open reading frame (ORF) is the gene region that encodes proteins, is first transcribed into messenger RNA, and then translated into protein. An open reading frame starts with an atg (Met) in most species and ends with a stop codon (taa, tag or tga). During our DD-PCR amplification, we elected to amplify the 3' end of all messenger RNA population by using the 3' oligo dT anchored primers (H-T₁₁M). Theoretically, all amplified DNA fragments should lie in the 3' open reading frame area of the gene sequences. Those DNA fragments corresponding to sequences in the 3' open reading frame of genes were then further investigated for differential expression by real-time PCR analysis.

### **1.6- Real Time RT-PCR Analysis:**

The levels of expression of selected genes were quantified using real-time RT-PCR analysis.

1.6.1-Isolation of total RNA and cDNA synthesis: Total RNA that was extracted from homogenized pig hippocampi in the first experiment was used in this experiment. Total RNA was reverse transcribed to synthesize first strand cDNA using the iScript cDNA synthesis kit (Bio-Rad). Briefly, the reverse transcription reaction was carried out in a total volume of 20 µl that contained 4 µl 5 x iScript reaction mixture buffer, 1 µl iScript reverse transcriptase, 1 µg total RNA template and nuclease-free water up to 20 µl. The reaction was carried out in the thermocycler which was adjusted to 25°C for 5 minutes followed by 42°C for 30 minutes then 85°C for 5 minutes and a final hold at 4°C.



1.6.2-Synthesis of real-time PCR primers: All oligonucleotide primers, specific for genes of interest, and used in real-time PCR analysis were designed using Vector NTI 10.1.1 software (Invitrogen). The successful real-time PCR reaction requires efficient amplification of the product and is dependent on the primer design. Primers for real-time PCR analysis should be 18-24 bp in length, have a GC content of 50-60%, and not have repeats of C's or G's longer than 3 bases. The primers should also display high melting temperature (between 50°C and 65°C) and produce an amplicon with length of 75-150 bp. The amplified template should have no secondary structures which can hinder the primer from annealing and prevent complete product extension by the polymerase. If there is a possibility of secondary structure formation, the annealing temperature used in real-time PCR amplification should be above the melting temperature for any template secondary structures. Secondary structure formation for any template at different annealing temperatures between 50°C and 65°C was analyzed using the DNA m-fold server (*Zuker, 2003*). 500- 800 bp sections of the targeted genes were analyzed for secondary structure at various temperatures. PCR primers were then designed to target linear DNA regions at the corresponding temperature. The designed primer pairs for each gene were analyzed by a BLAST search on NCBI GenBank database using Vector NTI software to determine the selectivity to the defined gene. Primer sets for the house keeping genes, glyceraldehyde-3-phosphate dehydrogenase (GAPDH) and acidic ribosomal phosphoprotein (Arbp or 36B4) were designed according to the published sequences AF141959 and NM_007475, respectively. The oligonucleotide primers were synthesized by Sigma-Genosys (St. Louis, MO). A confirmatory PCR amplification for each primer pair was performed at the designated annealing temperature to determine the

specificity of the primer set by the presence of a single product. The PCR product was resolved on a 1.2% agarose gel, stained with ethidium bromide and photographed under UV illumination using a Flour-S imager.

1.6.3-Real-time PCR analysis: The real-time PCR analysis of targeted genes in pig hippocampi was carried out in an iCycler My iQ Real-Time PCR Detection System (BioRad) using iQ SYBR Green Supermix (Bio-Rad). The real-time PCR reactions were carried out in a total volume of 25  $\mu$ l containing: 12.5  $\mu$ l iQ SYBR Green Supermix (BioRad), 11  $\mu$ l nuclease-free H₂O, 1  $\mu$ l 5  $\mu$ M primer mix solution (in 1X TE buffer) and 0.5  $\mu$ l cDNA template. The thermal cycling conditions were 95°C for 3 min, 45 repeats of two-step cycle; 10 sec at 95°C and 45 sec at 65°C. Melting curve analysis was carried out to determine the specificity of PCR products by presence of one product of PCR amplification reaction. Two house keeping genes, glyceraldehyde-3-phosphate dehydrogenase (GAPDH) and acidic ribosomal phosphoprotein (Arbp or 36B4) were used as internal controls. A negative control without cDNA was run simultaneously with every assay. Each sample was run in duplicate. A standard curve was performed for each primer set at the same real-time PCR reaction conditions using serial 10 fold dilutions of the hippocampi cDNA to determine the efficiency of amplification.

1.6.4-Gene expression analysis: Changes in gene expression in the hippocampus of heat stressed pigs were calculated relative to the gene expression in the hippocampus of control pigs according to the  $\Delta\Delta$ Ct method described by *Livak and Schmittgen*, (2001). The expression of the two house keeping genes was used as internal control for gene

expression analysis. Gene expression was calculated using an excel gene expression macro (Bio-Rad) that utilizes a modified  $\Delta\Delta C_t$  method described by *Vandesompele et al., 2002*. The modified  $\Delta\Delta C_t$  method allows the analysis of the results using multiple reference genes.

## **2- Experimental protocol 2: Effect of heat stress on SOD-1 gene and protein expression and SOD-1 activity in HT-22 cells.**

### **2.1- Cell culture:**

HT22 cells, a mouse hippocampal neuronal cell line, were a kind gift from Dr. David Schubert (The Salk Institute for Biological Studies, La Jolla, CA). Cells were cultured in either T-75 tissue culture flasks, 10 cm tissue culture dishes, 2 cm tissue culture dishes or 12-well plates according to experimental needs. Cells were grown in DMEM supplemented with 10% fetal calf serum, 100  $\mu\text{g/ml}$  streptomycin and 100 U/ml penicillin G and 0.25  $\mu\text{g/ml}$  amphotericin B at 37 °C in 5% CO₂. The medium was changed every other day and experiments were performed in HT-22 cells at 50-70% confluence (*Cumming and Schubert, 2005*).

To examine the effect of heat stress on HT-22 cells, cells were incubated in a 43°C water bath for 30 minutes and allowed to recover at 37°C in an incubator for different time points (0, 1, 2, 4, 8, 12, 24 and 48 hours).

## **2.2- Isolation of total RNA and cDNA synthesis from HT-22 cells:**

Total RNA was isolated from both control and heat stressed cells using Trizol reagent (Invitrogen) and RNeasy Mini kit (Qiagen).

2.2.1- Cell lysis: Medium was aspirated from 10 cm tissue culture dishes and cells were washed 2X in ice-cold PBS. Cells were disrupted and lysed directly in 1 ml Trizol per each 10 cm dish. Cell lysates were collected in 2 ml microcentrifuge tubes and incubated for 5 min at room temperature, and chloroform was added to each sample in a ratio of 0.2 ml per 1ml Trizol reagent. Each tube was shaken vigorously by hand for 15 seconds and incubated for 5 minutes at room temperature. Samples were centrifuged at 12,000 x g for 15 minutes at 4°C. Following centrifugation, the mixture was separated into three distinct layers; a lower red organic phase, an interphase and a colorless upper aqueous phase that contains the extracted RNA. The aqueous phases were transferred into fresh 2 ml microfuge tubes.

2.2.2- Isolation of total RNA using RNeasy mini kit: Total RNA was extracted from the above solution using the RNeasy mini kit (Qiagen). In brief, an equal volume of 70% ethanol was added to each homogenized lysate and mixed well by pipetting. Samples were transferred to RNeasy mini columns placed in 2ml collection tubes. Samples were centrifuged at 10,000 x g for 15 seconds at room temperature and the flow-through was discarded. RNA samples on the column membranes were washed with 700 µl RNeasy RW1 buffer and centrifuged at 10,000 x g for 15 seconds at room temperature and the flow-through was discarded. Columns were transferred into new 2 ml collection tubes and washed 2X with 500 µl RNeasy RPE buffer. Buffer solutions were removed by centrifugation for 2 minutes at 10,000 x g and the flow-through was discarded.

The RNeasy columns were transferred to new 1.5 ml collection tubes and total RNA was eluted from each sample by pipetting 50 µl RNase-free water directly to the silica-gel membrane, incubated at room temperature for 1 minute and centrifuged at 10,000 x g for 1 minute. RNA samples were stored at -80°C until further processing.

2.2.3- RNA qualitative and quantitative analysis: The purity of the isolated RNA samples was determined by denaturing-formaldehyde agarose gel electrophoresis. RNA was quantified spectrophotometrically. The absorption of RNA solutions at both 260 nm and 280 nm were assessed by UV spectroscopy (see section 1.3.5).

2.2.4- Reverse transcription and cDNA synthesis: Total RNA was reverse transcribed to synthesize cDNA using the iScript cDNA synthesis kit (section 1.6.1).

### **2.3- Measurement of SOD-1 gene expression by real-time RT-PCR:**

The expression of SOD-1 mRNA was determined by real-time RT-PCR using iQ SYBR Green Supermix and iCycler My iQ Real-Time PCR Detection System.

2.3.1- Real-time PCR analysis: The Real-time PCR reactions were carried out in a total volume of 25 µl containing: 12.5 µl iQ SYBR Green Supermix (BioRad), 11 µl nuclease-free H₂O, 1 µl 5 µM primer mix solution (in 1X TE) buffer) and 0.5 µl cDNA template. The thermal cycling conditions were adjusted at 95°C for 3 min, 45 repeats of two-step cycle; 10 sec at 95°C and 45 sec at 65°C. Melting curve analysis was carried out with each PCR amplification. Two house keeping genes, glyceraldehyde-3-phosphate dehydrogenase (GAPDH) and acidic ribosomal phosphoprotein (Arbp or 36B4) were used as internal controls. The following oligonucleotide primers were used: SOD-1 (accession number NM_000454), 5'-ACA GCA GGC TGT ACC AGT GCA GGT CCT

(sense) and 5'-CAT TGC CCA AGT CTC CAA CAT GCC TCT (antisense); GAPDH (accession number AF141959), 5'-TGC ACC ACC AAC TGT TAG C (sense) and 5'-GGC ATG GAC TGT GGT CAT GAG (antisense); 36B4 (accession number NM_007475), 5'-AAG CGC GTC CTG GCA TTG TCT (sense) and 5'-CCG CAG GGG GCA GCA GTG GT (antisense).

2.3.2- Gene expression analysis: The change in gene expression of SOD-1 in heat stressed HT-22 cells was calculated relative to the gene expression in non heated control samples according to the modified  $\Delta\Delta C_t$  method.

#### **2.4-Measurement of SOD-1 protein expression by western blotting:**

2.4.1- Preparation of whole Cell lysate: Medium was aspirated from 10 cm tissue culture dishes and cells were washed twice in ice-cold PBS, scraped with a rubber policeman, collected into ice-cold phosphate-buffered saline, pelleted at 2,000 x g for 5 min at 4°C, and solubilized in 200  $\mu$ l cell lysis buffer containing 50 mM Tris-HCl, pH 7.5, 100 mM NaCl, 2 mM EDTA, 1% Nonidet P-40, 100  $\mu$ M NaVO₄, 10  $\mu$ M NaF and 5  $\mu$ l/ml protease inhibitor cocktail. The lysate was centrifuged at 14,000 x g for 10 minutes at 4°C and the supernatant (cytosolic fraction) was collected (Luo and Defranco, 2006).

2.4.2- Determination of protein concentration: The protein concentration was determined using the DC protein assay kit (Bio-Rad) that utilizes the colorimetric assay procedures described by Peterson, 1979. In brief, BSA standards (0.1-1.5 mg/ml) were prepared from a stock solution (15 mg/ml). Reagent A1 was prepared by mixing 20  $\mu$ l

reagent S with 1ml reagent A. Five  $\mu$ l of each standard and cell lysate sample, 25  $\mu$ l of reagent A1 and 200  $\mu$ l of reagent B were added into each well of a 96-well microtiter plate, mixed thoroughly using a microplate mixer and incubated at room temperature for 15 minutes. The light absorbance of each sample was measured at 750 nm on a SpectraMax Plus microplate reader (Molecular Devices Corp., Palo Alto, CA). Protein concentration of each cell lysate samples were calculated based on the generated standard curve. All samples were normalized per microgram total protein based on the concentration of the lowest sample.

2.4.3- Western blotting: Equivalent amounts of cell lysate protein (15  $\mu$ g) were boiled in equal volumes of Laemmli sample buffer containing 5%  $\beta$ -mercaptoethanol for 5 minutes. Cell lysates were separated on 12% sodium dodecyl sulfate-polyacrylamide gel electrophoresis (SDS-PAGE) and then electrophoretically transferred to nitrocellulose membranes. Membranes were blocked for 1 hour at room temperature with 1X TBS-T (20 mM Tris; pH 7.6; 137 mM NaCl; and 0.1% Tween 20) containing 5% non-fat dry milk. Membranes were then incubated with SOD-1 rabbit anti-mouse polyclonal antibody (1:1000 dilution in blocking buffer) overnight at 4°C. Membranes were washed 3 x 5 minutes with 1X TBS-T at room temperature and then exposed to goat anti-rabbit IgG HRP-coupled antibodies (1:3000 dilution in blocking buffer) for 1 hour at room temperature. Membranes were again washed 5 x 5 minutes with 1X TBS-T and immunoreactive bands were detected by chemiluminescence using ECL plus western blotting detection system. Blots were scanned with a Flour-S multi imaging system (Bio-Rad) to visualize the bands. The densities of the resulting bands

were calculated using Quantity One software (Bio-Rad). Densitometry of western blots was normalized to expression of  $\beta$ -tubulin and protein expression was calculated as a percent from control.

### **2.5- Measurement of SOD-1 enzyme activity:**

A superoxide dismutase assay kit (Cayman Chemicals) was used to measure the SOD-1 activity as described by *Peskin and Winterbourn, 2000*.

2.5.1- Isolation of cytosolic lysate: Cells from two 10 cm dishes were washed and collected in ice-cold PBS by centrifugation at 2000 x g, for 10min at 4°C. Pellets were homogenized in 0.1 ml 20 mM HEPES buffer (pH 7.5) containing 210 mM mannitol, 70 mM sucrose and 1 mM EDTA with a syringe and a narrow-gauge (No. 27) needle. The homogenate was centrifuged at 1,500 x g for 5 minutes at 4 °C. The resulting supernatant was then centrifuged twice at 10,000 x g for 15 minutes at 4°C. The supernatant was collected as the cytosolic fraction and pellets as the mitochondrial fraction. The protein concentrations in the cytosolic fraction were determined using the DC protein assay kit (Bio-Rad) as described in section 2.4.2. The protein concentrations of all samples were adjusted to 2  $\mu$ g/ml using HEPES buffer.

2.5.2- Determination of SOD-1 activity: The superoxide dismutase activity kit utilizes a highly water-soluble, colorless tetrazolium salt, WST-1, which produces a water-soluble red formazan dye upon interaction with a superoxide anion generated by xanthine oxidase and hypoxanthine. The rate of reduction with superoxide anion is linearly related to the xanthine oxidase activity and is inhibited by superoxide dismutase. Inhibition of the red color production is proportional to the activity of the SOD-1 in the sample.



SOD-1 standard curve was performed using serial dilutions of SOD-1 standard stock solution (0.25 U/ml- 0.05 U/ml). Each sample was run in duplicate. To each standard, blank and test wells, 200 µl of the diluted radical detector (a solution of the WST-1 salt in 1X assay buffer (50 mM Tris-HCl, pH 8.0, containing 0.1 mM diethylenetriaminepentaacetic acid (DTPA) and 0.1 mM hypoxanthine) followed by addition of 10 µl per well of each standard solution, dd H₂O or samples respectively. The reaction was initiated by adding 20 µl of a xanthine oxidase solution diluted in 1X sample buffer (50 mM Tris-HCl, pH 8.0) to all the wells. The plate was incubated on a shaker for 20 min at room temperature. The absorbance at 450 nm was measured using a Fusion-alpha universal microplate analyzer (Perkin Elmer Inc., Wellesley, MA).

2.5.3- Calculation of the results: The average absorbance of each standard and test sample was calculated. The absorbance of the blank sample (no SOD activity) was divided by the absorbance of each standard and test sample to determine the linearized rate (LR) of each sample. A standard curve was created by plotting LR of different SOD-1 standard dilutions as a function of final SOD activity (U/ ml). The SOD activity in each test sample was calculated from the equation obtained from the linear regression of the standard curve using the following formula:

$$\text{SOD (U/ ml)} = \left[ \left( \frac{\text{Sample LR} - \text{Y-intercept}}{\text{Slope}} \right) \times \frac{0.23}{0.01} \right] \times \text{Sample dilution}$$

**3- Experimental protocol 3: Effect of heat stress on cell viability, reactive oxygen species (ROS) generation, cytochrome c release, and DNA fragmentation in HT-22 cells.**

**3.1- Cell proliferation assay:**

HT-22 cells were plated in 12-well plates and incubated in a 43°C water bath for 30 minutes and allowed to recover at 37°C in an incubator for different times (0, 1, 2, 4, 8, 12, 24 and 48 hours). Cell number was estimated using the CyQUANT Cell Proliferation Assay Kit (Molecular Probes) that utilizes a green fluorescent dye, CyQUANT GR, which exhibits strong fluorescence enhancement when bound to cellular nucleic acids. The fluorescence emitted by the dye is linearly proportional to the cell number. At designated time points, cells were trypsinized, suspended in culture media and collected by centrifugation for 5 min at 2000 x g. The supernatants were removed and the cell pellets were frozen at -80°C. Frozen cells were thawed and lysed by addition of 200 µl 1X cell lysis buffer containing the CyQUANT GR dye. The entire 200 µl corresponding to each sample was transferred to a 96-well microplate and fluorescence was measured directly at Ex/Em 480/520 nm using a Fusion-alpha universal microplate analyzer. A standard curve using known amount of cells (10,000- 50,000 cells) was created to convert the observed fluorescence values into cell number (*Jones et al., 2001*).

### **3.2- Determination of intracellular reactive oxygen species (ROS) levels:**

Intracellular ROS levels were determined by fluorescence microscopy using the Image-iT live green ROS detection kit (Molecular Probes) according to the method described by *Bass et al., 1983*. The kit uses the fluorescent probe, 6-carboxy-2', 7'-dichlorodihydrofluorescein diacetate (carboxy-H₂DCFDA) that enters cells freely and is cleaved by intracellular esterases giving the non-fluorescent compound H₂DCF. H₂DCF is oxidized by intracellular oxidants (ROS) to the green fluorescent carboxy-DCF. The change in the fluorescence is proportional to the amount of intracellular ROS and can be detected by fluorescence microscopy. To determine the effect of heat stress on ROS generation, HT-22 cells were plated on glass coverslips and exposed to heat stress; 43°C for 30 minutes, and allowed to recover at 37°C for 2 hours. Unheated control cells were incubated at 37°C for the all period of time. Another group of cells were exposed to *tert*-butyl hydroperoxide (100 µM) for 2 hours at 37°C as a positive control. The cells were then washed with warm HBSS buffer with Ca⁺² and Mg⁺² and labeled with 25 µM carboxy-H₂DCFDA in HBSS for 30 min at 37°C in the dark and with 1 µM Hoeschst 33342 nucleic acid blue fluorescent stain for the last 5 min. Cells were then washed three times with warm HBSS and mounted on glass slides and visualized using a Nikon Eclipse E 800 Fluorescence microscope (Nikon Inc., Melville, NY) at Ex/Em 495/529 nm (green) and Ex/Em 350/461 nm (blue). Slides were examined blindly for the detection of fluorescence.

### **3.3- Measurement of cytoplasmic cytochrome c:**

3.3.1- Separation of mitochondrial and cytosolic fractions: Both adherent and floating HT-22 cells under different experimental conditions were scraped and collected at 500 x g for 5 minutes at 4 °C, washed in ice-cold PBS and resuspended in 100 µl mitochondria isolation buffer (320 mM sucrose, 1 mM potassium-EDTA, 10 mM Tris-HCl, pH 7.4, 1mM PMSF, 1 µg/ml leupeptin, 21 µg/ml pepstatin, 31 µg/ml aprotinin), and triturated with a syringe and a narrow-gauge (No. 27) needle. The homogenate was centrifuged at 500 x g for 15 minutes at 4 °C. The resulting supernatant was centrifuged twice at 17,000 x g for 15 minutes at 4 °C, and the supernatant was collected as the cytosolic fraction. The pellet was incubated in 50 µl of RIPA lysis buffer supplemented with 1mM PMSF for 15 min on ice and then centrifuged at 13,000 x g for 4 minutes (*Sun and Leaman, 2005*). Protein concentrations were determined colorimetrically using the DC protein assay kit (Bio-Rad) as described in section 2.4.2.

3.3.2- Measurement of cytosolic release of cytochrome c by immunoblotting: Equal amounts of cytosolic protein (15 µg/lane) were separated on 12% SDS-PAGE gels and then electrophoretically transferred to nitrocellulose membranes. Membranes were blocked in TBS-T buffer containing 5% non-fat dried milk, incubated overnight with mouse anti-cytochrome c monoclonal antibody (1:500 dilution) at 4°C, washed 3 x 5 minutes in 1X TBS-T buffer and incubated with goat anti-mouse IgG HRP-coupled antibody (1:3000 dilution) 1 hour at room temperature. Blots were developed using ECL plus western blotting detection system. The intensities of the resultant bands were determined using the Bio-Rad Fluor-S imager. Densitometry of western blots was

normalized to the expression of  $\beta$ -tubulin. In vitro purified cytochrome c protein was used as positive control.

### **3.4- Analysis of DNA fragmentation:**

3.4.1- Isolation of genomic DNA: To determine whether heat stress caused DNA fragmentation, HT-22 cells were heat stressed as described and total genomic DNA was isolated from cell pellets by use of the DNeasy tissue kit (Qiagen). HT-22 cells grown in 10 cm dishes were scraped and collected by centrifugation. The cell pellets were washed 2X with ice-cold PBS. Cell pellets were resuspended in 20  $\mu$ l proteinase K and 200  $\mu$ l buffer AL and mixed well by vortexing. Samples were incubated at 70°C for 10 minutes and 200  $\mu$ l 100% ethanol was added to each sample and mixed thoroughly by vortexing. Samples were transferred to DNeasy mini spin columns placed in 2 ml collection tubes. Samples were centrifuged at 8,000 x g for 1 minute at room temperature and the flow-through was discarded. DNeasy mini spin columns were placed in new 2 ml collection tubes and DNA samples on the column membranes were washed with 500  $\mu$ l AW1 buffer and centrifuged at 8,000 x g for 1 minute at room temperature and the flow-through was discarded. DNeasy columns were transferred into new 2 ml collection tubes and 500  $\mu$ l buffer AW2 were added to each sample and then centrifuged at 20,000 x g for 3 minutes at room temperature. The flow-through was discarded and the mini spin columns were then transferred to new 1.5 ml collection tubes and genomic DNA was eluted from each sample by pipetting 100  $\mu$ l buffer AE directly onto the DNeasy membrane, incubated for 1 minute at room temperature, and centrifuged at 8,000 x g for 1 minute. DNA samples

were quantified to determine their concentrations by UV spectrophotometric analysis. DNA samples were stored at -20°C until further processing.

3.4.2- Measurement of DNA fragmentation by gel electrophoresis: Five micrograms of each DNA sample was separated electrophoretically on a 1.5 % horizontal agarose gel. Gels were prepared in 1X TE buffer. Gels were run at 100 V for 1 hour and were stained with ethidium bromide for 1 hour at room temperature. The DNA fragmentation was photographed using UV illumination on a Fluor-S imager (Bio-Rad) (*Baydas et al., 2005 & Choi et al., 2006*).

#### **4- Experimental protocol 4: Effect of the pretreatment with the SOD mimetic EUK-134 on cell viability, reactive oxygen species (ROS) generation, cytochrome c release , and DNA fragmentation in HT-22 cells.**

##### **4.1- Drug treatment:**

Synthetic SOD mimetics, salen manganese compounds (EUKs), are a group of compounds that are originally formed of five-ring structure containing Mn³⁺ and have both SOD and catalase activities such that they can scavenge both superoxide radical and its dismutation product, hydrogen peroxide. EUK-134 [manganese 3-methoxy *N, N'*-bis (salicylidene) ethylenediamine chloride] is the salen manganese compound used in this study (**Figure 7**). It was obtained from Cayman chemicals and a stock solution of 50 mM was prepared using dimethyl sulfoxide (DMSO) purged with N₂. Stock solution was aliquoted and kept at -20°C. EUK-134 stock solution was diluted to the desired concentration in culturing medium just before use. Three days after plating, cells were

treated with EUK-134. Cells were incubated in a medium in the presence of 10  $\mu$ M EUK-134 or its vehicle one hour before induction of heat stress by incubation in a 43°C water bath for 30 minutes and allowed to recover at 37°C for different times (0, 1, 2, 4, 8, 12, 24 and 48 hours). DMSO in dilution of (1:1000) in culturing medium was used as vehicle control. Cell proliferation, ROS generation, , cytochrome c release and DNA fragmentation were then measured in the cells as described above in experimental protocol 3.

### **5-Statistical analysis:**

All data were represented as mean  $\pm$  S.E.M. of the indicated number of samples. Statistical analysis between groups was made using one-way analysis of variance (ANOVA single factor). Student's t-test, F-test, correlation and regression analysis were used to analyze between groups.

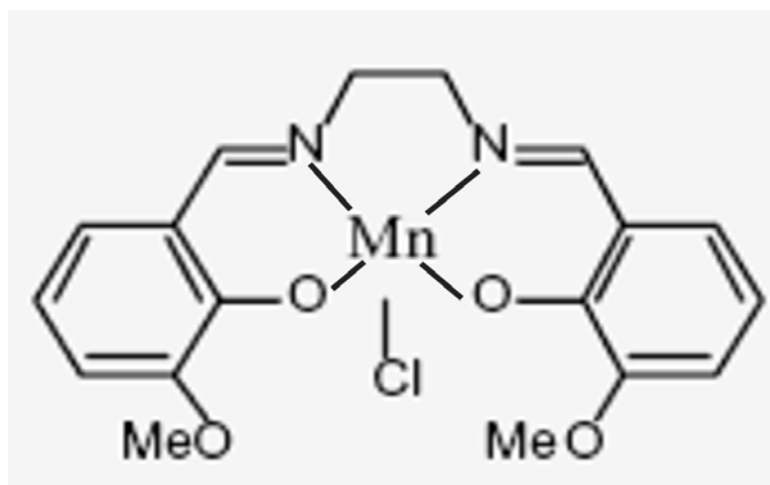


**Figure 7:** Chemical structure of EUK-134.



## RESULTS

### **Effect of heat stress on core body temperature, respiratory rate and heart rate of**

#### **pigs:**

Pigs were acclimated to 70 °F for 48 hours before being exposed to 90 °F for 4, 8, 12 or 24 hours. Core body temperature in control pigs at 12 and 24 hours was  $102.5 \pm 0.1$  °F and  $102.5 \pm 0.4$  °F respectively. Core body temperature in heat-stressed pigs at 12 and 24 hours was significantly elevated from control to  $104.5 \pm 0.5$  °F and  $104.0 \pm 0.6$  °F respectively.

Respiratory rate (breaths per minute) was elevated in heat-stressed pigs compared to control. All time points from 0-13 hours were significantly different between treatments. Time points 14 hours to 23 hours were not significant (**Figure 8**). There was no significant difference in heart rate at any time measured between heat-stressed and control pigs (**Figure 9**).

#### **Identification of total RNA quality and concentration:**

Pigs were used in this study as a model of human heat stress to identify novel genes associated with heat stress in the hippocampus using the mRNA Differential Display PCR method. A heat stress of 12 hours was chosen for this study. Pigs were maintained at either 70 °F (Control) or 90 °F (heat-stressed) for 12 hours. Three pigs were assigned to

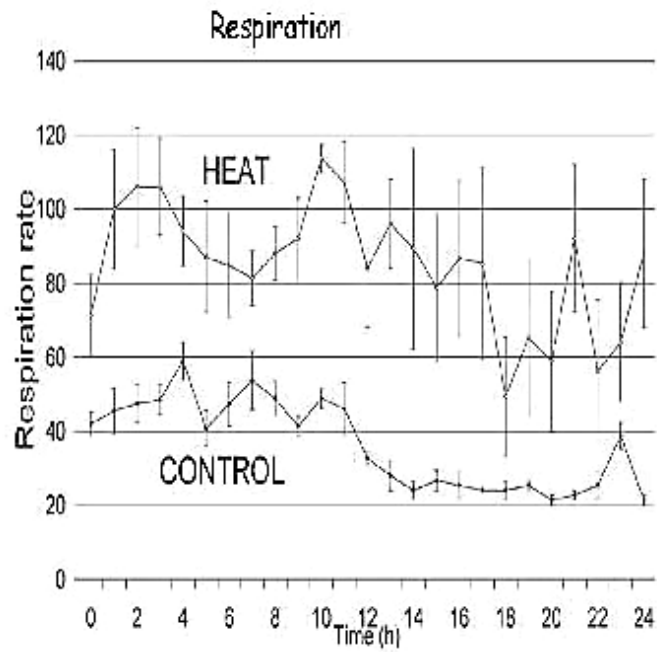


**Figure 8:** Effect of heat stress on respiratory rate. Change in respiratory rate (breath per minute) with time in both control and heat stressed pigs. All time points from 0 -13 h are significantly different between treatments ( $P \leq 0.05$ ). Points 14 h to 23h are not significant.

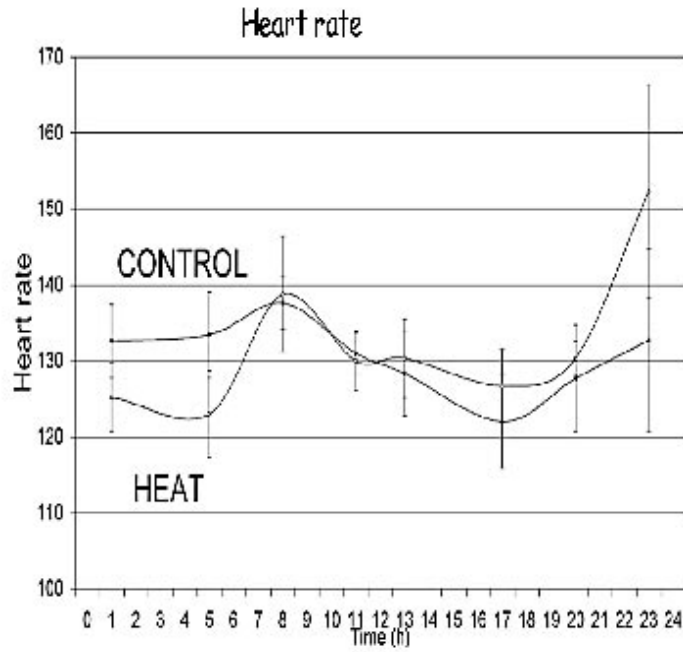


**Figure 9:** Effect of heat stress on heart rate. Change heart rate with time in both control and heat stressed pigs. No significant difference was recorded in heart rate at any of time points measured between heat stressed and control pigs.

each subgroup. At the end of each time period, the hippocampus was removed and total RNA was isolated from each sample. The integrity of each isolated total RNA sample was determined by denaturing-formaldehyde agarose gel electrophoresis. The integrity of each RNA sample was determined using the 28S and 18S ribosomal RNA bands which should be distinct from the background and the 28S band twice as bright as the 18S band (**Figure 10**). During the isolation of total RNA from pig hippocampus, one of the heat stress samples was determined to be degraded. Therefore, the hippocampus from three control and two heat stress pigs were used for DD-PCR. The concentration of total RNA in each sample was determined at 260nm UV spectroscopy. The yield (in  $\mu\text{g RNA/mg protein}$ ) of total RNA in all groups ranged from 576  $\mu\text{g /mg protein}$  to 2628  $\mu\text{g/mg protein}$  (**Table 3**).

#### **Differential display PCR and identification of differentially expressed bands:**

First strand (cDNA) was prepared from each RNA sample and differential display PCR was performed using a total of 240 different primer combinations. The PCR products were resolved on a total of 39 polyacrylamide gels. Gels were blotted on HPLC paper, dried and exposed to x-ray films. Differentially expressed DNA bands between heat-stressed and control samples were determined after auto-radiography (**Figure 11**). The molecular weight of DNA fragments separated on DNA sequencing gel ranged from 50 bp to 1Kbp, only fragments of intermediate size (150-750 bp) lying in the middle 3/5 of the gel were considered. Only the clear bands and those bands having the same pattern of expression in each sample among the same treatment condition were considered for further analysis (*Ma et al., 2001 & Yang et al., 2004*). Each band was designated by its

origin (hippocampus), the original primer pair used in DD-PCR amplification, the treatment condition and its number on the gel. Each differentially expressed DNA fragment was detected by visual examination of the autoradiograms on a light box. Thirty one differentially expressed DNA fragments were isolated (**Table 4** and **Figure 12**). The isolated DNA fragments were reamplified by RT-PCR and the PCR products were resolved on agarose gels to determine the molecular weights of the isolated DNA fragments. The molecular weight of the isolated 31 DNA fragment ranged from 150 bp to 500 bp (**Figure 13**).

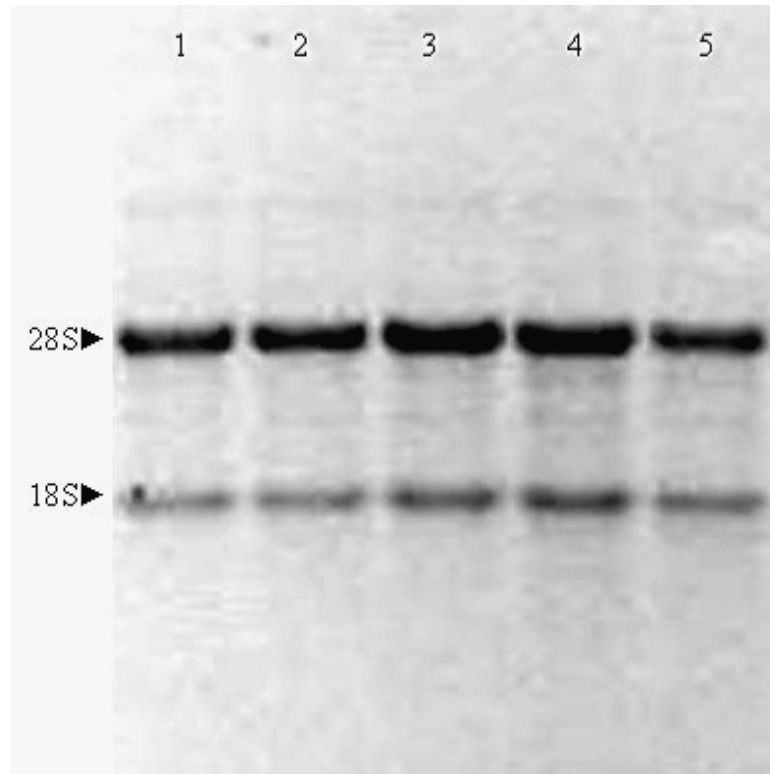


**Figure 10:** RNA integrity gel. The quality of the isolated RNA was assessed by denaturing-formaldehyde gel electrophoresis. Gel was stained with ethidium bromide and RNA bands were visualized and pictured using UV illumination on a Flour-S imager. On this picture two bands appear in each sample, the upper band is 28S ribosomal RNA which is twice as bright as the lower one that corresponds to 18S ribosomal RNA. Lanes 1-3 represent the RNA samples isolated from control pig hippocampuses and lanes 4 and 5 represent the RNA isolated from heat-stressed pig hippocampi.

Sample	Total RNA ( $\mu\text{g}/\text{mg}$ protein)	260/280 ratio
<b>4 hours:</b>		
C1	1190	2.1
C2	1191	2.1
C3	1530	2.1
H1	890	2.1
H2	1360	2.1
H3	1150	2.1
<b>8 hours:</b>		
C4	830	2.1
C5	950	2.1
C6	1051	2.1
H4	872	2.1
H5	1050	2.0
H6	1430	2.1
<b>12 hours:</b>		
C7	576	2.1
C8	1090	2.1
C9	930	2.1
H7	594	2.0
H8	885	2.0
H9	765	2.0
<b>24 hours:</b>		
C10	1070	2.0
C11	2628	1.9
C12	1261	2.1
H10	1298	1.8
H11	1233	2.0
H12	1297	1.9

**Table 3:** Total RNA concentrations in different experimental groups. **C** represents control samples; **H** represents heat-stressed samples. The RNA yield in  $\mu\text{g}/\text{mg}$  protein was calculated by multiplying the  $A_{260}$  x dilution factor x 40. The ratio of  $A_{260}$  to  $A_{280}$  values is a measure of RNA purity, and should fall in the range of 1.7 to 2.1. The highlighted sample is the sample found degraded during RNA isolation.

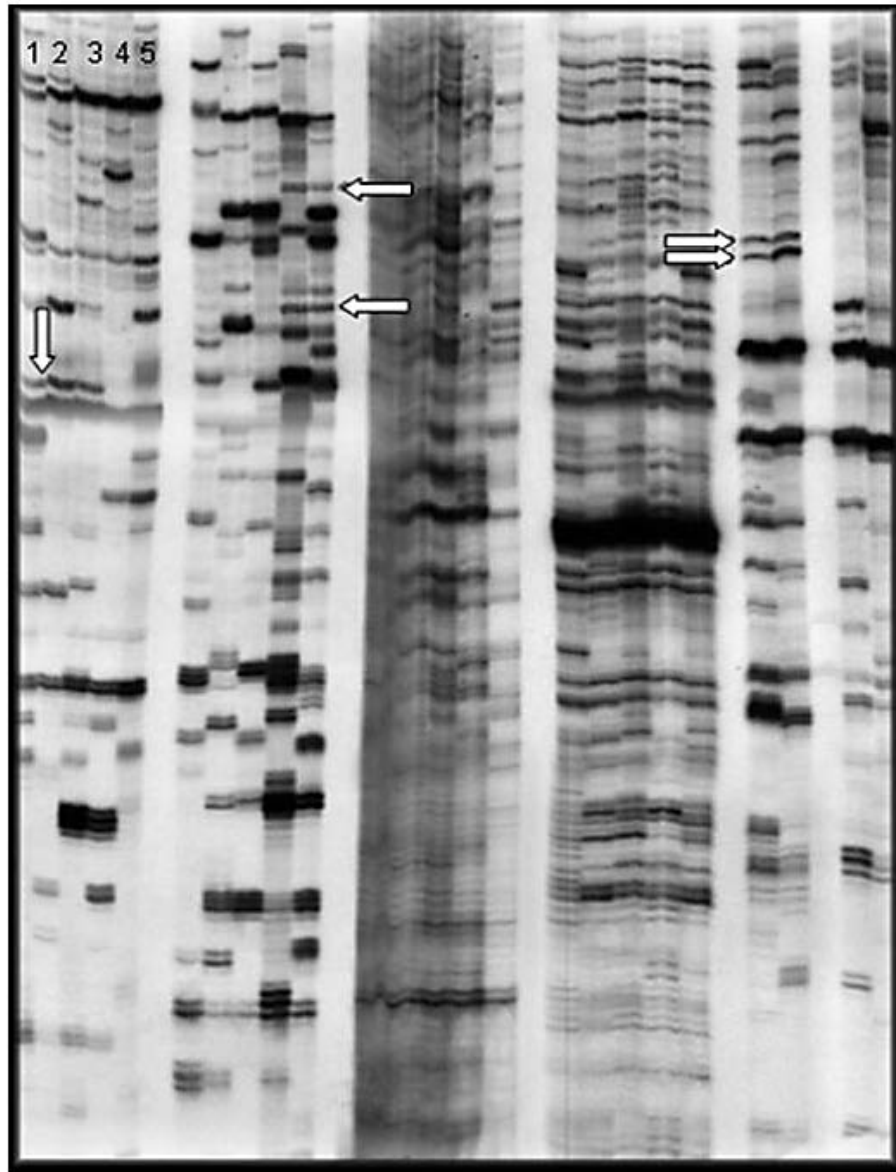


**Figure 11:** A representative autoradiograph of polyacrylamide sequencing gel displaying PCR fragments. The lanes labeled 1, 2 and 3 contain PCR fragments representing mRNA isolated from hippocampi of control pigs. The lanes labeled 4 and 5 show PCR fragments representing mRNA from hippocampi of heat-stressed (12 hours) pigs. The primers used for this experiment were anchored primer H-T₁₁A and the random primers HAP-62, 63, 64, 65 and 66 (from left to right). Arrows show some differentially expressed PCR fragments between control and heat stressed groups.



DNA fragment name	3` oligo dT anchored primers	The number of arbitrary 5` primers	More expression in	Number on the gel
Hi A2H	H-T ₁₁ A	HAP ₂	Heat-stressed	The only one
HiA2C	H-T ₁₁ A	HAP ₂	Control	The only one
HiA8C	H-T ₁₁ A	HAP ₈	Control	The only one
HiA9C	H-T ₁₁ A	HAP ₉	Control	The only one
HiC21H	H-T ₁₁ C	HAP ₂₁	Heat stress	The only one
HiC24C	H-T ₁₁ C	HAP ₂₄	Control	The only one
HiC25C	H-T ₁₁ C	HAP ₂₅	Control	The only one
HiC25H1	H-T ₁₁ C	HAP ₂₅	Heat-stressed	1
HiC25H2	H-T ₁₁ C	HAP ₂₅	Heat-stressed	2
HiA29H	H-T ₁₁ A	HAP ₂₉	Heat-stressed	The only one
HiA30H	H-T ₁₁ A	HAP ₃₀	Heat-stressed	The only one
HiG40C	H-T ₁₁ G	HAP ₄₀	Control	The only one
HiC45H1	H-T ₁₁ C	HAP ₄₅	Heat-stressed	1
HiC45H2	H-T ₁₁ C	HAP ₄₅	Heat-stressed	2
HiG47C	H-T ₁₁ G	HAP ₄₇	Control	The only one
HiG56H	H-T ₁₁ A	HAP ₅₆	Heat-stressed	The only one
HiA56C	H-T ₁₁ A	HAP ₅₆	Control	The only one
HiC58C	H-T ₁₁ C	HAP ₅₈	Control	The only one
HiA60H	H-T ₁₁ A	HAP ₆₀	Heat-stressed	The only one
HiG61H	H-T ₁₁ G	HAP ₆₁	Heat-stressed	The only one
HiC62C	H-T ₁₁ C	HAP ₆₂	Control	The only one
HiC63H1	H-T ₁₁ C	HAP ₆₃	Heat-stressed	1
HiC63H2	H-T ₁₁ C	HAP ₆₃	Heat-stressed	2
HiC66C1	H-T ₁₁ C	HAP ₆₆	Control	1
HiC66C2	H-T ₁₁ C	HAP ₆₆	Control	2
HiC71C1	H-T ₁₁ C	HAP ₇₁	Control	1
HiC71C2	H-T ₁₁ C	HAP ₇₁	Control	2
HiC72C	H-T ₁₁ C	HAP ₇₂	Control	The only one
HiA73C	H-T ₁₁ A	HAP ₇₃	Control	The only one
HiC73C	H-T ₁₁ C	HAP ₇₃	Control	The only one
HiA75H	H-T ₁₁ A	HAP ₇₅	Heat-stressed	The only one

**Table 4:** Differentially expressed DNA fragments on differential display PRC gels. Thirty one DNA fragments displayed differential expression between control and heat stress. Hi, hippocampus; C, control; H heat-stressed.

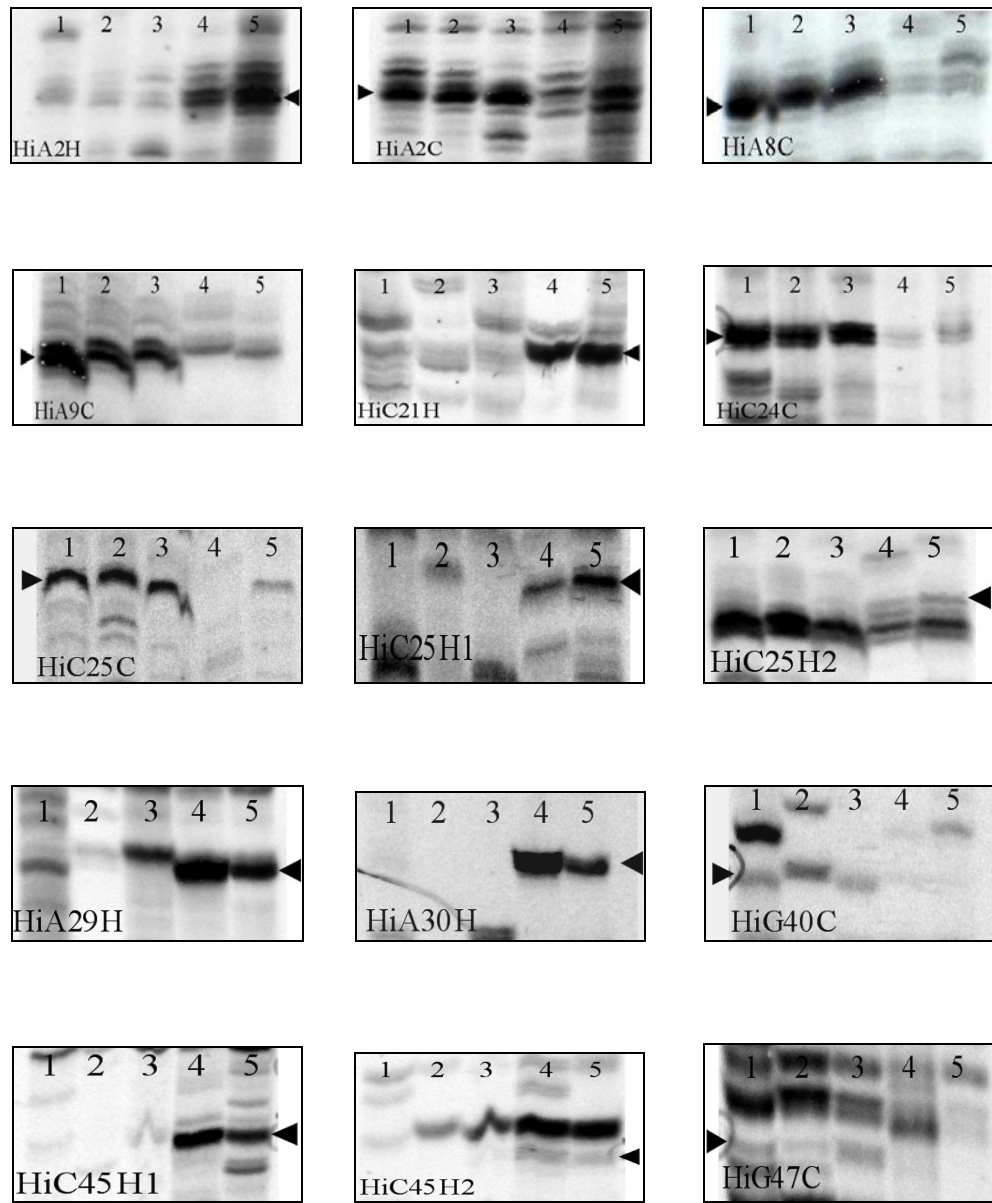


**Figure 12:** Differentially expressed DNA fragments in pig hippocampus. The lanes number 1, 2 and 3 represent DNA from hippocampi of control pigs. The lanes number 4 and 5 show represent DNA from hippocampi of 12 hours heat-stressed pigs.

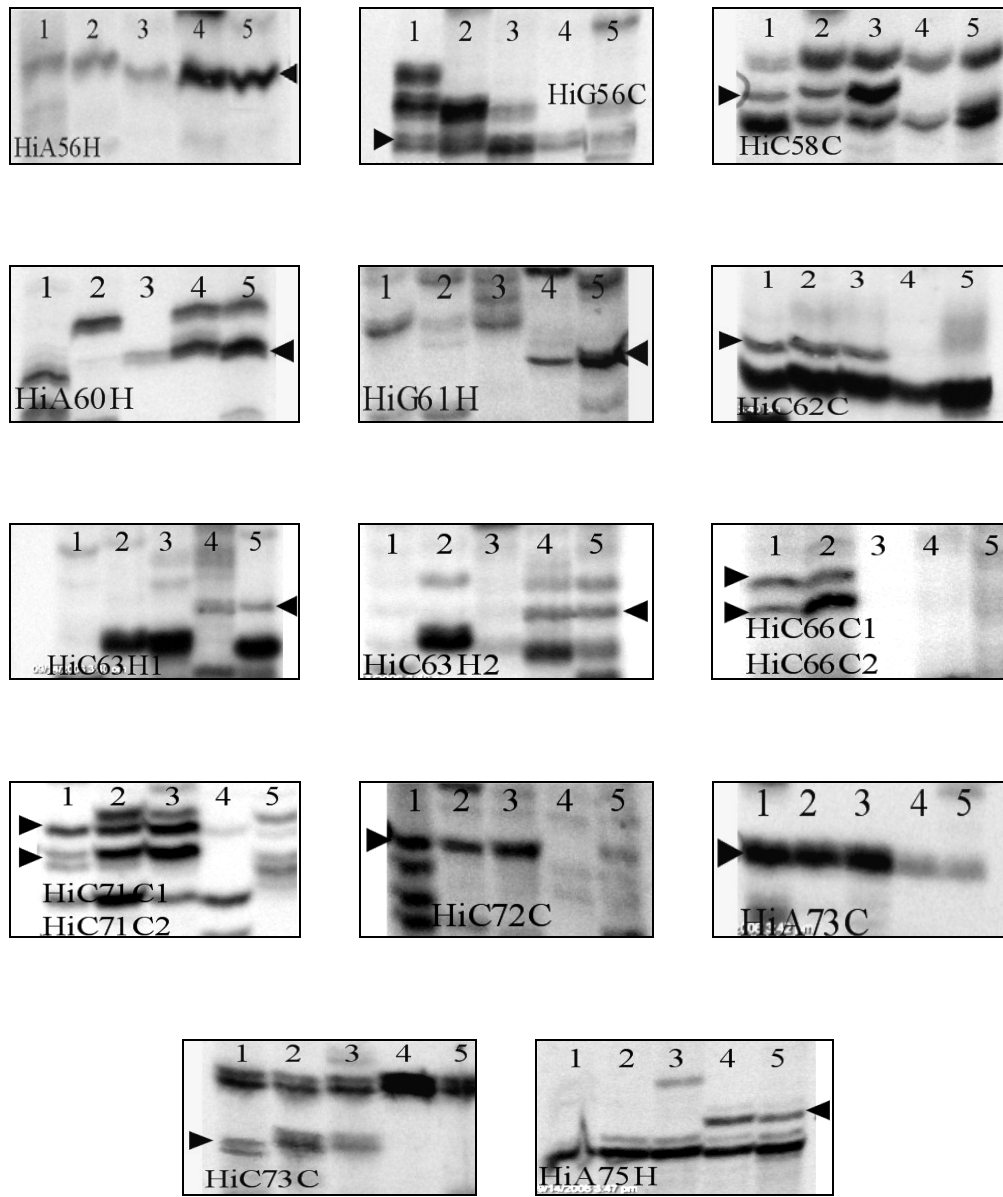


**Figure 12:** Differentially expressed DNA fragments in pig hippocampus. (Continued)

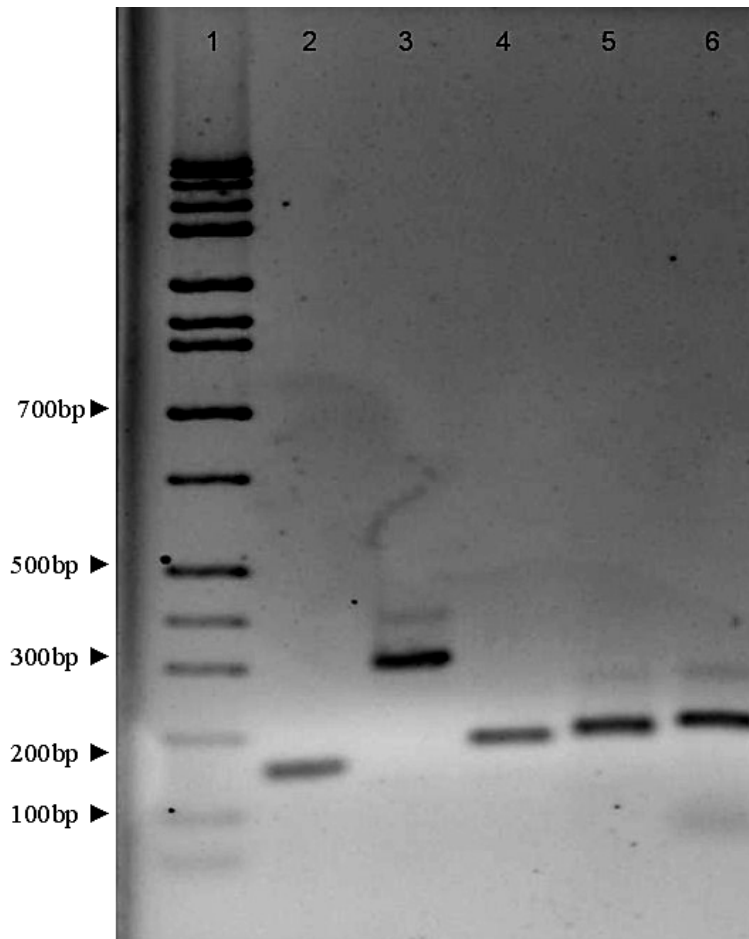


**Figure 13:** A representative reamplification gel of isolated DNA fragments. The cDNA bands that showed differential expression in DD-PCR polyacrylamide gel picture were extracted from the acrylamide gel and reamplified by PCR using the original primer pairs and resolved on an agarose gel to determine their size and purity (presence of one band). Lane 1 represents the DNA molecular weight marker; lanes 2-6 represent cDNA fragments HiA29H, HiA30H, HiA56A, HiA60H and HiA73C.

### **Sequences of isolated DNA fragments and BLAST search results on GenBank:**

The isolated 31 differentially expressed DNA fragments were ligated into linearized plasmid vector (PCR11), and transformed to *E. Coli* for blue/white screening. Plasmids were then isolated and the presence of our PCR inserts was confirmed by EcoRI restriction digestion analysis (**Figure 14**). The isolated plasmids were sequenced and the amplified DNA sequences were compared for homologous nucleic acid sequences by a BLAST search of the databases at NCBI GenBank using the software Vector NTI. Significant sequence similarity at the nucleotide level was defined by at least 96% identity over the entire length of the clone (*Wen, 2000*). BLAST search in GenBank identified 17 sequences that matched to known human or porcine genes, 5 sequences to human genes with unknown functions, 4 sequences to known genes of species other than human and pig and 5 sequences had no significant similarity with any database entry. The 17 inserts that matched to human or porcine genes are summarized in **Table 5**. These sequences were then subjected to further analysis to determine that the fragments corresponded to sequences in the 3' open reading frame of the genes. The 3' open reading frame was the target amplified by DD-PCR. Six sequences were found to match the 3' open reading frame of known human genes (**Table 6**). The six genes were DNA polymerase epsilon p12 subunit (PolE4), proteasome 26S non-ATPase subunit 10 (PSMD10), Cu/Zn superoxide dismutase (SOD-1), MutL homolog 1 (MLH1), cerebroside sulfotransferase (CST), and voltage-gated sodium channel, type I, beta subunit (SCN1B). These six genes were chosen for further analysis using real-time PCR.

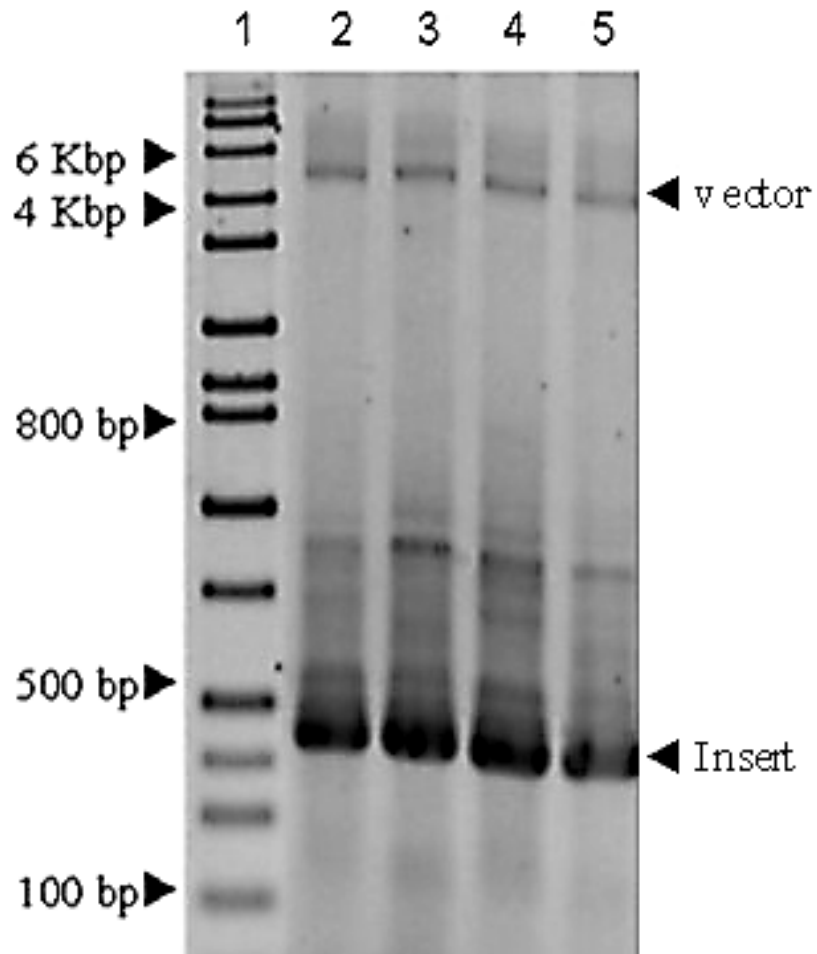


**Figure 14:** A representative *EcoRI* restriction digestion product on agarose gel. Plasmid vector containing the DNA insert was subjected to *EcoRI* restriction digestion to determine the presence of our ligated insert. Lane 1 represents the DNA molecular weight marker; lanes 2-5 represent 4 repeats of the same insert; the low molecular weight bands (~ 400bp) represent the DNA inserts while those of high molecular weight (~ 5 Kbp) represent the plasmid vector. This DNA fragment was HiC25C.

Gene Name	Accession number in gene bank	More expression in	Fragment name
*DNA polymerase epsilon p12 subunit gene,(PoIE4) gene.	AF261688	Heat stress	HiC25H1
CC chemokine gene cluster	AF088219	Heat stress	HiC25H2
Coagulation factor II (thrombin) receptor-like 1, (F2RL1) gene	AF400075	Control	HiA9C
Olfactomedin 1 (OLFM1) gene, transcript variant 2	NM_006334	Heat stress	HiA2H
AMY gene	D82343	Heat stress	HiC21H
Calcium channel alpha 12.2 subunit, CACNA1B gene.	AF238296	Control	HiC24C
*Proteasome (prosome, macropain )26S subunit, non-ATPase, 10 (PSMD10) gene	NM_002814	Heat stress	HiG61H
HLA-B gene for MHC class I antigen B 4006 allele	AJ300180	Heat stress	HiA56H
ITGB4 gene for integrin beta 4 subunit.	Y11107	Heat stress	HiA60H
OAT-1 (organic anion transporter).	AJ249369	Control	HiG56C
Carboxypeptidase D (CPD) gene.	NM_001304	Heat stress	HiA75H
ADAM9 gene. This gene encodes disintegrin and metalloprotease (ADAM) domain 9.	NM_003816	Control	HiC73C
*Cu/Zn superoxide dismutase, SOD-1.	NM_000454	Control	HiC62C
*MutL homolog 1 (MLH1) gene.	AY217549	Heat stress	HiC63H1
CGI-109 gene ( a membrane trafficking protein)	NM_181836	Heat stress	HiA56H
*CST gene for cerebroside sulfotransferase	AB029901	Heat stress	HiC63H2
*Voltage-gated sodium channel, type I, beta subunit (SCN1B)	BC030193	Control	HiC66C2
Pig mitochondrion, complete genome	AF034253	Control	HiA9C
Human chromosome 11, clone RP11-677N16	AC087207	Control	HiC21C
Human cDNA FLJ37747 fis, clone BRHIP2022986	AK095066	Heat stress	HiC45H1
Human cDNA FLJ11918 fis, clone HEMBB1000272	AK021980	Heat stress	HiC45H2
Human chromosome 3 clone RP11-739J4	AC113172	Heat stress	HiA30H
Human DNA sequence from clone CTA-212D2 on chromosome 6	AL353596	Control	HiC71C1

**Table 5:** Blast search results that matched the sequences of the isolated PCR fragments that appear to be differentially expressed after heat stress in pig hippocampi. The marked genes with the (*) are the genes that our sequences matched to their 3' open reading frames. Those genes were chose to confirm their differential expression with real-time PCR.

Gene name	Accession number	Function
PoIE4, DNA polymerase epsilon p12 subunit gene	AF261688	PoIE4 is a structural subunit of DNA polymerase $\epsilon$ that contains four subunits; catalytic subunit A (p261) and three regulatory subunits B (p59), C (p12) and D (p17) Polymerase $\epsilon$ is involved in both DNA replication and repair.
PSMD10, Proteasome 26S non-ATPase subunit 10 gene	NM_002814	The 26S proteasome is a multicatalytic proteinase complex with a highly ordered structure composed of 2 complexes, a 20S core and a 19S regulator and built by at least 32 different protein subunits. This gene encodes a non-ATPase type subunit 10 of the 19S regulator. 26S proteasome plays a central role in the degradation of intracellular proteins.
SOD-1, Cu/Zn superoxide dismutase or cytosolic superoxide dismutase gene	NM_000454	The protein encoded by this gene binds copper and zinc ions and is the responsible for destroying free superoxide radicals in the body. The encoded enzyme is a soluble cytoplasmic protein, acting as a homodimer to convert naturally-occurring but harmful superoxide radicals to molecular oxygen and hydrogen peroxide.
MLH1, MutL homolog 1 gene	AY217549	This gene is a member of the MutL-homolog (MLH) family of DNA mismatch repair (MMR) genes. MLH genes are implicated in maintaining genomic integrity during DNA replication and after meiotic recombination. The protein encoded by this gene function as a heterodimer with other MLH family members.
CST gene for cerebroside (galactosylceramide) sulfotransferase.	AB029901	Sulfonation, an important step in the metabolism of many drugs, xenobiotics, hormones, and neurotransmitters, is catalyzed by sulfotransferases. The product of this gene is galactosylceramide sulfotransferase which catalyzes the sulfation of membrane glycolipids. Seems to prefer beta-glycosides at the nonreducing termini of sugar chains attached to a lipid moiety. Catalyzes the synthesis of galactosylceramide sulfate (sulfatide), a major lipid component of the myelin sheath and of monogalactosylalkylacylglycerol sulfate (seminolipid), present in spermatocytes and involved in spermatogenesis. Also acts on lactosylceramide, galactosyl 1-alkyl-2-sn-glycerol and galactosyl diacylglycerol ( <i>in vitro</i> ).
SCN1B, Voltage-gated sodium channel, type I, beta subunit gene	BC030193	Voltage-gated sodium channels (VGSCs) are essential for the generation and propagation of action potentials in striated muscle and neuronal tissues. Voltage-sensitive sodium channels are heteromultimeric complexes consisting of a large central pore-forming $\alpha$ subunit and 1 or more, smaller auxiliary $\beta$ subunits, such as SCN1B. The $\alpha$ subunit of the brain sodium channels is sufficient for expression of functional voltage-gated Na ⁺ channels, but requires a beta-1 subunit for normal inactivation kinetics. The $\beta_1$ -subunit alters gating, voltage sensitivity and recovery from fast inactivation of VGSCs.

**Table 6:** The genes chosen to verify their heat-induced differential expression by real-time PCR analysis. The 3`open reading frames sequences of these genes were matched with sequences of six of our DD-PCR amplified DNA fragments.



### **Quantitative real-time PCR results on 12 hours heat stress:**

To determine whether the expressions of the six identified genes were altered by heat stress, real-time PCR was used to examine the expression of these six genes in the hippocampi of control and heat stressed pigs. The samples used for this analysis were the samples originally used for the DD-PCR. Oligonucleotide real-time PCR primers of the identified six genes were designed with Vector NTI software and the effectiveness of their PCR amplification was confirmed by the gel-based PCR. The expression of GAPDH (glyceraldehyde-3-Phosphate dehydrogenase) and 36B4 (acidic ribosomal phosphoprotein) were used as internal reference genes. Two of these six genes, MutL 1 and CST, unsuccessful real-time PCR amplification with three different primer pairs and no further analysis was carried out with these genes. The other four genes, PolE4, SCN1B, PSMD10, and SOD-1 were successfully amplified with the primer sets and their differential expression was determined by real-time PCR. A standard curve was performed for each primer pair to determine the efficiency of amplification (**Figure 15 A** and **15 B**). A list of primer sets that were designed for the selected genes is included in **Table 7**.

The differential expression of the four genes after 12 hours of heat stress with DD-PCR was confirmed by the real-time PCR analysis. The expression of both PolE4 and PSMD10 was upregulated significantly to  $2.55 \pm 0.38$  and  $2.6 \pm 0.28$  fold compared to control, respectively. On the other hand, the expression of both SCN1B and SOD-1 was downregulated to  $0.7 \pm 0.15$  and  $0.45 \pm 0.1$  fold compared to control, respectively (**Figure 16**).

Gene name	Accession number	Oligonucleotide sequence	Product length (bp)	Efficiency of PCR amplification
<b>Superoxide Dismutase-1 (SOD-1) gene.</b>	NM_000454	<b>Sense:</b> 5'-ACAGCAGGCTGTACCAGTGCAGGTCCT <b>Antisense:</b> 5'-CATTGCCCAAGTCTCCAACATGCCTCT	100	136.0%
<b>DNA polymease epsilon 12 subunit (POLE4) gene.</b>	AF261688	<b>Sense:</b> 5'-TGACGCTAGCGGGACAGGAAGCCAT <b>Antisense:</b> 5'CTGCTGAGCGCAACAGTAGGCATCTTTT	143	115.2%
<b>Proteasome 26 S subunit, non-ATPase type 10 (PSMD10) gene.</b>	NM_002814	<b>Sense:</b> 5'-TGCAGGTTGGTCTCCTCTTCATATTGCG <b>Antisense:</b> 5'CAGCATTCACCTGAGCACCTTTTCCCAG	92	112.0%
<b>Sodium Channel voltage-gated, type I,beta (SCN1B) gene.</b>	BC030193	<b>Sense:</b> 5'-GGCATCATTTCCCCTCCCGCTTCCT <b>Antisense:</b> 5'-TTCAAGGCTGGTGAGAGAGGGCGAG	104	100.1%
<b>Glyceraldehyde-3-phosphate dehydrogenase (GAPDH) gene.</b>	AF141959	<b>Forward:</b> 5'-TGCACCACCAACTGTTAGC <b>Reverse:</b> 5'-GGCATGGACTGTGGTCATGAG	93	108.5%
<b>Proteasome 26 S subunit beta type 9, (PSMB9) gene.</b>	X62741	<b>Sense:</b> 5'-CCATGGGATAGA AACTGGAGGAACCTCC <b>Antisense:</b> 5'-CCATGAGATGTGCAGACAAGTCCTCTCG	103	129.4%
<b>36B4, Acidic ribosomal phosphoprotein mRNA.</b>	NM_007475	<b>Sense:</b> 5'-AAGCGCGTCCTGGCATTGTCT <b>Antisense:</b> 5'-CCGCAGGGGGCAGCAGTGGT	136	91.0%

**Table 7:** Primers for all tested genes by real-time PCR.

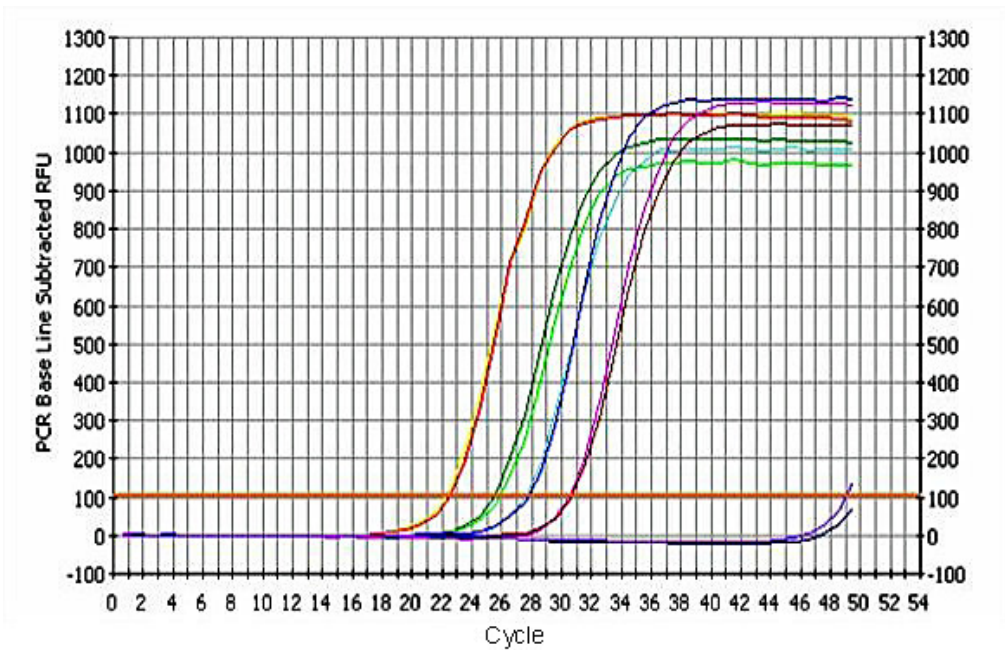
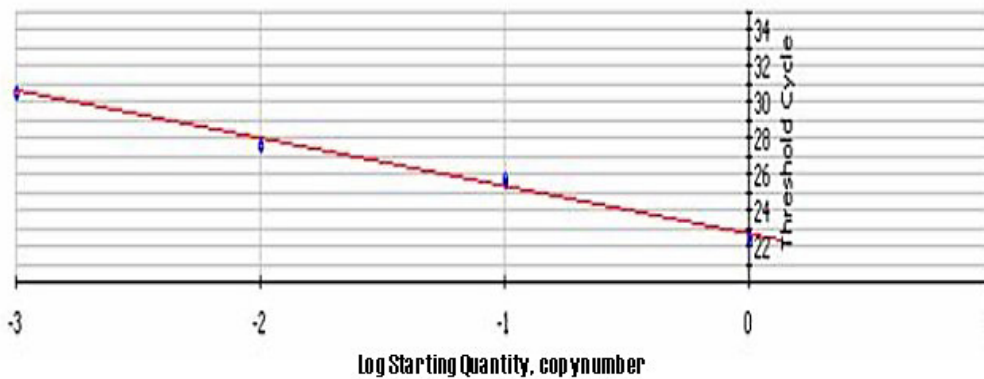


**Figure 15 A:** Real-time PCR quantification graph for standard curve. This standard curve was performed using cDNA concentration range from 1.0µg/µl- 1.0ng/µl to generate the standard curve for each PCR run.

Correlation Coefficient: 0.995 Slope: -2.661 Intercept: 22.612  $Y = -2.661X + 22.612$   
 PCR Efficiency: 136.0%



PCRStandard Curve: Data 12-Apr-05 S00-1ST.odm

**Figure 15 B:** Linear representation of real-time PCR standard curve. This figure represents the linear representation of the data generated in figure 15A.

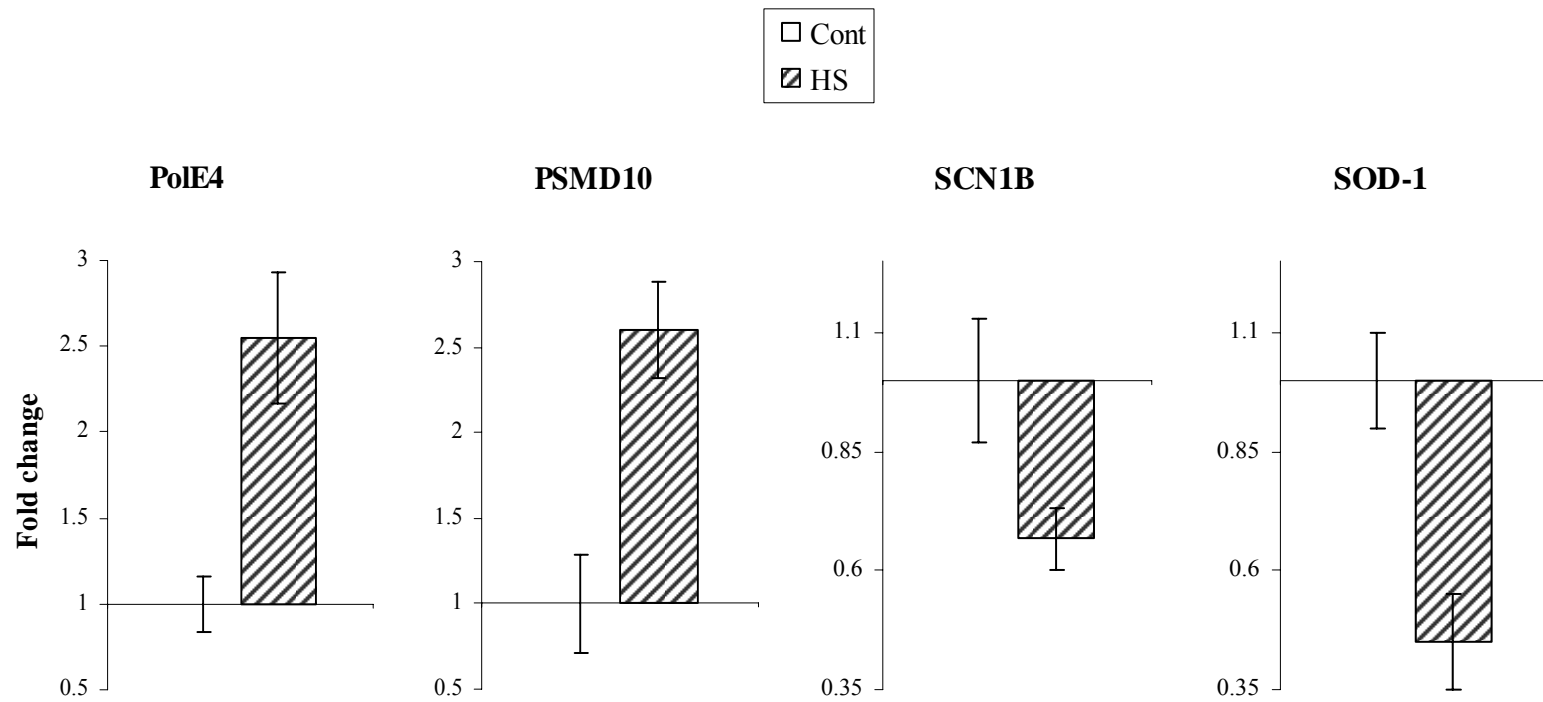


**Figure 16:** Quantitative real-time PCR analysis of gene expression in pig hippocampus after heat stress for 12 hours compared with control. Data represent means  $\pm$  S.E.M. of three pigs per group and the experiment was repeated two times (n=6). Relative expression of each gene after heat stress relative to control was determined using the gene expression macro software which utilizes the modified  $\Delta\Delta C_t$  method described by (Vandesompele *et al.*, 2002). GAPDH and 36B4 genes were used as internal standards for each sample.

### **Effect of heat stress on time course of gene expression:**

Real-time PCR confirmed the altered expression of 4 genes in the hippocampus of 12 hours heat stress pigs. To determine the time course of gene expression, pigs were heat stressed for 4, 8, 12 and 24 hours and the expression of PolE4, SCN1B, SOD-1, and PSMD10 was determined in the hippocampus using real-time PCR (**Figure 17 A**).

No significant change occurred in the level of PolE4 mRNA in the hippocampus of heat-stressed pigs after 4 hours. It was significantly decreased after 8 hours to  $0.23 \pm 0.05$  fold compared to control. On the other hand, the level was upregulated significantly after 12 hours of heat stress to  $2.55 \pm 0.38$  fold compared to control before returning approximately to basal levels by 24 hours.

The expression level of  $\beta 1$  subunit gene of voltage-gated sodium channels (SCN1B) was significantly reduced in the hippocampus of heat-stressed pigs at both 8 and 24 hours to  $0.59 \pm 0.09$  fold and  $0.67 \pm 0.07$  fold compared to control, respectively. The changes in gene expression of SCN1B at both 4 and 12 hours were not significant in comparison to control.

The expression level of SOD-1 mRNA was significantly downregulated in heat stressed pig hippocampus after both 8 and 12 hours to  $0.39 \pm 0.06$  fold and  $0.45 \pm 0.1$  fold compared to control, respectively. At 4 and 24 hours, the expression level from control was not significantly different from control.

The proteasomal subunit (PSMD10) gene had increased expression in the hippocampus of heat stressed pig in comparison to control. This increase in gene expression was only significant from control at 12 hours ( $2.6 \pm 0.28$  fold increase compared to control). The PSMD10 gene encodes a non-ATPase subunit of the 19S

regulatory element of the 26S proteasome. The 26S proteasome is a multisubunit ATPase-dependent protease that plays a central role in the degradation of intracellular proteins. The 26S proteasome is composed of the 20S proteolytic core and 19S regulatory element that caps the 20S at both ends (*Piccinini et al., 2003*). The 26S proteasome in its entirety is composed of at least 32 different protein subunits that are encoded by at least 32 different genes. The expression of the different proteasomal subunits has been reported to be affected by heat stress (*Anderson et al., 2004*). In our DD-PCR experiment, we only detected a change in the expression of the PSMD10 subunit and alteration in its mRNA expression was confirmed by real-time PCR analysis. We therefore designed a primer pair against another proteasomal subunit, PSMB9 (a 20S core beta subunit) to determine if its expression is also affected by heat stress. The expression of proteasomal subunit PSMB9 mRNA was increased significantly in heat-stressed pig hippocampus in comparison to control at all sampling times from 4 to 24 hours. The levels of PSMB9 gene expression were  $3.4 \pm 0.24$  fold,  $2.69 \pm 2.7$  fold,  $2.7 \pm 0.6$  fold and  $3.9 \pm 0.8$  fold compared to control at 4, 8, 12 and 24 hours, respectively (**Figure 17 B**).

It has been reported in several studies that heat stress stimulates the expression of heat shock proteins (HSPs) in the hippocampus of different animal species (*Maroni et al., 2003; Bechtold and Brown, 2003; Pavlik et al., 2003; Lim et al., 2003; Reynolds and Allen, 2003*). Heat shock proteins play an important role in cell protection and cell recovery from heat-induced damage through their role in preventing protein aggregation; catalyzing refolding of misfolded proteins, facilitating degradation of strongly damaged proteins as well as a role in DNA damage repair (*Pandita et al., 2004*). In our DD-PCR we did not detect any differentially expressed DNA fragment that correlated with any of

HSP genes. Due to the biological importance of this group of genes, we designed primer sets against one member of each HSP family. We measured the expression of HSP27 (low molecular weight), HSP70 (the most important form of HSPs and the intermediate molecular weight), and HSP90 (high molecular weight family) in pig hippocampus. The following oligonucleotide primers against different HSPs were used: HSP70 (accession number NM_213766), 5'-GTG ACC TTC GAC ATC GAC GCC AAC (sense) and 5'-TGG TGA TCT TGT TGG CCT TGC CC (antisense); HSP90 (accession number NM_213973), 5'-GCA GCA GCT GAA GGA GTT TGA GGG G (sense) and 5'-CCT CTT CAT CTT CCG GGA GCT CCA (antisense); HSP27 (accession number AB020027), 5'-TGT CCC TGG ATG TCA ACC ACT TCG C (sense) and 5'-CCT CTT CAT CTT CCG GGA GCT CCA (antisense). The expression of HSP90 and HSP27 mRNA were slightly but not significantly enhanced after heat stress at all sampling times up to 24 hours. HSP70 expression was significantly increased after 4 hours of heat stress compared to control ( $1.67 \pm 0.3$  fold) (**Figure 17 B**).

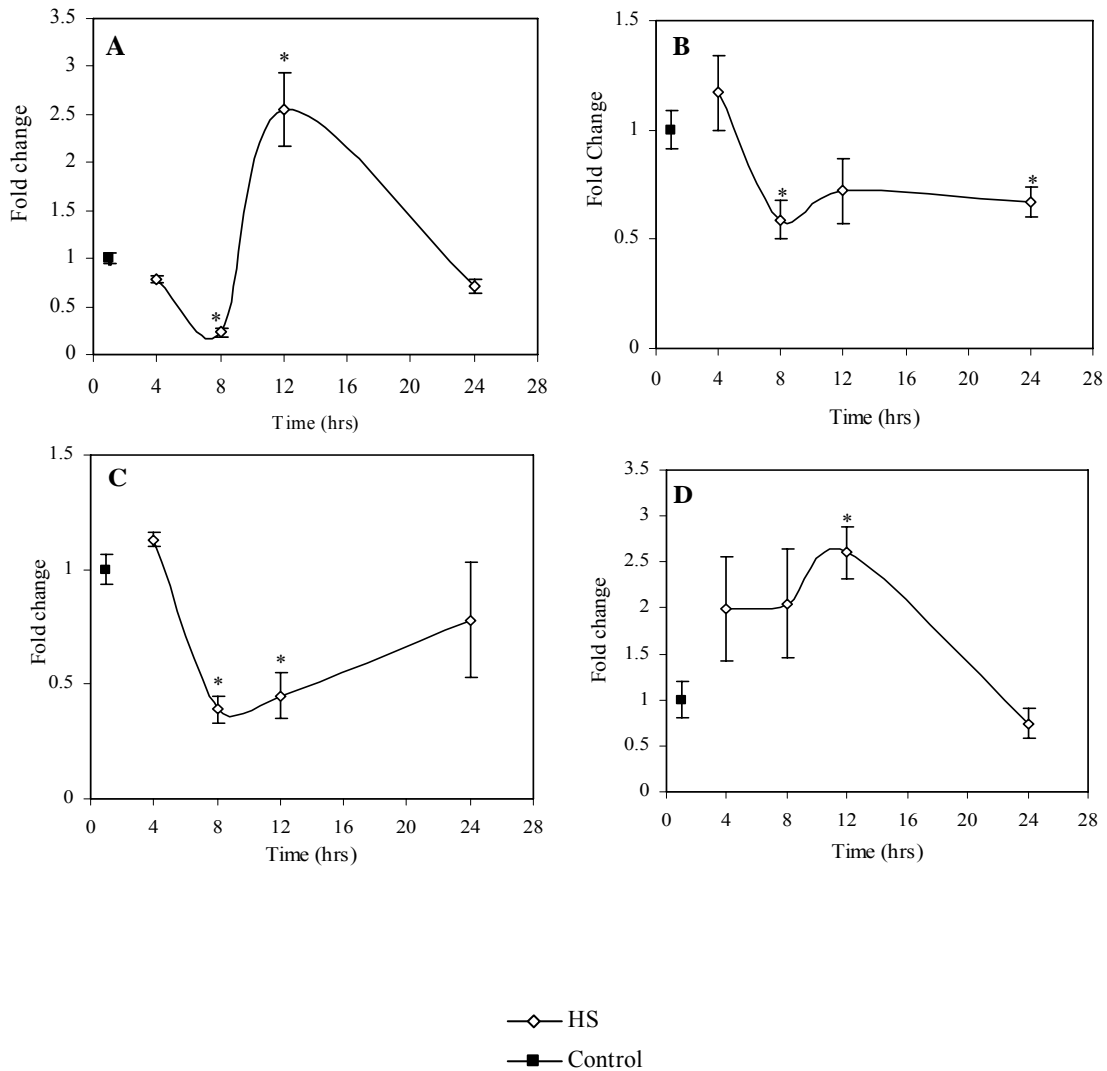


**Figure 17 A:** Quantitative real-time PCR analysis of gene expression in pig hippocampus after heat stress for 4, 8, 12 and 24 hours compared with control. **A**, PolE4; **B**, SCN1B; **C**, SOD-1; and **D**, PSMD10. Data represent means  $\pm$  S.E.M. of three pigs per group and the experiment was repeated two times (n=6). Relative expression of each gene after heat stress relative to control was determined using the gene expression macro software which utilizes the modified  $\Delta\Delta C_t$  method described by (Vandesompele *et al.*, 2002). GAPDH and 36B4 genes were used as internal standards for each sample. * indicates significant from control ( $P \leq 0.05$ ).



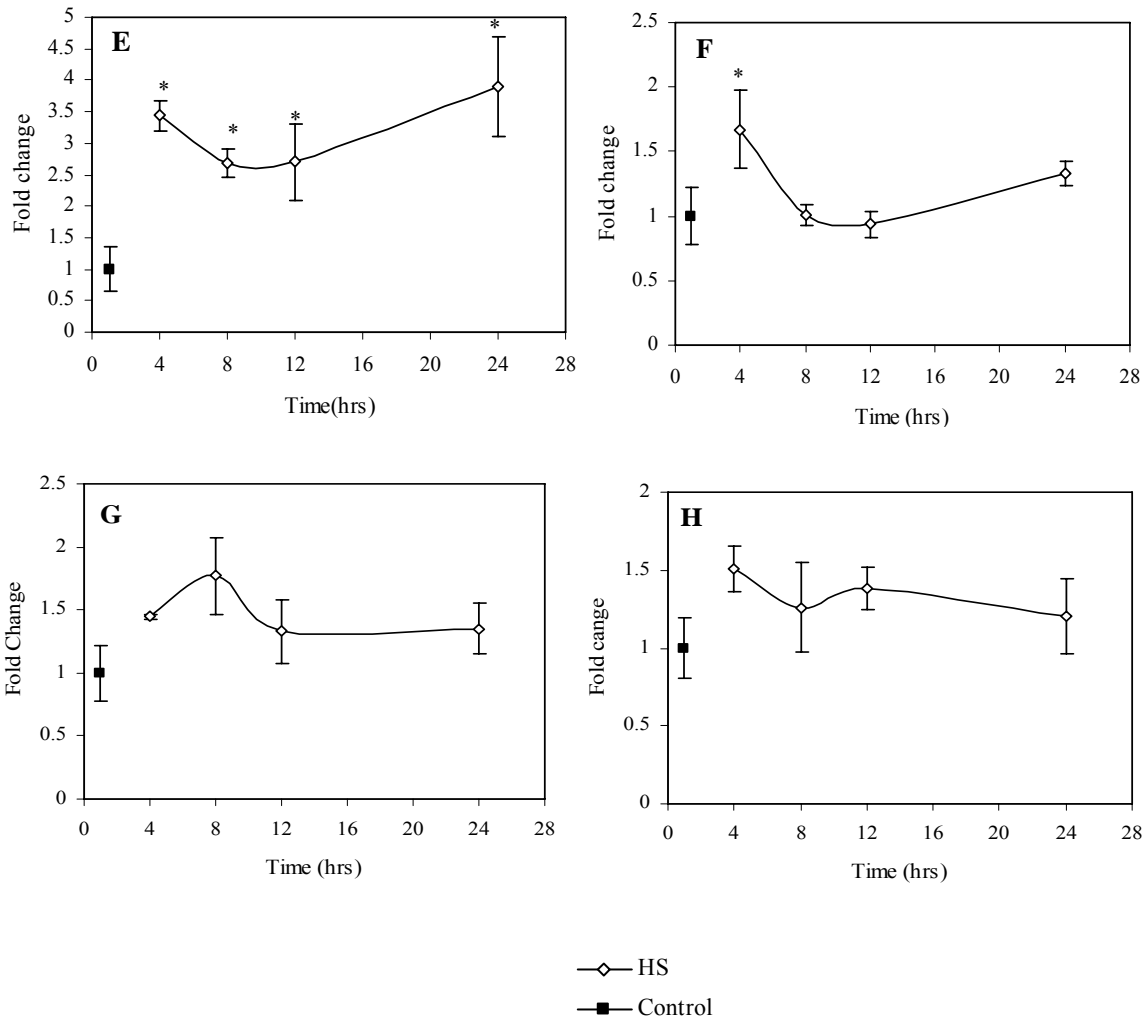


**Figure 17 B:** Quantitative real-time PCR analysis of gene expression in pig hippocampus after heat stress for 4, 8, 12 and 24 hours compared with control. **E**, PSMB9; **F**, HSP70; **G**, HSP27; **H**, HSP90. Data represent means  $\pm$  S.E.M. of three pigs per group and the experiment was repeated two times ( $n=6$ ). Relative expression of each gene after heat stress relative to control was determined using the gene expression macro software which utilizes the modified  $\Delta\Delta C_t$  method described by (Vandesompele *et al.*, 2002). GAPDH and 36B4 genes were used as internal standards for each sample. * indicates significant from control ( $P \leq 0.05$ ).

In the first part of this study, we utilized DD-PCR to identify novel genes in pig hippocampus that are involved in the molecular response of the brain to heat stress. Neuronal cells are more sensitive to the effect of different stressors than any other cell type in the neuronal tissues. This may be due to its limited mitotic activity and limited ability to regenerate. Neuronal injury is an important component in the progression of neuropathological disorders associated with many stressors and neurodegenerative diseases (*Zhang et al, 2006*). For this reason, we decided to investigate the effect of heat stress on hippocampal neuronal cells using the HT-22 cell line which has been suggested to be a good model to study the effect of oxidative toxicity (*Lewerenz et al, 2006*) in the second part of this study. We also focused our attention on the effects of heat stress on SOD-1 that we observed to be downregulation in the hippocampus of heat stressed pigs. SOD-1 is one of the key antioxidant enzymes that, along with another two isozymes, is involved in the dismutation of superoxide radical ( $O_2^{\cdot-}$ ) to  $H_2O_2$  and oxygen. SOD-1 is responsible for approximately 90% of total cellular SOD activity (*Busuttil et al, 2005 & Fridovich, 1997*). Overexpression of SOD-1 in neuronal cells is protective and delays apoptosis triggered by many insults that enhance production of ROS (*Schwartz et al, 1998*). By contrast, downregulation of SOD-1 can promote apoptosis (*Troy and Shelanski, 1994*). The hypothesis that was tested in the second part of this study was that the heat-induced inhibition of SOD-1 is responsible for accumulation of ROS and neuronal cell death associated with heat stress.

### **Effect of heat stress on both SOD-1 mRNA and protein levels in HT-22 cells:**

The hippocampal neuronal cell line (HT-22) was used as an *In vitro* model for hippocampal neuronal tissue. The morphology of HT-22 cells is shown in **Figure 18**. To induce heat stress in these cells, HT-22 cells were incubated in a 43°C water bath for 30 minutes and allowed to recover at 37°C for 0, 1, 2, 4, 8, 12, 24 and 48 hours. At the end of each experimental time period total RNA was isolated from the cells and cDNA was generated. SOD-1 mRNA expression in heat-stressed HT-22 cells relative to non-heated control cells was analyzed using real-time PCR using GAPDH and acidic ribosomal phosphoprotein (36B4) as house keeping genes. SOD-1 expression in response to heat stress was significantly decreased at all experimental sample times after heat stress from 1 hour to 48 hours (**Figure 19**). The expression of SOD-1 at 0 hour recovery was not different from non-heated control. At 12 hour recovery, SOD-1 expression was decreased by  $82.0 \pm 13\%$  compared to non-heated control cells. At 24 hours and 48 hours, the SOD-1 mRNA levels were increased from 12 hours but still significantly lower than non-heated control ( $0.6 \pm 0.18$  and  $0.81 \pm 0.057$  fold, respectively).

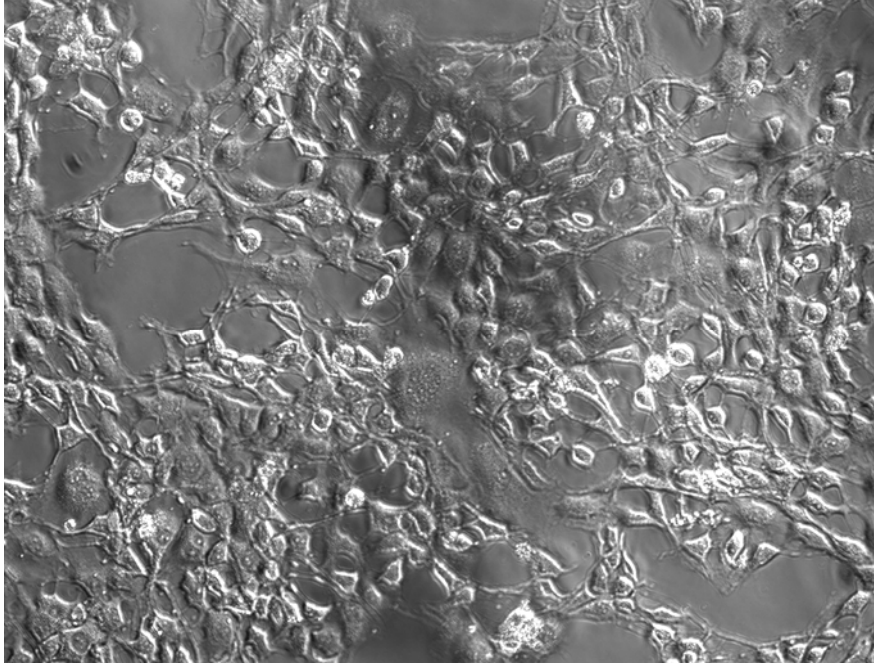


**Figure 18:** Phase contrast photograph of HT-22 cells. Magnification is 20 X.

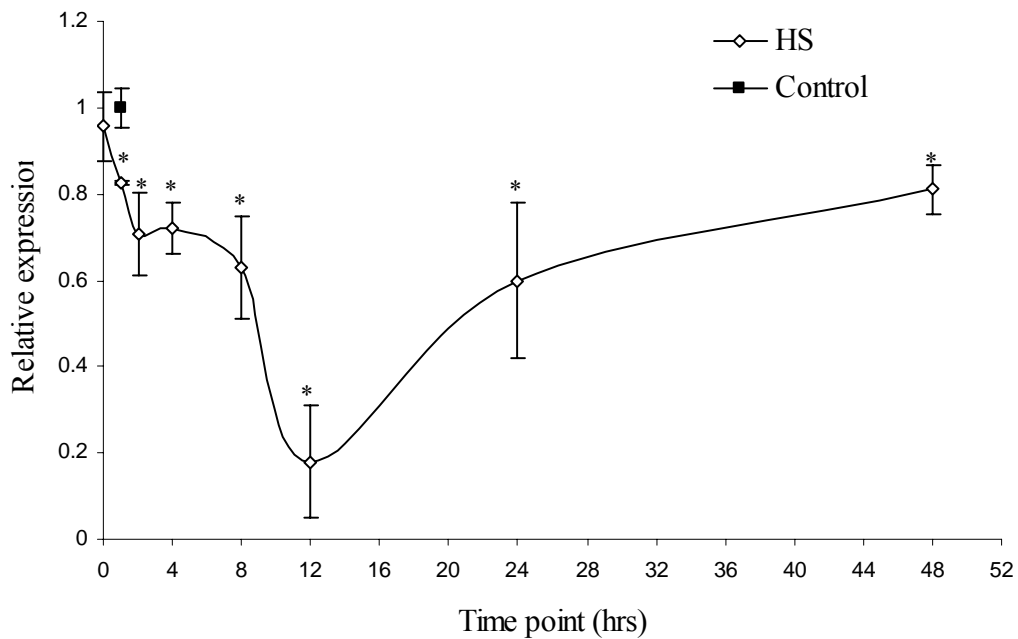


**Figure 19:** Effect of heat stress on SOD-1 mRNA expression in HT-22 cells. HT-22 cells were exposed to heat stress at 43°C for 30 min and allowed to recover at 37°C for up to 48 hours. At the end of each time period, total RNA was isolated, first strand cDNA was generated and SOD-1 mRNA expression was measured by real-time PCR. The expression at each sample time is calculated relative to non-heated control. (n=3); * indicates a significant difference from non-heated control cells ( $P \leq 0.05$ ).

To determine the effect of heat stress on SOD-1 protein expression, HT-22 cells were heat stressed and SOD-1 protein expression was measured by Western blotting. Cell lysates were collected at the end of each experimental time period and protein concentration was determined by DC protein assay kit. Fifteen micrograms of cell lysate proteins were separated by 12% SDS-PAGE and then electrophoretically transferred to nitrocellulose membranes. Membranes were then probed with anti-SOD-1 polyclonal antibody and incubated with HRP-coupled secondary antibody. The immunoreactive bands on membranes were detected by ECL-plus and visualized using a Flour-S Multi Imaging system. The densities of the resulting bands were calculated using Quantity One software. The expression of  $\beta$ -tubulin was used as an internal control. The protein expression in heat stressed cells at different experimental time points was calculated as a percent of non-heated control. SOD-1 protein expression slowly decreased over 48 hours recovery period after heat stress (**Figure 20**). This decrease in SOD-1 protein expression was significantly different from unheated control at 4 hours after heat stress and continued to decrease up to 48 hours after heat stress. The maximum decrease in SOD-1 protein expression was seen at 48 hours corresponding to a  $54.0 \pm 8.0\%$  decrease compared to non-heated control cells.

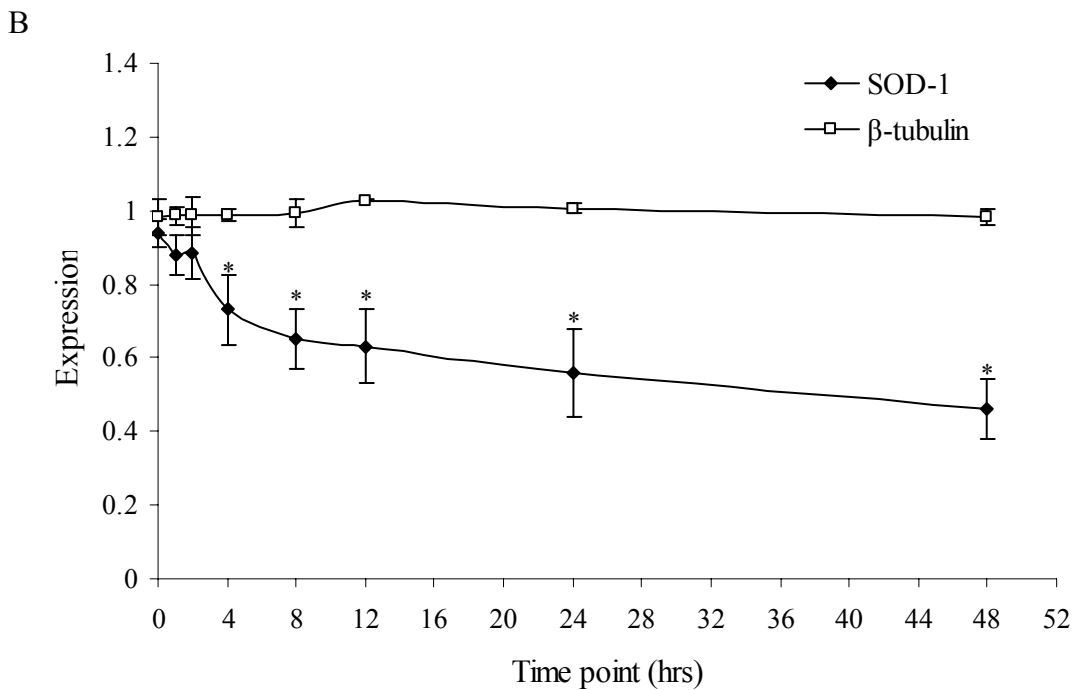
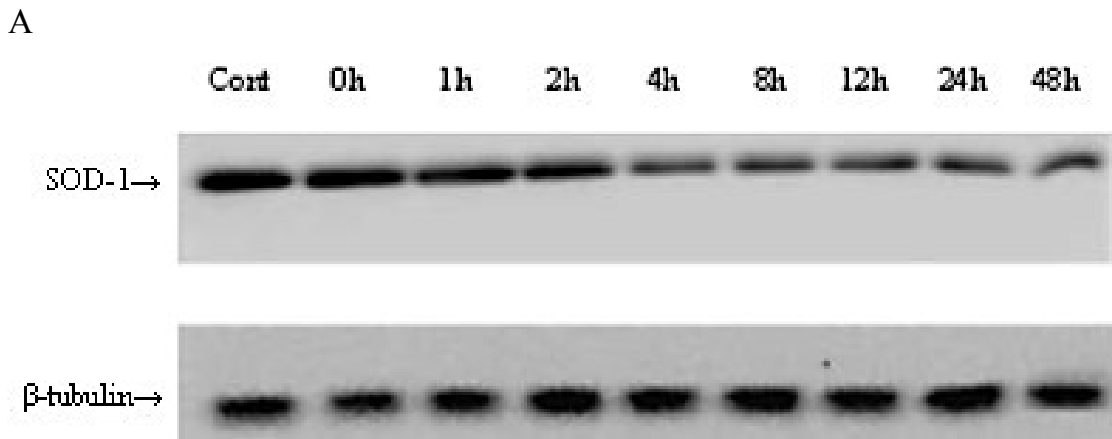


**Figure 20:** Effect of heat stress on SOD-1 protein level in HT-22 cells. Western blot analysis of SOD-1 protein level in lysates prepared from HT-22 cells exposed to heat at 43°C for 30 min and then allowed to recover at 37°C up to 48 hours. The cell lysates were separated by 12% SDS-PAGE, and the protein was detected by immunoblotting. **A**, Western blot showing the protein expression of SOD-1 (upper panel) and  $\beta$ -tubulin (lower panel) in both unheated control and heat stressed HT-22 cells. Lane 1, control; lane 2-lane 9, experimental time points during recovery after heat stress from 0 to 48 hours. **B**, quantitative analysis of SOD-1 protein level and  $\beta$ -tubulin. (n=3); * indicates a significant difference from unheated control cells ( $P \leq 0.05$ ).

### **Effect of heat stress on SOD-1 activity:**

The effect of heat stress on SOD-1 enzymatic activity in HT-22 cells was assessed by using a commercially available SOD activity kit (Cayman Chemicals). HT-22 cells were heat stressed and cell lysates were collected for determination of SOD-1 activity. The total protein concentration in each sample was adjusted to the same concentration (2  $\mu\text{g/ml}$ ). A standard curve using serial dilutions of SOD-1 standard stock solution (0.25 U/ml- 0.05 U/ml) was determined and the activity of SOD-1 in each sample was calculated according to the equation obtained from the linear regression of the standard curve (**Figure 21**). Basal SOD-1 activity in non-heated control cells was 3.94 U/ $\mu\text{g}$  protein. After 30 minutes heat stress, SOD-1 activity in HT-22 cells was reduced by  $35 \pm 5.5\%$  when compared to unheated control cells (**Figure 22**). SOD-1 activity continued to decrease after recovery and was reduced by  $84.0 \pm 4.0 \%$  at 12 hours and remained at this level for up to 48 hours.



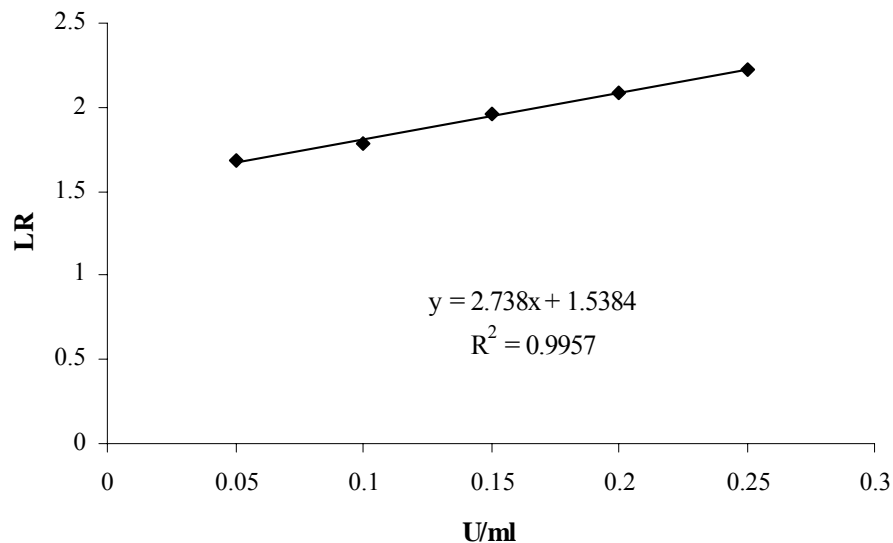


**Figure 21:** SOD-1 activity standard curve. SOD standards were prepared from serial dilutions of SOD standard stock solution (0.25U/ml- 0.05U/ml). The change in color in test and standard samples was measured at 450 nm. The absorbance of blank sample (no SOD activity) was divided by the absorbance of each standard and test sample to determine the linearized rate (LR) of each sample. Standard curve was created by plotting LRs of different SOD standard dilutions as a function of final SOD activity (U/ml). The SOD activity in each test sample was calculated from the equation obtained from the linear regression of the standard curve.

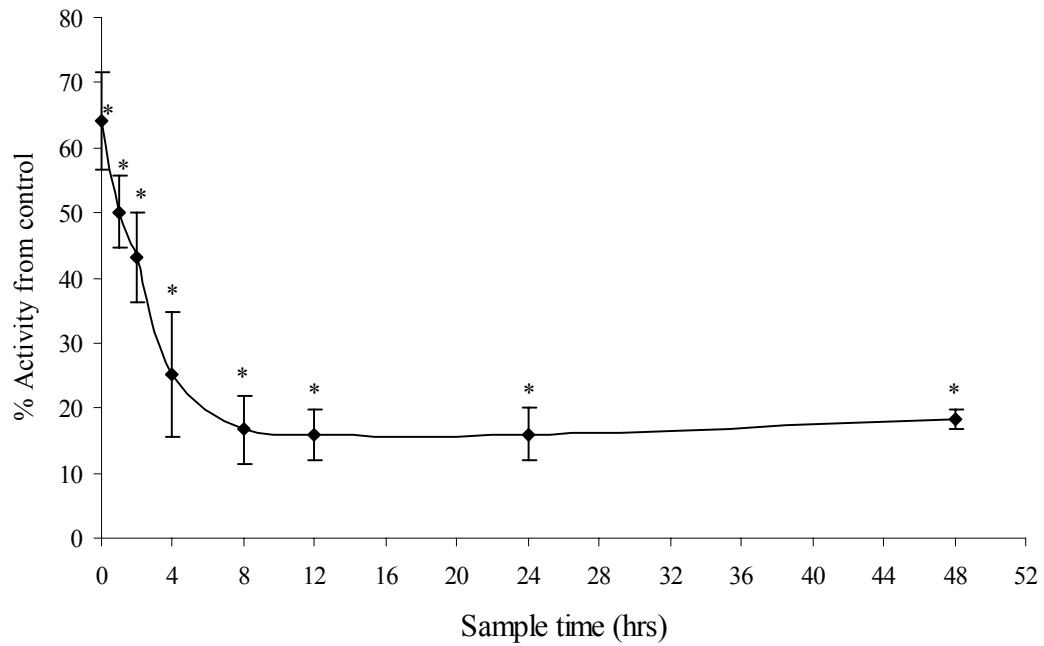


**Figure 22:** Effect of heat stress on SOD-1 activity in HT-22 cells. HT-22 cells were exposed to heat stress at 43°C for 30 min and then allowed to recover at 37°C for different times (0,1,2,4,8,12,24 and 48 hour). At the end of each sample time, cytosolic extracts were isolated. All samples were adjusted to the same total protein concentration and SOD-1 enzymatic activity was measured. (n=5); * indicates a significant difference from unheated control cells ( $P \leq 0.05$ ).

### **Heat stress diminishes HT-22 cell viability over time:**

To determine the effect of heat stress on HT-22 cell viability, HT-22 cells were exposed to heat stress at 43°C for 30 min and allowed to recover at 37°C for up to 48 hours. Unheated control cells were left incubated at 37°C for the same amount of time. At the end of each sample time, cells were examined microscopically, dislodged and cell number determined using the Cell Proliferation Assay kit (Molecular Probes). After a 30 minute heat stress, dead cells were clearly visible microscopically in the cultures. Rounded and detached cells were detected over the entire recovery time of up to 48 hours after heat stress. To quantify cell number following heat stress, a calibration standard curve was created for relating cell number to observed fluorescence (**Figure 23**). Heat stress caused a  $24.0 \pm 4.3\%$  decrease in cell number by 1 hour after heat stress in comparison with unheated control cells. The decline in cell number continued for up to 12 hours where there was a  $62.4 \pm 8.6\%$  decrease in cell number compared to unheated control. Cell number remained low for the entire 48 hour experiment period (**Figure 24**).

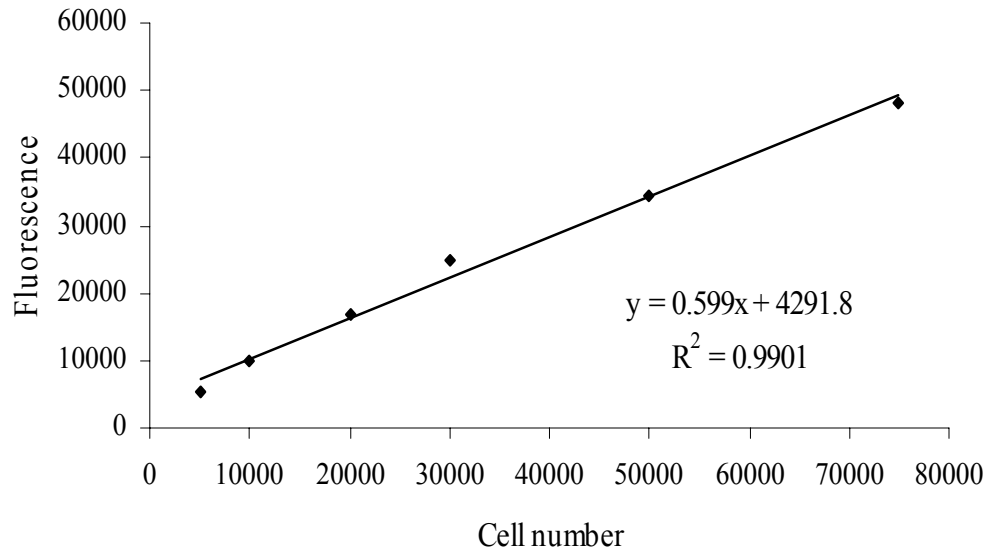


**Figure 23:** Cell proliferation assay calibration standard curve. Calibration curve was created for converting the observed fluorescence values in test samples into cell number according to the equation obtained from the linear regression of the standard curve.

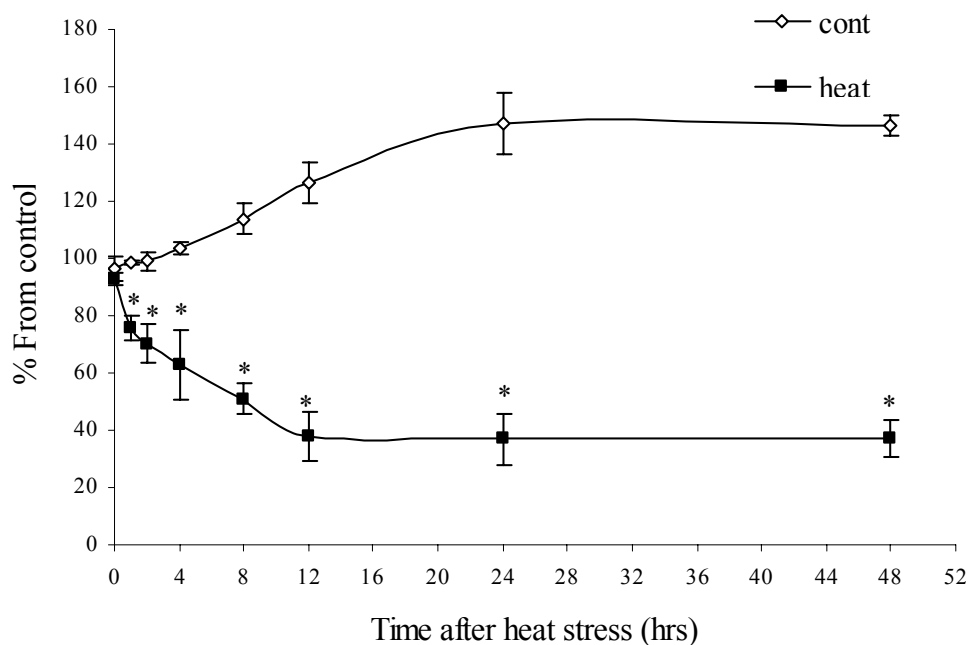


**Figure 24:** Effect of heat stress on HT-22 cell proliferation. HT-22 cells were exposed to heat stress at 43°C for 30 min and allowed to recover at 37°C for different times. Unheated control cells were maintained at 37°C for the same time. At each sample time, cell number was measured. (n=3); * indicates significantly different from unheated control cells ( $P \leq 0.05$ ).

**Effect of pretreatment with EUK-134 on heat-induced decrease in HT-22 cell viability:**

Experiments to date suggested that heating HT-22 cells to 43°C for 30 minutes causes a decline in SOD-1 gene and protein expression, and a decrease in cell viability. We determined to investigate the effect of pretreatment of HT-22 cells with a synthetic SOD-mimetic, EUK-134, on heat-induced decrease in cell viability. HT-22 cells were treated with EUK-134 (10-100  $\mu$ M) or its vehicle for 1 hour and exposed to heat stress as previously discussed. Cell number was determined using the Cell Proliferation Assay kit. Pretreatment of HT-22 cells with EUK-134 at 10  $\mu$ M, 50  $\mu$ M and 100  $\mu$ M 1 hour before heat stress completely protected HT-22 cells from heat-induced cell death (**Figure 25**). There was no difference in the effectiveness of the three concentrations and therefore the concentration of 10  $\mu$ M was chosen for all future work. Pretreatment of HT-22 with 10  $\mu$ M EUK-134 had no effect on growth rate in non-heated control cells but completely reversed the effect of heat stress on cell death (**Figure 26**).

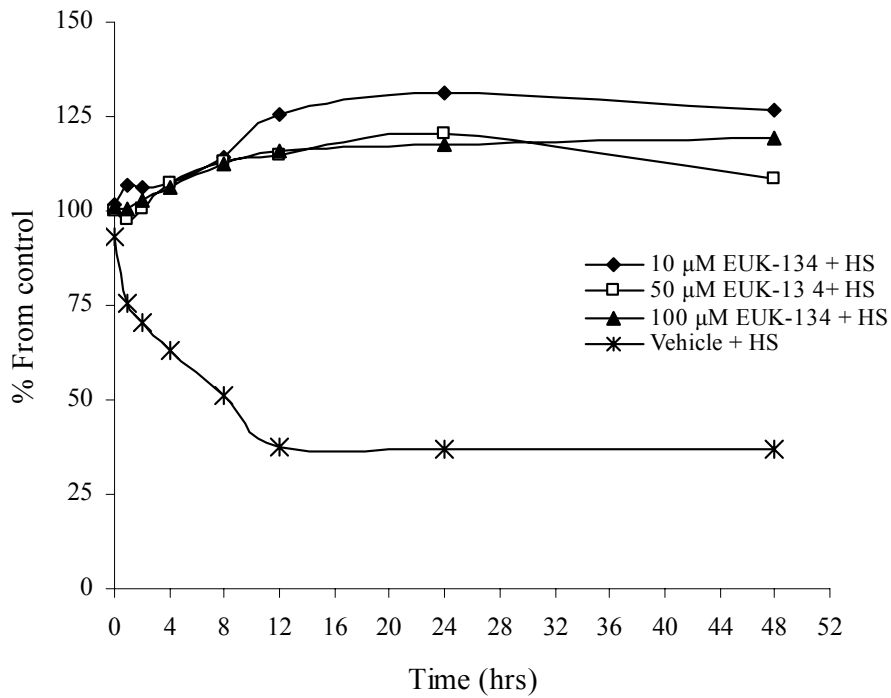


**Figure 25:** Effect of pretreatment of HT-22 cells with EUK-134 (10-100  $\mu$ M) on cell proliferation. HT-22 cells were treated with either 10  $\mu$ M, 50  $\mu$ M or 100  $\mu$ M EUK-134 or its vehicle for 1 hour and then exposed to heat stress at 43°C for 30 min and allowed to recover at 37°C for up to 48 hours. At each sample time cells were collected and cell viability was assayed. HS: heat stress.

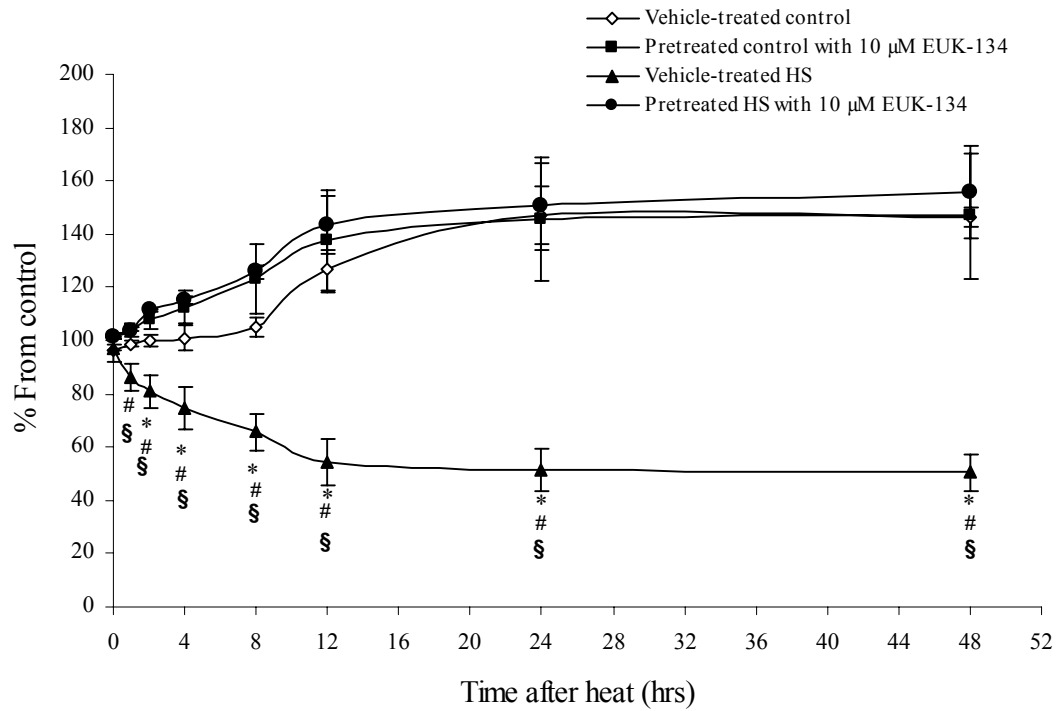


**Figure 26:** Effect of pretreatment with EUK-134 (10 μM) on heat-induced decrease in HT-22 cell proliferation. HT-22 cells were either treated with 10 μM EUK-134 or its vehicle for 1 hour and then exposed to heat stress at 43°C for 30 min and allowed to recover at 37°C for up to 48 hours. Control cells were treated with 10 μM EUK-134 or its vehicle and left incubated at 37°C for the same time. At each sample time, cells were collected and cell viability was assayed. HS: heat stress. (n=3); * indicates significantly different from vehicle-treated, non-heated control ( $P \leq 0.05$ ); # indicates significantly different from treated, non-heated control ( $P \leq 0.05$ ) and § indicates significantly different from pretreated heat stressed cells ( $P \leq 0.05$ ).



### **Effect of heat stress on intracellular ROS generation:**

To determine the effect of heat stress on intracellular reactive oxygen species (ROS) generation, HT-22 cells were exposed to heat stress at 43°C for 30 min and allowed to recover at 37°C for 2 hours. Unheated control cells were maintained at 37°C for the same period. Cells were labeled with carboxy-DCF fluorescent probe using the Image-iT Live Green ROS detection kit (Molecular Probes). The intensity of green fluorescence corresponding to oxidized DCF dye is directly proportional to the level of intracellular ROS and was determined qualitatively by fluorescence microscopy. tBHP (100 µM) was used as a positive control and enhanced the generation and accumulation of intracellular ROS as determined by elevated green fluorescence intensity inside the cells (**Figure 27**). The level of ROS accumulation in HT-22 cells was also enhanced markedly after heat stress when compared to non-heated control cells (**Figure 27**) suggesting that heat stress induces oxidative stress in HT-22 cells.

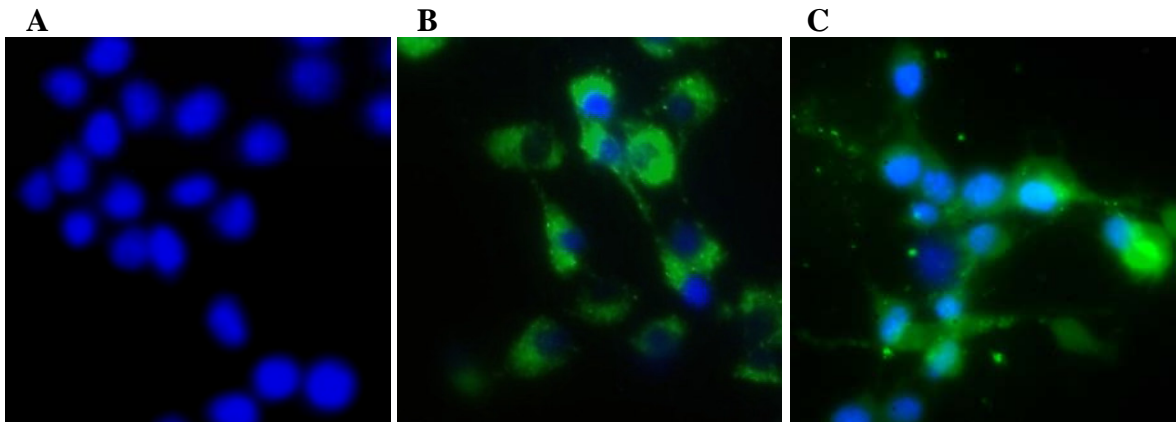


**Figure 27:** Effect of heat stress on ROS generation in HT-22 cells. HT-22 cells were exposed to heat stress at 43°C for 30 min and allowed to recover at 37°C for 2h. Unheated control cells were maintained at 37°C for the same period. HT-22 cells were treated with 100  $\mu$ M tBHP for 2h (as positive control). Cells were labeled with 25  $\mu$ M DCF and visualized under fluorescence microscope. **A**, unheated control cells; **B**, tBHP-treated cells; **C**, heat stressed cells. Pictures are representative of three independent experiments.

**Effect of pretreatment with 10  $\mu$ M EUK-134 on heat-induced ROS generation in HT-22 cells:**

Since the enzymatic activity of SOD-1 decreased in HT-22 cells in response to heat stress and the pretreatment of HT-22 cells with SOD-mimetic EUK-134 inhibited the heat-induced cell death, we determined whether pretreatment with EUK-134 could also reduce the heat-induced accumulation of ROS. HT-22 cells were treated with EUK-134 (10  $\mu$ M ) or its vehicle for 1 hour and then exposed to heat stress at 43°C for 30 min and allowed to recover at 37°C for 2 hours. Vehicle-treated control and EUK-134-treated control cells were maintained at 37°C for the same period. Cells were probed with carboxy-DCF fluorescent dye and the intensity of the green fluorescence that was determined by fluorescence microscopy. Pretreatment of HT-22 cells with EUK-134 inhibited the heat-induced accumulation of ROS. Cells pretreated with 10  $\mu$ M EUK-134 (EUK-134-treated, heat stressed and EUK-134-treated, unheated control) showed reduced intensity of green fluorescence and the number of DCF-labeled cells when compared to vehicle-treated, heat stressed HT-22 cells. In addition, there was no difference in DCF-labeling between EUK-134-treated, heat stressed HT-22 cells, EUK-134-treated, unheated HT-22 cells and vehicle-treated, unheated control HT-22 cells (**Figure 28**).

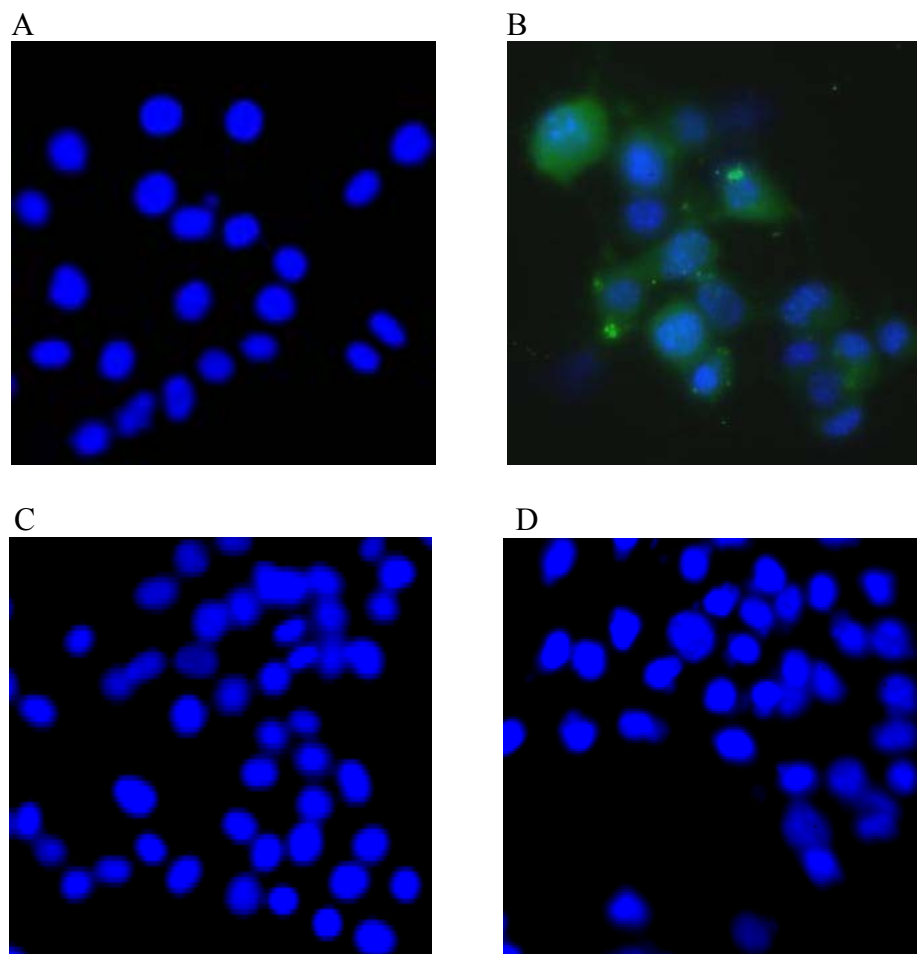


**Figure 28:** Effect of pretreatment with EUK-134 (10  $\mu$ M) on heat-induced generation of ROS in HT-22 cells. HT-22 cells were treated with EUK-134 (10  $\mu$ M) or its vehicle for 1 hour and then exposed to heat stress at 43°C for 30 min and allowed to recover at 37°C for 2 hours. Unheated control cells were treated with 10  $\mu$ M EUK-134 for 1 hour or its vehicle and then maintained at 37°C for the same period. Cells were labeled with 25  $\mu$ M H₂DCFDA and visualized under a fluorescence microscope. **A**, vehicle-treated, unheated control cells; **B**, vehicle-treated, heat stressed cells; **C**, EUK-134-treated unheated control cells; **D**, EUK-134-treated heat stressed cells. Pictures are representative of three independent experiments.

### **Effect of heat stress on apoptotic cell death in HT-22 cells:**

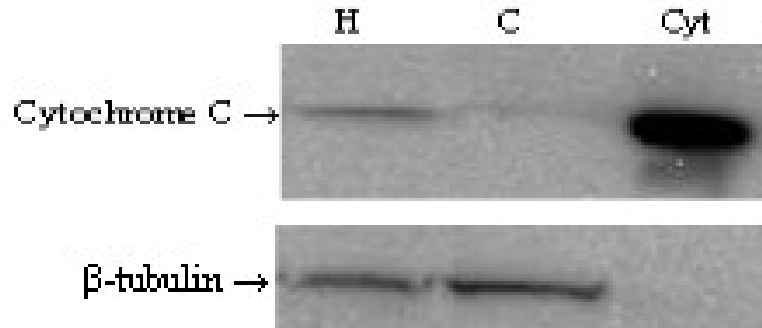
To determine the characteristic of heat-induced HT-22 cell death, mitochondrial release of cytochrome c were and genomic DNA fragmentation determined to assess apoptotic cell death.

Cytochrome c release from the mitochondria into the cytoplasm is another hallmark of apoptosis (*Lopez-Hernandez, et al., 2006*). Cytochrome c is an abundant hemoprotein that resides in the intermembrane space of mitochondria where it serves as an electron shuttle between Complex III and IV of the mitochondrial respiratory electron transport chain (*Bayir et al., 2006*). It plays a key role in the initiation of apoptosis when released into the cytoplasm (*Baydas et al., 2005*). The effect of heat stress on cytochrome c release from the mitochondrial intermembrane space to the cytoplasm was examined by immunoblotting. HT-22 cells were exposed to heat stress at 43°C for 30 min and allowed to recover at 37°C for 12 hours. Unheated control cells were maintained at 37°C for the same period. Cytosolic protein fractions were collected and protein concentration was determined by DC protein assay kit. Fifteen micrograms of cell lysates proteins were separated by 12% SDS-PAGE and then transferred to nitrocellulose membranes. Membranes were then probed with anti-cytochrome c monoclonal antibody and incubated with HRP-coupled secondary antibody. The immunoreactive bands on the membranes were detected by ECL-plus and visualized using a Flour-S Multi Imaging system. The densities of the resulting bands were calculated using Quantity One software. The expression of  $\beta$ -tubulin was used as internal control. Cytochrome c levels were barely detected in the cytosol of non-heated control cells (**Figure 29**). Twenty four hours after

heat stress, there was a 3.1 fold increase in cytosolic cytochrome c level compared to non-heated control cells (**Figure 29**).

To determine whether pretreatment with EUK-134 was effective in preventing heat-induced cytochrome c release from the mitochondria, HT-22 were treated with EUK-134 (10  $\mu$ M ) or its vehicle for 1 hour and exposed to heat stress at 43°C for 30 min and allowed to recover at 37°C for 24 hours. Non-heated control cells were treated with EUK-134 (10  $\mu$ M) or its vehicle for 1 hour and maintained at 37°C for 24 hours at 37°C. Cytosolic protein fractions were collected and cytochrome c release to the cytoplasm was determined by Western blot analysis. Pretreatment with EUK-134 (10  $\mu$ M) almost completely blocked the heat-induced translocation of cytochrome c into the cytosol. Analysis of cytochrome c demonstrated that immunoreactivity was undetectable in the cytosolic fraction of both vehicle-treated, non-heated control, non-heated, EUK-134-treated control cells and EUK-134-treated, heat stressed cells. Cytochrome c release was dramatically increased in vehicle-treated, heat stressed cells when compared to vehicle-treated, non-heated control (**Figure 30**).

**A**



**B**

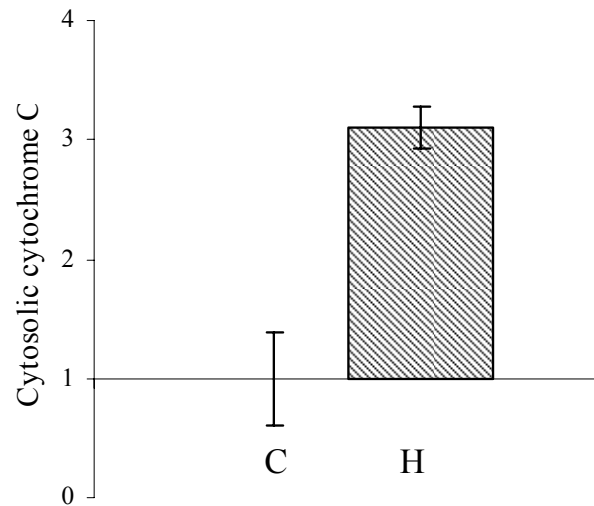


**Figure 29:** Effect of heat stress on cytochrome c release to the cytoplasm in HT-22 cells. Western blot analysis of cytochrome c release in cytosolic fraction of cell lysate prepared from HT-22 cells exposed to heat at 43°C for 30 min and then allowed to recover at 37°C up to 48 hours. The cell lysates were separated by 12% SDS-PAGE and the protein were detected by Western blot analysis. **A**, Western blotting showing cytochrome c (upper panel) and  $\beta$ -tubulin (lower panel) in cytosolic cell lysates prepared from both unheated control and heat stressed HT-22 cells. C, control; H, heat stressed cells; Cyt, *In vitro* purified cytochrome c protein as a positive control. **B**, quantitative analysis of cytoplasmic cytochrome c protein level.

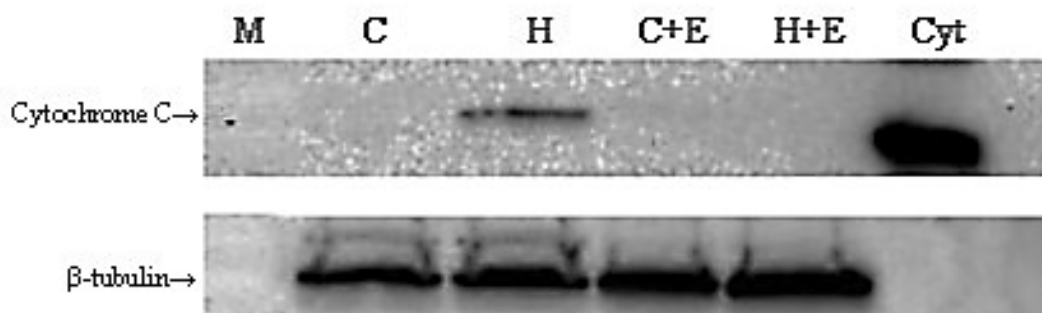


**Figure 30:** Effect of pretreatment with EUK-134 (10  $\mu$ M) on heat-induced cytochrome c release to the cytoplasm in HT-22 cells. Western blot analysis to determine cytochrome c protein level in cytosolic fraction prepared from HT-22 cells. Cells were treated with 10  $\mu$ M EUK-134 for 1 hour or its vehicle and then exposed to heat stress at 43°C for 30 min and allowed to recover at 37°C for 12 h. Non-heated control cells were treated with 10  $\mu$ M EUK-134 for 1 hour or its vehicle incubated at 37°C for 12 h at 37°C. Western blot analysis showing cytochrome c (upper panel) and  $\beta$ -tubulin (lower panel) in cytosolic cell lysates prepared from both vehicle-treated, non-heated control, vehicle-treated, heat stressed, EUK-134-treated, non-heated control, and EUK-134-treated, heat stressed HT-22 cells. M, Molecular weight marker; C, vehicle-treated, non-heated control; H, vehicle-treated, heat stressed; C+E, EUK-134-treated, non-heated control; H+E, EUK-134-treated, heat stressed; Cyt, *In vitro* purified cytochrome c protein as a positive control.  $\beta$ -tubulin was used as internal control (lower panel). Blot is a representative of three independent experiments.



DNA fragmentation or ladder pattern of genomic DNA was examined using agarose gel electrophoresis (*Wang et al., 2005*). HT-22 cells were exposed to heat stress at 43°C for 30 min and allowed to recover at 37°C for 24 hours. Non-heated control cells were maintained at 37°C for 24 hours. Genomic DNA was isolated and electrophoretically separated on a 1.5 % agarose gel. The DNA fragmentation was visualized using UV illumination on a Fluor-S imager. DNA fragmentation was observed in the heat stress HT-22 cells in comparison to non-heated control cells (**Figure 31**).

To determine the effect of pretreatment with EUK-134 on heat-induced DNA fragmentation, HT-22 were treated with EUK-134 (10 µM) or its vehicle for 1 hour and exposed to heat stress at 43°C for 30 min and allowed to recover at 37°C for 24 hours. Non-heated control cells were treated with EUK-134 (10 µM) or its vehicle for 1 hour and maintained at 37°C for 24 hours at 37°C. Genomic DNA was isolated from HT-22 cells and DNA fragmentation was assessed by agarose gel electrophoresis. EUK-134 alone had no effect on DNA fragmentation in non heated control cells but completely blocked the DNA fragmentation induced by heat stress (**Figure 32**).

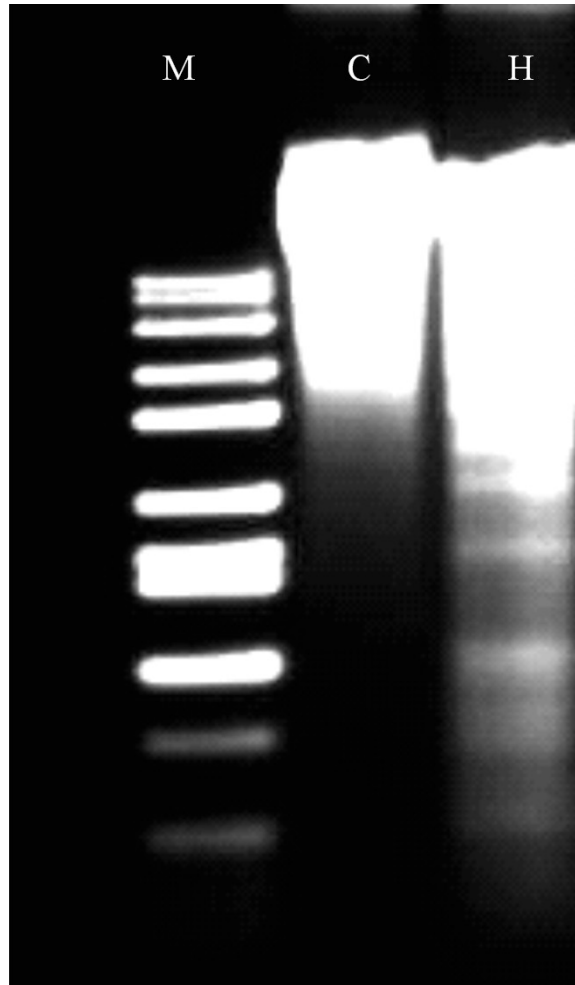


**Figure 31:** Effect of heat stress on DNA fragmentation in HT-22 cells. HT-22 cells were exposed to heat stress at 43°C for 30 min and allowed to recover at 37°C for 24 hours. Unheated control cells were maintained at 37°C for 24 hour at 37°C. Genomic DNA was isolated and assessed by agarose gel electrophoresis and DNA fragmentation was visualized using UV illumination on a Flour-S imager. M, DNA ladder; C, unheated control; H, heat stressed cells. Picture is representative of three independent experiments.

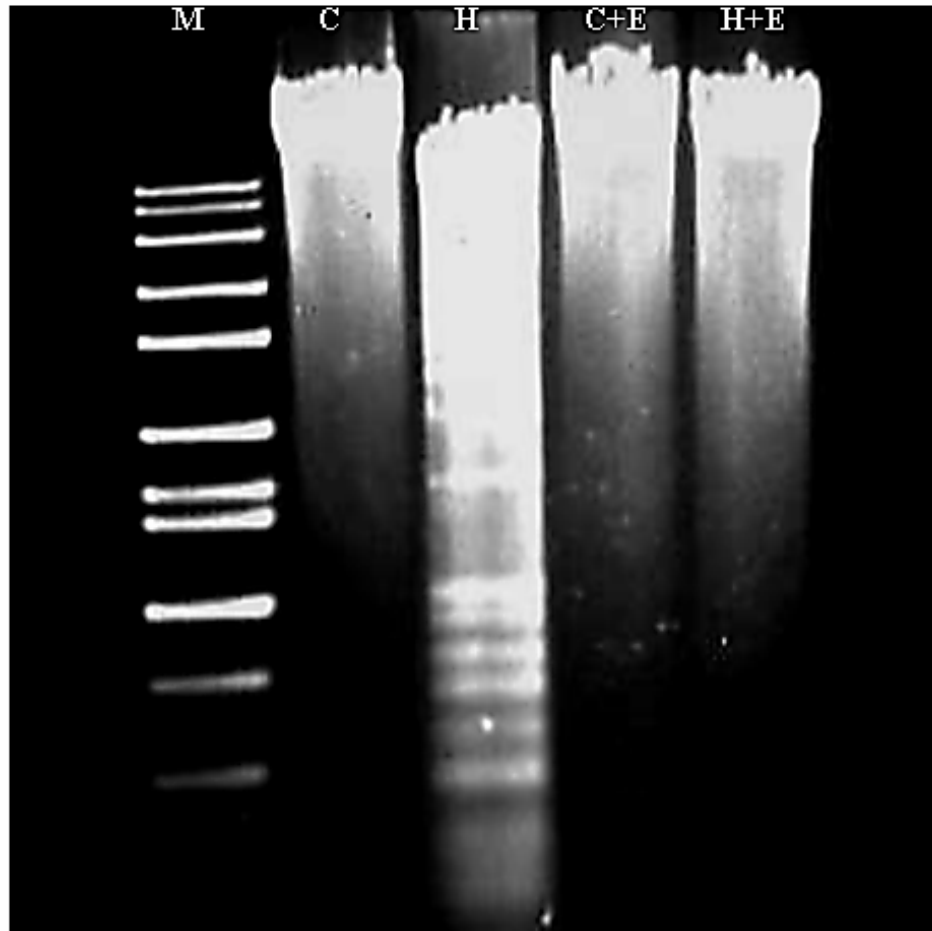


**Figure 32:** Effect of pretreatment with EUK-134 (10  $\mu$ M) on heat-induced DNA fragmentation in HT-22 cells. HT-22 cells were treated with EUK-134 (10  $\mu$ M ) or its vehicle for 1 hour and then exposed to heat stress at 43°C for 30 min and allowed to recover at 37°C for 24 h. Control cells were treated with EUK-134 or its vehicle and incubated at 37°C for 24 h at 37°C. Genomic DNA was isolated from both heated and control cells and separated on 1.5% agarose gels, stained with ethidium bromide and visualized under UV light on Flour-S imager. M, DNA ladder; C, untreated, vehicle-treated control cells; H, heat stressed cells; C+E, EUK-134-treated control; H+E, heat stressed cells pretreated with EUK-134. Electrophoretic pattern of DNA fragmentation results are representative of three independent experiments.

## DISCUSSION

This study was undertaken to determine the effect of heat stress on gene expression in the hippocampus. In the first part of the study, we used differential display PCR to examine the effect of a mild heat stress in pigs on hippocampal gene expression. In the second part of the study, we used a hippocampal neuronal cell line to investigate the protective effect of superoxide dismutase-1 on heat stressed hippocampal neurons.

In the first part of this study, we investigated the change in porcine hippocampal gene expression in response to heat stress. We used pigs in this study because of the genetic similarity and value of this model in human medicine. The pigs were maintained at either 70°F (control) or 90°F (heat stressed) for 4, 8, 12 or 24 hours. They were monitored for changes in body temperature, heart rate, and respiratory rate. Both core body temperature and respiratory frequencies were elevated over the time course of the experiment which is a good indication of heat-stress in these animals (*Huynh et al., 2005 & Berman, 2005*).

To determine the effect of heat stress on hippocampal gene expression, hippocampi were excised from 12 hour control or heat stressed pigs for mRNA differential display RT-PCR analysis. Hyperthermia, like many other stressors, triggers a reactive cellular response through activation of specific transduction pathways that leads to the alteration in the expression of several gene categories aimed at either cell protection against heat damage or cell death (*Maroni et al., 2003*). Among the thirty one differentially expressed DNA fragments we isolated, six were identified to be similar to

known human genes with sequence similarity within 3'-ORF of these genes. The differential expression of four of these genes (PolE4, PSMD10, SOD-1 and SCN1B) was further confirmed and quantified with real-time PCR.

DNA polymerase  $\epsilon$  p12 (PolE4) gene expression was slightly decreased after 8 hours of heat stress, but was upregulation to more than 2.5 fold after 12 hours of heat stress. PolE4 is a structural subunit of DNA polymerase  $\epsilon$  that contains four subunits; large catalytic subunit A (p261) and three smaller regulatory subunits B (p59), C (p12) and D (p17) (*Pospiech and Syvaaja, 2003*). Polymerase  $\epsilon$  is involved in replication and repair of cellular DNA. DNA polymerase  $\epsilon$  p12 has also been implicated in the recombinational process in the cell (*Takahashi et al., 2005 & Rusyn et al., 2004*). It has been reported that polymerase  $\epsilon$  is mainly involved in DNA repair but not DNA synthesis in adult rat brain (*Prapura and Rao, 1997 & Raji et al., 2002*). The increase in PolE4 expression observed in the present study suggests that there may be an upregulation of the complete DNA polymerase  $\epsilon$  enzyme (*Lee et al., 2001*). Steinau et al. reported an elevation in the gene expression of DNA pol  $\epsilon$  p12 subunit in blood cells of chronic fatigue syndrome (CFS) patients following exercise. CFS is a potentially disabling disorder that is closely linked to impaired energy metabolism and increased oxidative stress (*Chaudhuri and Behan, 2004*). We propose that the heat-induced increase in the expression of PolE4 occurs as a defense mechanism against the heat stress-induced oxidative DNA damage. This agrees with previous reports in that the levels of DNA repair genes were increased in response to chemical-induced oxidative stress in mouse liver (*Rusyn et al., 2004 & Cabelof et al., 2002*) and after transient focal ischemia and reperfusion in rat brain (*Lan et al., 2003*).

The expression of the proteasomal subunit gene, PSMD10, was also found to be upregulated by heat stress. PSMD10 encodes a non-ATPase subunit of the 19S regulator of 26S proteasome. The 26S proteasome is a multisubunit ATPase-dependent protease, distributed in the cytoplasmic and nuclear compartments (*Anderson et al., 2004*). It is composed of at least 32 different protein subunits that are encoded by at least 32 different genes (*Anderson et al., 2004*). The 26S proteasome consists of the 20S proteolytic core and 19S regulatory element that caps the 20S at both ends (*Bose et al., 2004 & Piccinini et al., 2003*). In the present study, we also looked at the expression of PSMB9 gene and found it to be enhanced in response to heat stress. PSMD9 encodes a member of the proteasome  $\beta$ -type family that is a 20S core beta subunit. The 26S proteasome plays a central role in the degradation of intracellular proteins. It degrades abnormal proteins and mediates post-translational modification and degradation of proteins. It appears to be essential for most cellular processes such as cell cycling, DNA repair, cell signaling, gene transcription and apoptosis (*Ardley et al., 2005*). The genes encoding the 26S proteasome subunits (PSM genes) and its component proteins have been reported to be induced by heat stress and are suggested to be involved in cellular protection against stressful conditions in yeast cells (*Hahn et al., 2006*), mouse liver (*Anderson et al., 2004*) and human fibroblasts (*Beedholm et al., 2004*). The induction of PSM genes expression in response to heat stress is thought to be an adaptation to the decrease in the levels of functional proteasomes (*Meiners et al., 2003*). The activity of the catalytic core subunits of the proteasome 26S is inhibited as a result of heat-induced accumulation of abnormal denatured proteins (*Piccinini et al., 2003*). The diminished proteasomal activity triggers an increase in PSM gene transcription as an autoregulatory feedback mechanism that

helps in the compensation of reduced proteasomal activity. This is supported by our data for HSPs gene expression in porcine hippocampus. In our study, we found only a small induction of the HSP genes, HSP70, HSP90 and HSP27 ( $\leq 1.7$  fold) in response to heat stress. Heat shock proteins play an important role in cell protection and cell recovery from heat-induced damage through their role in preventing protein aggregation; catalyzing refolding of misfolded proteins, facilitating degradation of strongly damaged proteins and DNA damage repair (*Pandita et al., 2004*). Several studies have reported the induction of heat shock protein mRNA and /or protein levels in the hippocampus after heat stress (*Maroni et al., 2003; Bechtold and Brown, 2003; Pavlik et al., 2003; Lim et al., 2003 & Reynold and Allen, 2003*) even though the hippocampus shows the weakest heat shock response compared to other body tissues in response to hyperthermia (*Maroni et al., 2003*). Also, the hippocampal neurons were unable to induce heat shock response after heat stress due to lack of HSF-1 (*Marcuccilli et al., 1996 and Kaariranata et al., 2002*). The disruption in the heat shock response leads to the accumulation of denatured and damaged proteins which in turn alters the proteasomal activity leading to heat-induced upregulation of proteasomal subunits genes as feed back of reduced activity (*Rattan, 2004*). The upregulation of proteasomal subunits by heat stress could be a possible explanation for our HSPs data in that the stimulation of proteasome expression helps in rapid turnover of denatured proteins (*Friant et al., 2003*) which may negatively affect HSF-HSPs complex and activation of HSF-1 (*Awasthi and Wagner, 2005*).

The  $\beta_1$  subunit of the voltage-gated sodium channel gene (SCN1B) was also downregulated in heat-stressed pig hippocampus. The voltage-gated sodium channel (VGSCs) is a membrane protein that plays an important role in electrical signaling by

generation and propagation of action potentials in excitable tissues by mediating the rapid entry of Na⁺ ions upon voltage changes across the plasma membrane (*Qin et al., 2003 & Takahashi et al., 2003*). The VGSCs are heteromultimeric proteins consisting of a pore-forming  $\alpha$ -subunit which is responsible for the voltage-sensitive characteristic of the channel and auxiliary  $\beta$ -subunits that act as regulators for the  $\alpha$ -subunit function. The  $\beta_1$ -subunit alters gating, voltage sensitivity and recovery from fast inactivation of VGSCs (*Takahashi et al., 2003*). Downregulation of SCN1B gene expression has been reported in rat brain following pilocarpine-induced seizures (*Ellerkmann et al., 2003 & Lu et al., 2004*) and has been suggested to play a key role in the neurophysiologic recovery from brain injury (*Fung, 2000*). The downregulation of the  $\beta_1$  accessory subunit in our study could be a compensatory mechanism by which brain cells modify VGSCs activity. This modification may be important in reducing sodium influx, decreasing neuronal excitability and diminishing cellular energy demand. These adaptations may increase the resilience of neuronal cells to toxic insults and provide neuroprotection against oxidative damage (*Obrenovitch, 1998*).

The expression of superoxide dismutase-1 gene (Cu/Zn SOD or SOD-1) was also decreased in response to heat stress in pig hippocampus. SOD-1 is a cytosolic antioxidant enzyme that is involved in superoxide radical (O₂^{•-}) detoxification during normal cellular metabolism and after cell injury. SOD-1 catalyzes the dismutation of superoxide radical to H₂O₂ (*Peluffo et al., 2005*). Many stressors and pathological conditions associated with accumulation of reactive oxygen species (ROS) and development of oxidative stress have been reported to decrease the level of SOD-1 mRNA with or without decline in protein content and/or enzymatic activity in different tissues and species (*Peluffo et al., 2005*).



Such conditions include cold stress (*Nakao et al., 1999*), immobilization stress (*Oishi and Machida, 2002*), septic shock (*Ghosh et al., 1996*), hypoxia/ischemia (*Martin et al., 2002 & Rawal et al., 2004*), chronic fatigue syndrome (*Steinau et al., 2004*), inflammatory bowel disease (*Segui et al., 2004*), type-II diabetes (*Sakuraba et al., 2002*) and chemical-induced excitotoxic injury (*Peluffo et al., 2005*). In the CNS, SOD-1 plays an important role in neuroprotection and has been reported to be rapidly downregulated after several types of CNS injury (*Peluffo et al., 2005*). Hyperthermia is associated with accumulation of ROS such as superoxide anion ( $O_2^{\cdot-}$ ) and hydrogen peroxide ( $H_2O_2$ ) (*Zhao et al., 2006; Pérez-Crespo et al., 2005; Arnaud et al., 2002 & Niu et al., 2003*) and the downregulation of SOD-1 expression in the present study could be a consequence of increased oxidative stress (*Li et al., 2004 & De et al., 2006*). An alternative explanation for heat-induced downregulation of SOD-1 is that heat stress inhibits the activation and translocation of transcription factor NF- $\kappa$ B (*Kitamura, et al., 2006 & Chen et al., 2004*) which plays a role in the regulation of SOD-1 gene expression (*Alia, et al., 2005; Rojo et al., 2004 & Kinnula and Crapo, 2003*).

The heat-induced alteration in the expression of various genes in pig hippocampus represents a good step to identify novel genes that may be involved in the molecular response of the brain to heat stress. In light of the fact that SOD-1 expression was decreased in response to mild heat stress in pig hippocampus, we decided to focus our attention on the role of SOD-1 in heat stress. SOD-1 is responsible for approximately 90% of the total cellular superoxide radical dismutation activity (*Busuttill et al, 2005 & Fridovich, 1997*). Overexpression of SOD-1 has been shown to be protective in neuronal cells and delays apoptosis triggered by many oxidative insults (*Schwartz et al, 1998*). On

the contrary, downregulation of SOD-1 promotes apoptosis (*Troy and Shelanski, 1994*). The hypothesis we tested in the second part of this study was that the decrease in SOD-1 gene expression plays a role in heat-induced brain injury by decreasing the antioxidant capacity of the brain. Neuronal cell injury is an important component in the progression of neuropathological disorders associated with many stressors (*Zhang et al, 2006*). We therefore utilized a hippocampal cell line (HT-22) to investigate the role of SOD-1 in neuronal cell injury associated with heat stress. HT-22 cells are a mouse immortalized hippocampal cell line that was reported to be a good model for studying the effect of oxidative toxicity on neuronal cells (*Lewerenz et al, 2006*).

In the second part of this study, we exposed HT-22 cells to a 43°C heat stress for 30 minutes followed by recovery at 37°C. Heat stress caused a time-dependent decrease in SOD-1 mRNA and protein expression and diminished SOD-1 enzymatic activity. Inhibition of SOD-1 activity following exposure to elevated temperature has been reported in rat brain (*Niu et al., 2003 & Yang and Lin, 2002*), gold fish brain (*Lushchak and Bagnyukova, 2006*), rat liver (*Morrison et al., 2005 & Zhang et al., 2003*) and in PC-3 cells (*Moriyama-Gonda et al., 2002*). The heat-induced inhibition of SOD-1 activity is thought to be a consequence of the decrease in SOD-1 mRNA and protein synthesis or due to the thermal and oxidative disruption to the SOD-1 protein (*Lushchak and Bagnyukova, 2006*).

Altered expression and/or mutation of the SOD-1 gene or SOD-1 activity have been identified in several degenerative neurologic disorders such as familial and sporadic amyotrophic lateral sclerosis (ALS), Parkinson's disease (PD), Alzheimer's disease, and Down's syndrome (*Kitzberger et al., 2005 & Noor et al., 2002*). Alteration in SOD-1

expression and activity are also involved in a broad range of other pathologic conditions including diabetes, cancer, inflammatory diseases, atherosclerosis, pulmonary fibrosis, diseases of ischemia and reperfusion injuries and aging (*McCord and Edeas, 2005 & Thannickal and Fanburg, 2000*). The reduction in SOD-1 activity associated with heat stress may contribute to the diminished antioxidant capacity of the brain leading to neuronal injury following heat stress and may represent a new approach to develop neuroprotective therapeutic strategies against heat-induced neuronal damage.

The heat stress-induced reduction in SOD-1 enzymatic activity in the present study is associated with an elevation in intracellular ROS and a decrease in cell number. The heat stress induced generation of ROS such as superoxide anion ( $O_2^{\cdot-}$ ) (*Zhao et al., 2006*) has been reported to be mediated by stimulation of the mitochondrial electron transport chain (*Morrison et al., 2005*). The oxidative stress is a result of an imbalance between production of ROS and antioxidant defense systems. These defense mechanisms include antioxidant enzymes such as SOD-1, which is a key antioxidant enzyme that represents as much as 90% of the total cellular SOD activity (*Busuttill et al., 2005 & Noor et al., 2002*). In our study, we propose that the antioxidant activity of HT-22 cells following heat stress was insufficient in handling the heat-induced elevation of ROS generation. As a result, ROS accumulated in the cells as indicated by fluorescence microscopy. We also propose that the accumulation of ROS in HT-22 cells caused a cytotoxic effect that initiated cell death by apoptotic and non-apoptotic mechanisms as seen by others (*Galli et al., 2005a & Galli et al., 2005b*).

Neuronal apoptosis is a process characterized by changes in plasma membrane organization, and redistribution of the proapoptotic protein (BAX) to the mitochondrial

membrane, causing the release of cytochrome c from the mitochondria to the cytoplasm. Cytochrome c plays a key role in the initiation of apoptosis when released into the cytoplasm where it binds to Apaf-1 and triggers a series of caspase activations (*Baydas et al., 2005*). Activation of the caspase cascade leads to cleavage of cellular proteins and DNA fragmentation, and the orderly demise of the neuronal cell (*Tabakman et al., 2004*). To elucidate the features of the cellular death that occurred after heat stress, we examined two hallmarks of apoptosis; the release of the mitochondrial cytochrome c to the cytoplasm and DNA fragmentation. Heat stress increased the cytoplasmic accumulation of cytochrome c and caused DNA fragmentation suggesting that apoptosis contributes to heat-induced cell death in HT-22 cells. Heat stress has been reported to induce apoptotic cell death in other cell types like striatal neuronal cells (*White et al., 2003*), oligodendrocytes (*Goldbaum and Richter-Landsberg, 2001*) and fibroblasts (*Matsumoto et al., 1997*). Oxidative stress is a common element of heat-induced apoptotic cell death (*Petrosillo, et al., 2003a*). The accumulated ROS promote cytochrome c release and subsequent apoptotic process (*Pstrosillo et al., 2003b*).

The pretreatment of HT-22 cells with the salen manganese antioxidant SOD-mimetic compound (EUK-134) rescued HT-22 cells from heat-induced death. EUK-134 is a synthetic SOD-mimetic drug that has the ability to scavenge superoxide anions and its dismutation product hydrogen peroxide (*Pong et al., 2001*). EUK-134 has been shown to be protective against oxidative injury in many types of cells including rat cortical neurons (*Pong et al., 2001*) and motoneurons (*Sanchez-Carbenete et al., 2005*). In our study, EUK-134 protected HT-22 cells against heat stress-induced accumulation of intracellular ROS, mitochondrial cytochrome c release, DNA fragmentation and most importantly cell

death. These data suggest that oxidative stress plays a major role in heat induced-neuronal cell damage and EUK-134 is protective via an antioxidant mechanism. Interestingly, salen manganese SOD-mimetic drugs (EUKs) have been used successfully to abrogate oxidative stress-induced cellular damage and apoptosis in different cell types and tissues associated with neurodegenerative disorders like Alzheimer's disease (*Anderson et al., 2001*), Parkinson's disease (*Peng et al., 2005*) and amyotrophic lateral sclerosis (*Jung et al., 2001*). They have also been used in the treatment of cell injuries in other pathological conditions such as diabetes (*Olcott et al., 2004*), inflammatory immune diseases (*Decraene et al., 2004a*), ischemia-reperfusion injuries (*Li et al., 2005*), heat stress-induced liver injury (*Zhang et al., 2006 & Zhang et al., 2004*), stroke (*Peng et al., 2005*), septic shock (*Bianca et al., 2002*) and heavy metal-induced toxicity (*Yang et al., 2005*). One novel aspect of this study was the use of SOD-mimetic drugs in the treatment of heat-induced neuronal cell injury. Oxidative stress is implicated in triggering the neuronal cell damage associated with heat stress as well as many other types of stressors and neuropathological disorders. Strategies aimed to prevent the increase in ROS accumulation during the course of these stresses or disorders may attenuate or stop neuronal injury and therefore may have significant clinical applications.

## SUMMARY

Heat induced an alteration in the gene expression pattern in pig hippocampus in comparison with control. Our results revealed that 31 cDNA fragments were differentially expressed between heat stress and control hippocampus. Four of these fragments were identified as known genes and their altered expression was confirmed using real-time PCR. Our results indicate that DNA polymease epsilon 12 subunit (PolE4) gene and proteasome 26S non-ATPase type subunit 10 (PSMD10) gene were upregulated and superoxide dismutase-1 gene and voltage-gated sodium channel  $\beta_1$  subunit gene were downregulated in the hippocampus of heat stressed pigs.

In HT-22 hippocampal neuronal cells, SOD-1 gene and protein expression and enzyme activity were reduced following heat stress. The decrease in SOD-1 activity was associated with accumulation of ROS and the release of mitochondrial cytochrome c, DNA fragmentation and cell death. Pretreatment of HT-22 cells with the synthetic SOD-mimetic, EUK-134, protected the HT-22 cells against accumulation of ROS and heat-induced cell death.

## **CONCLUSION**

These results suggest that the downregulation of hippocampal SOD-1 by the effect of heat diminishes the antioxidant capacity of neuronal cells leading to accumulation of ROS. The resultant oxidative stress may play a role in brain injury and neuronal cell death following heat stress.

The data also suggest that therapeutic strategies aimed at maintaining cellular redox potential, such as SOD-mimetics, may be useful in the treatment or prevention of neuronal cell death and brain tissue injuries associated with oxidative stress. In addition, SOD-mimetics may be effective in slowing the progression or lessening the effect of neurodegenerative disorders such as Alzheimer's disease, Parkinson's disease, stroke and traumatic brain injuries, all of which are known to involve oxidative stress as a contributing factor.

## REFERENCES

1. Adler, V., Schaffer, A., Kim, J., Dolan, L. and Ronai, Z., 1995. UV irradiation and heat shock mediate JNK activation via alternate pathways. *J Biol Chem.* 270, 26071-26077.
2. Ahn, S. G., Kim, S. A., Yoon, J. H. and Vacratsis, P., 2005. Heat-shock cognate 70 is required for the activation of heat-shock factor 1 in mammalian cells. *Biochem J.* 392, 145-152.
3. Ahn, S. G., Liu, P. C., Klyachko, K., Morimoto, R. I. and Thiele, D. J., 2001. The loop domain of heat shock transcription factor 1 dictates DNA-binding specificity and responses to heat stress. *Genes Dev.* 15, 2134-2145.
4. Alm, P., Sharma, H. S., Sjoquist, P. O. and Westman, J., 2000. A new antioxidant compound H-290/51 attenuates nitric oxide synthase and heme oxygenase expression following hyperthermic brain injury. An experimental study using immunohistochemistry in the rat. *Amino Acids.* 19, 383-394.
5. Anderson, I., Adinolfi, C., Doctrow, S., Huffman, K., Joy, K. A., Malfroy, B., Soden, P., Rupniak, H. T. and Barnes, J. C., 2001. Oxidative signalling and inflammatory pathways in Alzheimer's disease. *Biochem Soc Symp.* 141-149.
6. Anderson, S. P., Howroyd, P., Liu, J., Qian, X., Bahnemann, R., Swanson, C., Kwak, M. K., Kensler, T. W. and Corton, J. C., 2004. The transcriptional response to a peroxisome proliferator-activated receptor alpha agonist includes increased expression of proteome maintenance genes. *J Biol Chem.* 279, 52390-52398.
7. Ardley, H. C., Hung, C. C. and Robinson, P. A., 2005. The aggravating role of the ubiquitin-proteasome system in neurodegeneration. *FEBS Lett.* 579, 571-576.
8. Arnaud, C., Joyeux, M., Garrel, C., Godin-Ribuot, D., Demenge, P. and Ribuot, C., 2002. Free-radical production triggered by hyperthermia contributes to heat stress-induced cardioprotection in isolated rat hearts. *Br J Pharmacol.* 135, 1776-1782.



9. Awasthi, N. and Wagner, B. J., 2005. Upregulation of heat shock protein expression by proteasome inhibition: an antiapoptotic mechanism in the lens. *Invest Ophthalmol Vis Sci.* 46, 2082-2091.
10. Balcer-Kubiczek, E. K., Harrison, G. H., Davis, C. C., Haas, M. L. and Koffman, B. H., 2000. Expression analysis of human HL60 cells exposed to 60 Hz square- or sine-wave magnetic fields. *Radiat Res.* 153, 670-678.
11. Bass, D. A., Parce, J. W., Dechatelet, L. R., Szejda, P., Seeds, M. C. and Thomas, M., 1983. Flow cytometric studies of oxidative product formation by neutrophils: a graded response to membrane stimulation. *J Immunol.* 130, 1910-1917.
12. Batulan, Z., Nalbantoglu, J. and Durham, H. D., 2005. Nonsteroidal anti-inflammatory drugs differentially affect the heat shock response in cultured spinal cord cells. *Cell Stress Chaperones.* 10, 185-196.
13. Batulan, Z., Shinder, G. A., Minotti, S., He, B. P., Doroudchi, M. M., Nalbantoglu, J., Strong, M. J. and Durham, H. D., 2003. High threshold for induction of the stress response in motor neurons is associated with failure to activate HSF1. *J Neurosci.* 23, 5789-5798.
14. Baudry, M., Etienne, S., Bruce, A., Palucki, M., Jacobsen, E. and Malfroy, B., 1993. Salen-manganese complexes are superoxide dismutase-mimics. *Biochem Biophys Res Commun.* 192, 964-968.
15. Baydas, G., Reiter, R. J., Akbulut, M., Tuzcu, M. and Tamer, S., 2005. Melatonin inhibits neural apoptosis induced by homocysteine in hippocampus of rats via inhibition of cytochrome c translocation and caspase-3 activation and by regulating pro- and anti-apoptotic protein levels. *Neuroscience.* 135, 879-886.
16. Bayir, H., Fadeel, B., Palladino, M. J., Witasz, E., Kurnikov, I. V., Tyurina, Y. Y., Tyurin, V. A., Amoscato, A. A., Jiang, J., Kochanek, P. M., DeKosky, S. T., Greenberger, J. S., Shvedova, A. A. and Kagan, V. E., 2006. Apoptotic interactions of cytochrome c: redox flirting with anionic phospholipids within and outside of mitochondria. *Biochim Biophys Acta.* 1757, 648-659.
17. Bazille, C., Megarbane, B., Bensimhon, D., Lavergne-Slove, A., Baglin, A. C., Loirat, P., Woimant, F., Mikol, J. and Gray, F., 2005. Brain damage after heat stroke. *J Neuropathol Exp Neurol.* 64, 970-975.
18. Bechtold, D. A. and Brown, I. R., 2003. Induction of Hsp27 and Hsp32 stress proteins and vimentin in glial cells of the rat hippocampus following hyperthermia. *Neurochem Res.* 28, 1163-1173.

19. Becker, L. B., 2004. New concepts in reactive oxygen species and cardiovascular reperfusion physiology. *Cardiovasc Res.* 61, 461-470.
20. Beedholm, R., Clark, B. F. and Rattan, S. I., 2004. Mild heat stress stimulates 20S proteasome and its 11S activator in human fibroblasts undergoing aging in vitro. *Cell Stress Chaperones.* 9, 49-57.
21. Behl, C., 1997. Amyloid beta-protein toxicity and oxidative stress in Alzheimer's disease. *Cell Tissue Res.* 290, 471-480.
22. Behl, C., Lezoualc'h, F., Trapp, T., Widmann, M., Skutella, T. and Holsboer, F., 1997. Glucocorticoids enhance oxidative stress-induced cell death in hippocampal neurons in vitro. *Endocrinology.* 138, 101-106.
23. Berman, A., 2005. Estimates of heat stress relief needs for Holstein dairy cows. *J Anim Sci.* 83, 1377-1384.
24. Bianca, R. V., Wayman, N. S., McDonald, M. C., Pinto, A., Shape, M. A., Chatterjee, P. K. and Thiernemann, C., 2002. Superoxide dismutase mimetic with catalase activity, EUK-134, attenuates the multiple organ injury and dysfunction caused by endotoxin in the rat. *Med Sci Monit.* 8, BR1-7.
25. Bijur, G. N. and Jope, R. S., 2000. Opposing actions of phosphatidylinositol 3-kinase and glycogen synthase kinase-3beta in the regulation of HSF-1 activity. *J Neurochem.* 75, 2401-2408.
26. Borges, J. C. and Ramos, C. H., 2005. Protein folding assisted by chaperones. *Protein Pept Lett.* 12, 257-261.
27. Bose, S., Stratford, F. L., Broadfoot, K. I., Mason, G. G. and Rivett, A. J., 2004. Phosphorylation of 20S proteasome alpha subunit C8 (alpha7) stabilizes the 26S proteasome and plays a role in the regulation of proteasome complexes by gamma-interferon. *Biochem J.* 378, 177-184.
28. Bouchama, A., 2006. Heatstroke: facing the threat. *Crit Care Med.* 34, 1272-1273.
29. Bouchama, A. and Knochel, J. P., 2002. Heat stroke. *N Engl J Med.* 346, 1978-1988.
30. Boveris, A., Valdez, L. B., Zaobornyj, T. and Bustamante, J., 2006. Mitochondrial metabolic states regulate nitric oxide and hydrogen peroxide diffusion to the cytosol. *Biochim Biophys Acta.* 1757, 535-542.
31. Bukau, B., Weissman, J. and Horwich, A., 2006. Molecular chaperones and protein quality control. *Cell.* 125, 443-451.

32. Busuttil, R. A., Garcia, A. M., Cabrera, C., Rodriguez, A., Suh, Y., Kim, W. H., Huang, T. T. and Vijg, J., 2005. Organ-specific increase in mutation accumulation and apoptosis rate in CuZn-superoxide dismutase-deficient mice. *Cancer Res.* 65, 11271-11275.
33. Cabelof, D. C., Raffoul, J. J., Yanamadala, S., Guo, Z. and Heydari, A. R., 2002. Induction of DNA polymerase beta-dependent base excision repair in response to oxidative stress in vivo. *Carcinogenesis.* 23, 1419-1425.
34. Camello-Almaraz, C., Gomez-Pinilla, P. J., Pozo, M. J. and Camello, P. J., 2006. Mitochondrial reactive oxygen species and Ca²⁺ signaling. *Am J Physiol Cell Physiol.* 291, C1082-1088.
35. Carroll, M. C., Outten, C., Proescher, J. B., Rosenfeld, L., Watson, W. H., Whitson, L. J., Hart, P. J., Jensen, L. T. and Culotta, V. C., 2006. The effects of glutaredoxin and copper activation pathways on the disulfide and stability of Cu/Zn superoxide dismutase. *J Biol Chem.* 281 (39), 28648-28656.
36. CDC, 2005. Heat-related mortality--Arizona, 1993-2002, and United States, 1979-2002. *MMWR Morb Mortal Wkly Rep.* 54, 628-630.
37. Chaudhuri, A. and Behan, P. O., 2004. In vivo magnetic resonance spectroscopy in chronic fatigue syndrome. Prostaglandins *Leukot Essent Fatty Acids.* 71, 181-183.
38. Chen, J., Small-Howard, A., Yin, A. and Berry, M. J., 2005. The responses of HT22 cells to oxidative stress induced by buthionine sulfoximine (BSO). *BMC Neurosci.* 6, 10.
39. Chen, Y., Arrigo, A. P. and Currie, R. W., 2004. Heat shock treatment suppresses angiotensin II-induced activation of NF-kappaB pathway and heart inflammation: a role for IKK depletion by heat shock? *Am J Physiol Heart Circ Physiol.* 287, H1104-1114.
40. Chia, S. E. and Teo, K. J., 2003. Prognosis of adult men with heat exhaustion with regard to postural stability and neurobehavioral effects: a 6-month follow-up study. *Neurotoxicol Teratol.* 25, 503-508.
41. Chiueh, C. C., 1994. Neurobiology of NO[•] and [•]OH: basic research and clinical relevance. *Ann N Y Acad Sci.* 738, 279-281.
42. Choi, H., Kim, S. H., Chun, Y. S., Cho, Y. S., Park, J. W. and Kim, M. S., 2006. In vivo hyperoxic preconditioning prevents myocardial infarction by expressing bcl-2. *Exp Biol Med (Maywood).* 231, 463-472.

43. Chou, Y. T., Lai, S. T., Lee, C. C. and Lin, M. T., 2003. Hypothermia attenuates circulatory shock and cerebral ischemia in experimental heatstroke. *Shock*. 19, 388-393.
44. Cook, J. A., Gius, D., Wink, D. A., Krishna, M. C., Russo, A. and Mitchell, J. B., 2004. Oxidative stress, redox, and the tumor microenvironment. *Semin Radiat Oncol*. 14, 259-266.
45. Coris, E. E., Ramirez, A. M. and Van Durme, D. J., 2004. Heat illness in athletes: the dangerous combination of heat, humidity and exercise. *Sports Med*. 34, 9-16.
46. Coris, E. E., Walz, S. M., Duncanson, R., Ramirez, A. M. and Roetzheim, R. G., 2006. Heat illness symptom index (HISI): a novel instrument for the assessment of heat illness in athletes. *South Med J*. 99, 340-345.
47. Cuddy, M. L., 2004. The effects of drugs on thermoregulation. *AACN Clin Issues*. 15, 238-253.
48. Cumming, R. C. and Schubert, D., 2005. Amyloid-beta induces disulfide bonding and aggregation of GAPDH in Alzheimer's disease. *FASEB J*. 19, 2060-2062.
49. De, K., Ghosh, G., Datta, M., Konar, A., Bandyopadhyay, J., Bandyopadhyay, D., Bhattacharya, S. and Bandyopadhyay, A., 2004. Analysis of differentially expressed genes in hyperthyroid-induced hypertrophied heart by cDNA microarray. *J Endocrinol*. 182, 303-314.
50. De Keulenaer, G. W., Chappell, D. C., Ishizaka, N., Nerem, R. M., Alexander, R. W. and Griendling, K. K., 1998. Oscillatory and steady laminar shear stress differentially affects human endothelial redox state: role of a superoxide-producing NADH oxidase. *Circ Res*. 82, 1094-1101.
51. Decraene, D., Smaers, K., Gan, D., Mammone, T., Matsui, M., Maes, D., Declercq, L. and Garmyn, M., 2004a. A synthetic superoxide dismutase/catalase mimetic (EUK-134) inhibits membrane-damage-induced activation of mitogen-activated protein kinase pathways and reduces p53 accumulation in ultraviolet B-exposed primary human keratinocytes. *J Invest Dermatol*. 122, 484-491.
52. Decraene, D., Van Laethem, A., Agostinis, P., De Peuter, L., Degreef, H., Bouillon, R. and Garmyn, M., 2004b. AKT status controls susceptibility of malignant keratinocytes to the early-activated and UVB-induced apoptotic pathway. *J Invest Dermatol*. 123, 207-212.

53. DeMeester, S. L., Buchman, T. G. and Cobb, J. P., 2001. The heat shock paradox: does NF-kappaB determine cell fate? *FASEB J.* 15, 270-274.
54. Dinh, H. K., Zhao, B., Schuschereba, S. T., Merrill, G. and Bowman, P. D., 2001. Gene expression profiling of the response to thermal injury in human cells. *Physiol Genomics.* 7, 3-13.
55. Doctrow, S. R., Huffman, K., Marcus, C. B., Tocco, G., Malfroy, E., Adinolfi, C. A., Kruk, H., Baker, K., Lazarowych, N., Mascarenhas, J. and Malfroy, B., 2002. Salen-manganese complexes as catalytic scavengers of hydrogen peroxide and cytoprotective agents: structure-activity relationship studies. *J Med Chem.* 45, 4549-4558.
56. Drevet, J. R., 2006. The antioxidant glutathione peroxidase family and spermatozoa: a complex story. *Mol Cell Endocrinol.* 250, 70-79.
57. Drobotz, K. J. and Macintire, D. K., 1996. Heat-induced illness in dogs: 42 cases (1976-1993). *J Am Vet Med Assoc.* 209, 1894-1899.
58. Droge, W., 2001. Free Radicals in the Physiological Control of Cell Function. *Physiol Rev.* 82, 47-77.
59. Ellerkmann, R. K., Remy, S., Chen, J., Sochivko, D., Elger, C. E., Urban, B. W., Becker, A. and Beck, H., 2003. Molecular and functional changes in voltage-dependent Na⁺ channels following pilocarpine-induced status epilepticus in rat dentate granule cells. *Neuroscience.* 119, 323-333.
60. Emerit, J., Edeas, M. and Bricaire, F., 2004. Neurodegenerative diseases and oxidative stress. *Biomed Pharmacother.* 58, 39-46.
61. Fan, C. Y., Lee, S. and Cyr, D. M., 2003. Mechanisms for regulation of Hsp70 function by Hsp40. *Cell Stress Chaperones.* 8, 309-316.
62. Flanagan, S. W., Moseley, P. L. and Buettner, G. R., 1998. Increased flux of free radicals in cells subjected to hyperthermia: detection by electron paramagnetic resonance spin trapping. *FEBS Lett.* 431, 285-286.
63. Fountoulakis, M., Tsangaris, G. T., Maris, A. and Lubec, G., 2005. The rat brain hippocampus proteome. *J Chromatogr B Analyt Technol Biomed Life Sci.* 819, 115-129.
64. Franklin, T. B., Krueger-Naug, A. M., Clarke, D. B., Arrigo, A. P. and Currie, R. W., 2005. The role of heat shock proteins Hsp70 and Hsp27 in cellular protection of the central nervous system. *Int J Hyperthermia.* 21, 379-392.

65. Friant, S., Pecheur, E. I., Eugster, A., Michel, F., Lefkir, Y., Nourrisson, D. and Letourneur, F., 2003. Ent3p Is a PtdIns (3,5)P₂ effector required for protein sorting to the multivesicular body. *Dev Cell*. 5, 499-511.
66. Fridovich, I., 1995. Superoxide radical and superoxide dismutases. *Annu Rev Biochem*. 64, 97-112.
67. Fridovich, I., 1997. Superoxide anion radical (O₂⁻), superoxide dismutases, and related matters. *J Biol Chem*. 272, 18515-18517.
68. Fung, M. L., 2000. Role of voltage-gated Na⁺ channels in hypoxia-induced neuronal injuries. *Clin Exp Pharmacol Physiol*. 27, 569-574.
69. Galli, A., Svegliati-Baroni, G., Ceni, E., Milani, S., Ridolfi, F., Salzano, R., Tarocchi, M., Grappone, C., Pellegrini, G., Benedetti, A., Surrenti, C. and Casini, A., 2005a. Oxidative stress stimulates proliferation and invasiveness of hepatic stellate cells via a MMP2-mediated mechanism. *Hepatology*. 41, 1074-1084.
70. Galli, F., Piroddi, M., Annetti, C., Aisa, C., Floridi, E. and Floridi, A., 2005b. Oxidative stress and reactive oxygen species. *Contrib Nephrol*. 149, 240-260.
71. Garrido, C., Gurbuxani, S., Ravagnan, L. and Kroemer, G., 2001. Heat shock proteins: endogenous modulators of apoptotic cell death. *Biochem Biophys Res Commun*. 286, 433-442.
72. Ghosh, B., Hanevold, C. D., Dobashi, K., Orak, J. K. and Singh, I., 1996. Tissue differences in antioxidant enzyme gene expression in response to endotoxin. *Free Radic Biol Med*. 21, 533-540.
73. Gill, M. S., Olsen, A., Sampayo, J. N. and Lithgow, G. J., 2003. An automated high-throughput assay for survival of the nematode *Caenorhabditis elegans*. *Free Radic Biol Med*. 35, 558-565.
74. Gius, D., Mattson, D., Bradbury, C. M., Smart, D. K. and Spitz, D. R., 2004. Thermal stress and the disruption of redox-sensitive signalling and transcription factor activation: possible role in radiosensitization. *Int J Hyperthermia*. 20, 213-223.
75. Glazer, J. L., 2005. Management of heatstroke and heat exhaustion. *Am Fam Physician*. 71, 2133-2140.
76. Goldbaum, O. and Richter-Landsberg, C., 2001. Stress proteins in oligodendrocytes: differential effects of heat shock and oxidative stress. *J Neurochem*. 78, 1233-1242.

77. Gupta, S. and Knowlton, A. A., 2005. HSP60, Bax, apoptosis and the heart. *J Cell Mol Med.* 9, 51-58.
78. Hadad, E., Rav-Acha, M., Heled, Y., Epstein, Y. and Moran, D. S., 2004. Heat stroke: a review of cooling methods. *Sports Med.* 34, 501-511.
79. Hahn, J. S., Neef, D. W. and Thiele, D. J., 2006. A stress regulatory network for co-ordinated activation of proteasome expression mediated by yeast heat shock transcription factor. *Mol Microbiol.* 60, 240-251.
80. Halliwell, B., 2001. Role of free radicals in the neurodegenerative diseases: therapeutic implications for antioxidant treatment. *Drugs Aging.* 18, 685-716.
81. Hermesh, H., Shiloh, R., Epstein, Y., Manaim, H., Weizman, A. and Munitz, H., 2000. Heat intolerance in patients with chronic schizophrenia maintained with antipsychotic drugs. *Am J Psychiatry.* 157, 1327-1329.
82. Higgins, C. M., Jung, C., Ding, H. and Xu, Z., 2002. Mutant Cu, Zn superoxide dismutase that causes motoneuron degeneration is present in mitochondria in the CNS. *J Neurosci.* 22, RC215.
83. Holmberg, C. I., Leppa, S., Eriksson, J. E. and Sistonen, L., 1997. The phorbol ester 12-O-tetradecanoylphorbol 13-acetate enhances the heat-induced stress response. *J Biol Chem.* 272, 6792-6798.
84. Huber, A., Stuchbury, G., Burkle, A., Burnell, J. and Munch, G., 2006. Neuroprotective therapies for Alzheimer's disease. *Curr Pharm Des.* 12, 705-717.
85. Huynh, T. T., Aarnink, A. J., Verstegen, M. W., Gerrits, W. J., Heetkamp, M. J., Kemp, B. and Canh, T. T., 2005. Effects of increasing temperatures on physiological changes in pigs at different relative humidities. *J Anim Sci.* 83, 1385-1396.
86. Jallali, N., Ridha, H., Thrasivoulou, C., Underwood, C., Butler, P. E. and Cowen, T., 2005. Vulnerability to ROS-induced cell death in ageing articular cartilage: the role of antioxidant enzyme activity. *Osteoarthritis Cartilage.* 13, 614-622.
87. Jiang, F., Guo, Y., Salvemini, D. and Dusting, G. J., 2003. Superoxide dismutase mimetic M40403 improves endothelial function in apolipoprotein (E)-deficient mice. *Br J Pharmacol.* 139, 1127-1134.
88. Jin, Y. X., Lee, J. Y., Choi, S. H., Kim, T., Cui, X. S. and Kim, N. H., 2006. Heat shock induces apoptosis related gene expression and apoptosis in porcine parthenotes developing in vitro. *Anim Reprod Sci.* [Epub ahead of print].

89. Jolly, C. and Morimoto, R. I., 2000. Role of the heat shock response and molecular chaperones in oncogenesis and cell death. *J Natl Cancer Inst.* 92, 1564-1572.
90. Jones, L. J., Gray, M., Yue, S. T., Haugland, R. P. and Singer, V. L., 2001. Sensitive determination of cell number using the CyQUANT cell proliferation assay. *J Immunol Methods.* 254, 85-98.
91. Jung, C., Rong, Y., Doctrow, S., Baudry, M., Malfroy, B. and Xu, Z., 2001. Synthetic superoxide dismutase/catalase mimetics reduce oxidative stress and prolong survival in a mouse amyotrophic lateral sclerosis model. *Neurosci Lett.* 304, 157-160.
92. Kaarniranta, K., Oksala, N., Karjalainen, H. M., Suuronen, T., Sistonen, L., Helminen, H. J., Salminen, A. and Lammi, M. J., 2002. Neuronal cells show regulatory differences in the hsp70 gene response. *Brain Res Mol Brain Res.* 101, 136-140.
93. Kamijo, Y. and Nose, H., 2006. Heat illness during working and preventive considerations from body fluid homeostasis. *Ind Health.* 44, 345-358.
94. Kampinga, H. H., 2006a. Cell biological effects of hyperthermia alone or combined with radiation or drugs: a short introduction to newcomers in the field. *Int J Hyperthermia.* 22, 191-196.
95. Kampinga, H. H., 2006b. Chaperones in preventing protein denaturation in living cells and protecting against cellular stress. *Handb Exp Pharmacol*, 1-42.
96. Karlin, S. and Altschul, S. F., 1990. Methods for assessing the statistical significance of molecular sequence features by using general scoring schemes. *Proc Natl Acad Sci U S A.* 87, 2264-2268.
97. Kelly, K. J., 2005. Heat shock (stress response) proteins and renal ischemia/reperfusion injury. *Contrib Nephrol.* 148, 86-106.
98. Khosla, R. and Guntupalli, K. K., 1999. Heat-related illnesses. *Crit Care Clin.* 15, 251-263.
99. Kinnula, V. L. and Crapo, J. D., 2003. Superoxide dismutases in the lung and human lung diseases. *Am J Respir Crit Care Med.* 167, 1600-1619.
100. Kinoshita, S., Kaneko, G., Lee, J. H., Kikuchi, K., Yamada, H., Hara, T., Itoh, Y. and Watabe, S., 2001. A novel heat stress-responsive gene in the marine diatom *Chaetoceros compressum* encoding two types of transcripts, a trypsin-like protease and its related protein, by alternative RNA splicing. *Eur J Biochem.* 268, 4599-4609.



101. Kitamura, C., Nishihara, T., Ueno, Y., Chen, K. K., Morotomi, T., Yano, J., Nagayoshi, M. and Terashita, M., 2006. Effects of sequential exposure to lipopolysaccharide and heat stress on dental pulp cells. *J Cell Biochem.* 99(3), 797-806.
102. Kitzberger, R., Madl, C. and Ferenci, P., 2005. Wilson disease. *Metab Brain Dis.* 20, 295-302.
103. Kowluru, R. A. and Abbas, S. N., 2003. Diabetes-induced mitochondrial dysfunction in the retina. *Invest Ophthalmol Vis Sci.* 44, 5327-5334.
104. Kregel, K. C. and Zhang, H. J., 2006. An Integrated View of Oxidative Stress in Aging: Basic Mechanisms, Functional Effects and Pathological Considerations. *Am J Physiol Regul Integr Comp Physiol.* [Epub ahead of print].
105. Kultz, D., 2003. Evolution of the cellular stress proteome: from monophyletic origin to ubiquitous function. *J Exp Biol.* 206, 3119-3124.
106. Kysely, J., 2004. Mortality and displaced mortality during heat waves in the Czech Republic. *Int J Biometeorol.* 49, 91-97.
107. Lan, J., Li, W., Zhang, F., Sun, F. Y., Nagayama, T., O'Horo, C. and Chen, J., 2003. Inducible repair of oxidative DNA lesions in the rat brain after transient focal ischemia and reperfusion. *J Cereb Blood Flow Metab.* 23, 1324-1339.
108. Latchman, D. S., 2005. HSP27 and cell survival in neurones. *Int J Hyperthermia.* 21, 393-402.
109. Le Greves, P., Sharma, H. S., Westman, J., Alm, P. and Nyberg, F., 1997. Acute heat stress induces edema and nitric oxide synthase upregulation and down-regulates mRNA levels of the NMDAR1, NMDAR2A and NMDAR2B subunits in the rat hippocampus. *Acta Neurochir Suppl.* 70, 275-278.
110. Lee, B. P., Rushlow, W. J., Chakraborty, C. and Lala, P. K., 2001. Differential gene expression in premalignant human trophoblast: role of IGFBP-5. *Int J Cancer.* 94, 674-684.
111. Lee, J. Y., Kim, J. W., Lim, H. S., Joo, W. H., Cho, Y. K. and Moon, J. Y., 2005. Changes in antioxidant defense systems by 2,2',5,5'-tetrachlorobiphenyl exposure in neuronal SK-N-MC cells. *Toxicol Lett.* 157, 139-149.
112. Lee, S. and Tsai, F. T., 2005. Molecular chaperones in protein quality control. *J Biochem Mol Biol.* 38, 259-265.

113. Lewerenz, J., Klein, M. and Methner, A., 2006. Cooperative action of glutamate transporters and cystine/glutamate antiporter system Xc⁻ protects from oxidative glutamate toxicity. *J Neurochem.* 98, 916-925.
114. Li, H., Gu, Y., Zhang, Y., Lucas, M. J. and Wang, Y., 2004. High glucose levels down-regulate glucose transporter expression that correlates with increased oxidative stress in placental trophoblast cells in vitro. *J Soc Gynecol Investig.* 11, 75-81.
115. Li, L., Zhou, Q. X. and Shi, J. S., 2005. Protective effects of icariin on neurons injured by cerebral ischemia/reperfusion. *Chin Med J (Engl).* 118, 1637-1643.
116. Liang, P., Zhu, W., Zhang, X., Guo, Z., O'Connell, R. P., Averboukh, L., Wang, F. and Pardee, A. B., 1994. Differential display using one-base anchored oligo-dT primers. *Nucleic Acids Res.* 22, 5763-5764.
117. Lim, M. C., Brooke, S. M. and Sapolsky, R. M., 2003. gp120 neurotoxicity fails to induce heat shock defenses, while the over expression of hsp70 protects against gp120. *Brain Res Bull.* 61, 183-188.
118. Lin, M. T., 1997. Heatstroke-induced cerebral ischemia and neuronal damage. Involvement of cytokines and monoamines. *Ann N Y Acad Sci.* 813, 572-580.
119. Livak, K. J. and Schmittgen, T. D., 2001. Analysis of relative gene expression data using real-time quantitative PCR and the 2⁻(Delta Delta C(T)) Method. *Methods.* 25, 402-408.
120. Lopez-Hernandez, F. J., Ortiz, M. A. and Piedrafita, F. J., 2006. The extrinsic and intrinsic apoptotic pathways are differentially affected by temperature upstream of mitochondrial damage. *Apoptosis.* 11, 1339-1347.
121. Lord-Fontaine, S. and Averill-Bates, D. A., 2002. Heat shock inactivates cellular antioxidant defenses against hydrogen peroxide: protection by glucose. *Free Radic Biol Med.* 32, 752-765.
122. Lu, X. C., Williams, A. J., Yao, C., Berti, R., Hartings, J. A., Whipple, R., Vahey, M. T., Polavarapu, R. G., Woller, K. L., Tortella, F. C. and Dave, J. R., 2004. Microarray analysis of acute and delayed gene expression profile in rats after focal ischemic brain injury and reperfusion. *J Neurosci Res.* 77, 843-857.

123. Lugo-Amador, N. M., Rothenhaus, T. and Moyer, P., 2004. Heat-related illness. *Emerg Med Clin North Am.* 22, 315-327.
124. Lushchak, V. I. and Bagnyukova, T. V., 2006. Temperature increase results in oxidative stress in goldfish tissues. 2. Antioxidant and associated enzymes. *Comp Biochem Physiol C Toxicol Pharmacol.* 143, 36-41.
125. Ma, J., Svoboda, P., Schultz, R. M. and Stein, P., 2001. Regulation of zygotic gene activation in the preimplantation mouse embryo: global activation and repression of gene expression. *Biol Reprod.* 64, 1713-1721.
126. Mager, W. H. and De Kruijff, A. J., 1995. Stress-induced transcriptional activation. *Microbiol Rev.* 59, 506-531.
127. Malago, J. J., Koninkx, J. F. and van Dijk, J. E., 2002. The heat shock response and cytoprotection of the intestinal epithelium. *Cell Stress Chaperones.* 7, 191-199.
128. Malassagne, B., Ferret, P. J., Hammoud, R., Tulliez, M., Bedda, S., Trebeden, H., Jaffray, P., Calmus, Y., Weill, B. and Batteux, F., 2001. The superoxide dismutase mimetic MnTBAP prevents Fas-induced acute liver failure in the mouse. *Gastroenterology.* 121, 1451-1459.
129. Marcuccilli, C. J., Mathur, S. K., Morimoto, R. I. and Miller, R. J., 1996. Regulatory differences in the stress response of hippocampal neurons and glial cells after heat shock. *J Neurosci.* 16, 478-485.
130. Maroni, P., Bendinelli, P., Tiberio, L., Rovetta, F., Piccoletti, R. and Schiaffonati, L., 2003. In vivo heat-shock response in the brain: signalling pathway and transcription factor activation. *Brain Res Mol Brain Res.* 119, 90-99.
131. Martin, R., Fitzl, G., Mozet, C., Martin, H., Welt, K. and Wieland, E., 2002. Effect of age and hypoxia/reoxygenation on mRNA expression of antioxidative enzymes in rat liver and kidneys. *Exp Gerontol.* 37, 1481-1487.
132. Marto, N., 2005. [Heat waves: health impacts]. *Acta Med Port.* 18, 467-474.
133. Matsumoto, H., Takahashi, A., Wang, X., Ohnishi, K. and Ohnishi, T., 1997. Transfection of p53-knockout mouse fibroblasts with wild-type p53 increases the thermosensitivity and stimulates apoptosis induced by heat stress. *Int J Radiat Oncol Biol Phys.* 39, 197-203.

134. Matsuzuka, T., Ozawa, M., Nakamura, A., Ushitani, A., Hirabayashi, M. and Kanai, Y., 2005. Effects of heat stress on the redox status in the oviduct and early embryonic development in mice. *J Reprod Dev.* 51, 281-287.
135. Mattheus, N., Ekramoddoullah, A. K. and Lee, S. P., 2003. Isolation of high-quality RNA from white spruce tissue using a three-stage purification method and subsequent cloning of a transcript from the PR-10 gene family. *Phytochem Anal.* 14, 209-215.
136. Mayer, M. P. and Bukau, B., 2005. Hsp70 chaperones: cellular functions and molecular mechanism. *Cell Mol Life Sci.* 62, 670-684.
137. McCord, J. M. and Edeas, M. A., 2005. SOD, oxidative stress and human pathologies: a brief history and a future vision. *Biomed Pharmacother.* 59, 139-142.
138. McDonald, M. C., d'Emmanuele di Villa Bianca, R., Wayman, N. S., Pinto, A., Sharpe, M. A., Cuzzocrea, S., Chatterjee, P. K. and Thiemermann, C., 2003. A superoxide dismutase mimetic with catalase activity (EUK-8) reduces the organ injury in endotoxic shock. *Eur J Pharmacol.* 466, 181-189.
139. McEwen, B. S., 2005. Glucocorticoids, depression, and mood disorders: structural remodeling in the brain. *Metabolism.* 54, 20-23.
140. Meiners, S., Heyken, D., Weller, A., Ludwig, A., Stangl, K., Kloetzel, P. M. and Kruger, E., 2003. Inhibition of proteasome activity induces concerted expression of proteasome genes and de novo formation of Mammalian proteasomes. *J Biol Chem.* 278, 21517-21525.
141. Meloni, B. P., Van Dyk, D., Cole, R. and Knuckey, N. W., 2005. Proteome analysis of cortical neuronal cultures following cycloheximide, heat stress and MK801 preconditioning. *Proteomics.* 5, 4743-4753.
142. Miller, A. F., 2004. Superoxide dismutases: active sites that save, but a protein that kills. *Curr Opin Chem Biol.* 8, 162-168.
143. Minowada, G. and Welch, W. J., 1995. Clinical implications of the stress response. *J Clin Invest.* 95, 3-12.
144. Morimoto, B. H. and Koshland, D. E., Jr., 1990. Excitatory amino acid uptake and N-methyl-D-aspartate-mediated secretion in a neural cell line. *Proc Natl Acad Sci U S A.* 87, 3518-3521.

145. Morimoto, R. I., Kline, M. P., Bimston, D. N. and Cotto, J. J., 1997. The heat-shock response: regulation and function of heat-shock proteins and molecular chaperones. *Essays Biochem.* 32, 17-29.
146. Moriyama-Gonda, N., Igawa, M., Shiina, H., Urakami, S., Shigeno, K. and Terashima, M., 2002. Modulation of heat-induced cell death in PC-3 prostate cancer cells by the antioxidant inhibitor diethyldithiocarbamate. *BJU Int.* 90, 317-325.
147. Morrison, A. L., Dinges, M., Singleton, K. D., Odoms, K., Wong, H. R. and Wischmeyer, P. E., 2006. Glutamine's protection against cellular injury is dependent on heat shock factor-1. *Am J Physiol Cell Physiol.* 290, C1625-1632.
148. Morrison, J. P., Coleman, M. C., Aunan, E. S., Walsh, S. A., Spitz, D. R. and Kregel, K. C., 2005. Aging reduces responsiveness to BSO- and heat stress-induced perturbations of glutathione and antioxidant enzymes. *Am J Physiol Regul Integr Comp Physiol.* 289, R1035-1041.
149. Mortola, J. P., 2005. Influence of temperature on metabolism and breathing during mammalian ontogenesis. *Respir Physiol Neurobiol.* 149, 155-164.
150. Mosser, D. D. and Morimoto, R. I., 2004. Molecular chaperones and the stress of oncogenesis. *Oncogene.* 23, 2907-2918.
151. Munzel, T., Hink, U., Heitzer, T. and Meinertz, T., 1999. Role for NADPH/NADH oxidase in the modulation of vascular tone. *Ann N Y Acad Sci.* 874, 386-400.
152. Nakai, A., 1999. New aspects in the vertebrate heat shock factor system: Hsf3 and Hsf4. *Cell Stress Chaperones.* 4, 86-93.
153. Nethery, D., Stofan, D., Callahan, L., DiMarco, A. and Supinski, G., 1999. Formation of reactive oxygen species by the contracting diaphragm is PLA(2) dependent. *J Appl Physiol.* 87, 792-800.
154. Niakao, C., Ookawara, T., Kizaki, T., Suzuki, K., Haga, S., Sato, Y. and Ohno, H., 1999. Effects of acute cold stress on mRNA expression and immunoreactivity of three superoxide dismutase isoenzymes in genetically obese mice. *Res Commun Mol Pathol Pharmacol.* 106, 47-61.
155. Nishimura, R. N. and Sharp, F. R., 2005. Heat shock proteins and neuromuscular disease. *Muscle Nerve.* 32, 693-709.

- 156.** Niu, K. C., Lin, K. C., Yang, C. Y. and Lin, M. T., 2003. Protective effects of alpha-tocopherol and mannitol in both circulatory shock and cerebral ischaemia injury in rat heatstroke. *Clin Exp Pharmacol Physiol.* 30, 745-751.
- 157.** Noor, R., Mittal, S. and Iqbal, J., 2002. Superoxide dismutase--applications and relevance to human diseases. *Med Sci Monit.* 8, RA210-215.
- 158.** Obrenovitch, T. P., 1998. Neuroprotective strategies: voltage-gated Na⁺-channel down-modulation versus presynaptic glutamate release inhibition. *Rev Neurosci.* 9, 203-211.
- 159.** Ohnishi, T., Wang, X., Ohnishi, K., Matsumoto, H. and Takahashi, A., 1996. P53-dependent induction of WAF1 by heat treatment in human glioblastoma cells. *J Biol Chem.* 271, 14510-14513.
- 160.** Oishi, K. and Machida, K., 2002. Different effects of immobilization stress on the mRNA expression of antioxidant enzymes in rat peripheral organs. *Scand J Clin Lab Invest.* 62, 115-121.
- 161.** Olcott, A. P., Tocco, G., Tian, J., Zekzer, D., Fukuto, J., Ignarro, L. and Kaufman, D. L., 2004. A salen-manganese catalytic free radical scavenger inhibits type 1 diabetes and islet allograft rejection. *Diabetes.* 53, 2574-2580.
- 162.** Osorio, R. A., Christofani, J. S., D'Almeida, V., Russo, A. K. and Picarro, I. C., 2003. Reactive oxygen species in pregnant rats: effects of exercise and thermal stress. *Comp Biochem Physiol C Toxicol Pharmacol.* 135, 89-95.
- 163.** Pandita, T. K., 2005. Role of HSPs and telomerase in radiotherapy. *Int J Hyperthermia.* 21, 689-694.
- 164.** Pandita, T. K., Higashikubo, R. and Hunt, C. R., 2004. HSP70 and genomic stability. *Cell Cycle.* 3, 591-592.
- 165.** Park, H. G., Han, S. I., Oh, S. Y. and Kang, H. S., 2005. Cellular responses to mild heat stress. *Cell Mol Life Sci.* 62, 10-23.
- 166.** Patel, M. N., 2003. Metalloporphyrins improve the survival of Sod2-deficient neurons. *Aging Cell.* 2, 219-222.
- 167.** Pavlik, A., Aneja, I. S., Lexa, J. and Al-Zoabi, B. A., 2003. Identification of cerebral neurons and glial cell types inducing heat shock protein Hsp70 following heat stress in the rat. *Brain Res.* 973, 179-189.

168. Peluffo, H., Acarin, L., Faiz, M., Castellano, B. and Gonzalez, B., 2005. Cu/Zn superoxide dismutase expression in the postnatal rat brain following an excitotoxic injury. *J Neuroinflammation*. 2, 12.
169. Peng, J., Stevenson, F. F., Doctrow, S. R. and Andersen, J. K., 2005. Superoxide dismutase/catalase mimetics are neuroprotective against selective paraquat-mediated dopaminergic neuron death in the substantia nigra: implications for Parkinson disease. *J Biol Chem*. 280, 29194-29198.
170. Perez-Crespo, M., Ramirez, M. A., Fernandez-Gonzalez, R., Rizo, D., Lonergan, P., Pintado, B. and Gutierrez-Adan, A., 2005. Differential sensitivity of male and female mouse embryos to oxidative induced heat-stress is mediated by glucose-6-phosphate dehydrogenase gene expression. *Mol Reprod Dev*. 72, 502-510.
171. Peskin, A. V. and Winterbourn, C. C., 2000. A microtiter plate assay for superoxide dismutase using a water-soluble tetrazolium salt (WST-1). *Clin Chim Acta*. 293, 157-166.
172. Pespeni, M., Hodnett, M. and Pittet, J. F., 2005. In vivo stress preconditioning. *Methods*. 35, 158-164.
173. Peterson, G. L., 1979. Review of the Folin phenol protein quantitation method of Lowry, Rosebrough, Farr and Randall. *Anal Biochem*. 100, 201-220.
174. Petrosillo, G., Di Venosa, N., Pistolese, M., Casanova, G., Tiravanti, E., Colantuono, G., Federici, A., Paradies, G. and Ruggiero, F. M., 2006. Protective effect of melatonin against mitochondrial dysfunction associated with cardiac ischemia-reperfusion: role of cardiolipin. *FASEB J*. 20, 269-276.
175. Petrosillo, G., Ruggiero, F. M. and Paradies, G., 2003a. Role of reactive oxygen species and cardiolipin in the release of cytochrome c from mitochondria. *FASEB J*. 17, 2202-2208.
176. Petrosillo, G., Ruggiero, F. M. and Paradies, G., 2003b. Role of reactive oxygen species and cardiolipin in the release of cytochrome c from mitochondria. *FASEB J*. 17, 2202-2208.
177. Picard, D., 2002. Heat-shock protein 90, a chaperone for folding and regulation. *Cell Mol Life Sci*. 59, 1640-1648.

- 178.** Piccinini, M., Mostert, M., Croce, S., Baldovino, S., Papotti, M. and Rinaudo, M. T., 2003. Interferon-gamma-inducible subunits are incorporated in human brain 20S proteasome. *J Neuroimmunol.* 135, 135-140.
- 179.** Pirkkala, L., Nykanen, P. and Sistonen, L., 2001. Roles of the heat shock transcription factors in regulation of the heat shock response and beyond. *FASEB J.* 15, 1118-1131.
- 180.** Pong, K., Doctrow, S. R., Huffman, K., Adinolfi, C. A. and Baudry, M., 2001. Attenuation of staurosporine-induced apoptosis, oxidative stress, and mitochondrial dysfunction by synthetic superoxide dismutase and catalase mimetics, in cultured cortical neurons. *Exp Neurol.* 171, 84-97.
- 181.** Pospiech, H. and Syvaaja, J. E., 2003. DNA polymerase epsilon - more than a polymerase. *ScientificWorldJournal.* 3, 87-104.
- 182.** Prapurna, D. R. and Rao, K. S., 1997. DNA polymerases delta and epsilon in developing and aging rat brain. *Int J Dev Neurosci.* 15, 67-73.
- 183.** Pritts, T. A., Wang, Q., Sun, X., Moon, M. R., Fischer, D. R., Fischer, J. E., Wong, H. R. and Hasselgren, P. O., 2000. Induction of the stress response in vivo decreases nuclear factor-kappa B activity in jejunal mucosa of endotoxemic mice. *Arch Surg.* 135, 860-866.
- 184.** Qin, N., D'Andrea, M. R., Lubin, M. L., Shafae, N., Codd, E. E. and Correa, A. M., 2003. Molecular cloning and functional expression of the human sodium channel beta1B subunit, a novel splicing variant of the beta1 subunit. *Eur J Biochem.* 270, 4762-4770.
- 185.** Rahman, I. and Kilty, I., 2006. Antioxidant therapeutic targets in COPD. *Curr Drug Targets.* 7, 707-720.
- 186.** Raji, N. S., Krishna, T. H. and Rao, K. S., 2002. DNA-polymerase alpha, beta, delta and epsilon activities in isolated neuronal and astroglial cell fractions from developing and aging rat cerebral cortex. *Int J Dev Neurosci.* 20, 491-496.
- 187.** Rattan, S. I., 2004. Mechanisms of hormesis through mild heat stress on human cells. *Ann N Y Acad Sci.* 1019, 554-558.
- 188.** Rawal, A. K., Muddeshwar, M. G. and Biswas, S. K., 2004. Rubia cordifolia, Fagonia cretica linn and Tinospora cordifolia exert neuroprotection by modulating the antioxidant system in rat hippocampal slices subjected to oxygen glucose deprivation. *BMC Complement Altern Med.* 4, 11.



189. Reynolds, L. P. and Allen, G. V., 2003. A review of heat shock protein induction following cerebellar injury. *Cerebellum*. 2, 171-177.
190. Rojas, A., Figueroa, H., Morales, M. A. and Re, L., 2006a. Facing up the ROS labyrinth--Where to go? *Curr Vasc Pharmacol*. 4, 277-289.
191. Rojas, A., Figueroa, H., Re, L. and Morales, M. A., 2006b. Oxidative stress at the vascular wall. Mechanistic and pharmacological aspects. *Arch Med Res*. 37, 436-448.
192. Rojo, A. I., Salinas, M., Martin, D., Perona, R. and Cuadrado, A., 2004. Regulation of Cu/Zn-superoxide dismutase expression via the phosphatidylinositol 3 kinase/Akt pathway and nuclear factor-kappa B. *J Neurosci*. 24, 7324-7334.
193. Ross, A. D., Sheng, H., Warner, D. S., Piantadosi, C. A., Batinic-Haberle, I., Day, B. J. and Crapo, J. D., 2002. Hemodynamic effects of metalloporphyrin catalytic antioxidants: structure-activity relationships and species specificity. *Free Radic Biol Med*. 33, 1657-1669.
194. Rusyn, I., Asakura, S., Pachkowski, B., Bradford, B. U., Denissenko, M. F., Peters, J. M., Holland, S. M., Reddy, J. K., Cunningham, M. L. and Swenberg, J. A., 2004. Expression of base excision DNA repair genes is a sensitive biomarker for in vivo detection of chemical-induced chronic oxidative stress: identification of the molecular source of radicals responsible for DNA damage by peroxisome proliferators. *Cancer Res*. 64, 1050-1057.
195. Rusyniak, D. E. and Sprague, J. E., 2006. Hyperthermic syndromes induced by toxins. *Clin Lab Med*. 26, 165-184.
196. Sakuraba, H., Mizukami, H., Yagihashi, N., Wada, R., Hanyu, C. and Yagihashi, S., 2002. Reduced beta-cell mass and expression of oxidative stress-related DNA damage in the islet of Japanese Type II diabetic patients. *Diabetologia*. 45, 85-96.
197. Salvemini, D., Mazzon, E., Dugo, L., Riley, D. P., Serraino, I., Caputi, A. P. and Cuzzocrea, S., 2001. Pharmacological manipulation of the inflammatory cascade by the superoxide dismutase mimetic, M40403. *Br J Pharmacol*. 132, 815-827.
198. Sanchez-Carbente, M. R., Castro-Obregon, S., Covarrubias, L. and Narvaez, V., 2005. Motoneuronal death during spinal cord development is mediated by oxidative stress. *Cell Death Differ*. 12, 279-291.

- 199.** Santoro, M. G., 2000. Heat shock factors and the control of the stress response. *Biochem Pharmacol.* 59, 55-63.
- 200.** Satoh, T., Ishige, K. and Sagara, Y., 2004. Protective effects on neuronal cells of mouse afforded by ebselen against oxidative stress at multiple steps. *Neurosci Lett.* 371, 1-5.
- 201.** Scandalios, J. G., 2005. Oxidative stress: molecular perception and transduction of signals triggering antioxidant gene defenses. *Braz J Med Biol Res.* 38, 995-1014.
- 202.** Scheibel, T. and Buchner, J., 2006. Protein aggregation as a cause for disease. *Handb Exp Pharmacol.* 199-219.
- 203.** Schwartz, P. J., Reaume, A., Scott, R. and Coyle, J. T., 1998. Effects of over- and under-expression of Cu, Zn-superoxide dismutase on the toxicity of glutamate analogs in transgenic mouse striatum. *Brain Res.* 789, 32-39.
- 204.** Segui, J., Gironella, M., Sans, M., Granell, S., Gil, F., Gimeno, M., Coronel, P., Pique, J. M. and Panes, J., 2004. Superoxide dismutase ameliorates TNBS-induced colitis by reducing oxidative stress, adhesion molecule expression, and leukocyte recruitment into the inflamed intestine. *J Leukoc Biol.* 76, 537-544.
- 205.** Seto, C. K., Way, D. and O'Connor, N., 2005. Environmental illness in athletes. *Clin Sports Med.* 24, 695-718.
- 206.** Shamovsky, I. and Gershon, D., 2004. Novel regulatory factors of HSF-1 activation: facts and perspectives regarding their involvement in the age-associated attenuation of the heat shock response. *Mech Ageing Dev.* 125, 767-775.
- 207.** Shanley, T. P., Ryan, M. A., Eaves-Pyles, T. and Wong, H. R., 2000. Heat shock inhibits phosphorylation of I-kappaBalpha. *Shock.* 14, 447-450.
- 208.** Sharma, H. S., 2006 a. Hyperthermia influences excitatory and inhibitory amino acid neurotransmitters in the central nervous system. An experimental study in the rat using behavioural, biochemical, pharmacological, and morphological approaches. *J Neural Transm.* 113, 497-519.
- 209.** Sharma, H. S., 2006 b. Hyperthermia induced brain oedema: current status and future perspectives. *Indian J Med Res.* 123, 629-652.

- 210.** Sharma, H. S., Drieu, K., Alm, P. and Westman, J., 2000. Role of nitric oxide in blood-brain barrier permeability, brain edema and cell damage following hyperthermic brain injury. An experimental study using EGB-761 and Gingkolide B pretreatment in the rat. *Acta Neurochir Suppl.* 76, 81-86.
- 211.** Sharma, H. S. and Hoopes, P. J., 2003. Hyperthermia induced pathophysiology of the central nervous system. *Int J Hyperthermia.* 19, 325-354.
- 212.** Sharpe, M. A., Ollosson, R., Stewart, V. C. and Clark, J. B., 2002. Oxidation of nitric oxide by oxomanganese-salen complexes: a new mechanism for cellular protection by superoxide dismutase/catalase mimetics. *Biochem J.* 366, 97-107.
- 213.** Sherman, M. Y. and Goldberg, A. L., 2001. Cellular defenses against unfolded proteins: a cell biologist thinks about neurodegenerative diseases. *Neuron.* 29, 15-32.
- 214.** Shin, H. K., Lee, J. H., Kim, C. D., Kim, Y. K., Hong, J. Y. and Hong, K. W., 2003. Prevention of impairment of cerebral blood flow autoregulation during acute stage of subarachnoid hemorrhage by gene transfer of Cu/Zn SOD-1 to cerebral vessels. *J Cereb Blood Flow Metab.* 23, 111-120.
- 215.** Sikora, E., Grassilli, E., Radziszewska, E., Bellesia, E., Barbieri, D. and Franceschi, C., 1993. Transcription factors DNA-binding activity in rat thymocytes undergoing apoptosis after heat-shock or dexamethasone treatment. *Biochem Biophys Res Commun.* 197, 709-715.
- 216.** Simon, H. B., 1993. Hyperthermia. *N Engl J Med.* 329, 483-487.
- 217.** Sonna, L. A., Fujita, J., Gaffin, S. L. and Lilly, C. M., 2002. Invited review: Effects of heat and cold stress on mammalian gene expression. *J Appl Physiol.* 92, 1725-1742.
- 218.** Sorensen, J. G., Nielsen, M. M., Kruhoffer, M., Justesen, J. and Loeschcke, V., 2005. Full genome gene expression analysis of the heat stress response in *Drosophila melanogaster*. *Cell Stress Chaperones.* 10, 312-328.
- 219.** Sreedhar, A. S., Pardhasaradhi, B. V., Khar, A. and Srinivas, U. K., 2002. A cross talk between cellular signalling and cellular redox state during heat-induced apoptosis in a rat histiocytoma. *Free Radic Biol Med.* 32, 221-227.
- 220.** Stein, U., Jurchott, K., Walther, W., Bergmann, S., Schlag, P. M. and Royer, H. D., 2001. Hyperthermia-induced nuclear translocation of transcription factor YB-1 leads to enhanced expression of multidrug resistance-related ABC transporters. *J Biol Chem.* 276, 28562-28569.

- 221.** Steinau, M., Unger, E. R., Vernon, S. D., Jones, J. F. and Rajeevan, M. S., 2004. Differential-display PCR of peripheral blood for biomarker discovery in chronic fatigue syndrome. *J Mol Med.* 82, 750-755.
- 222.** Stofan, J. R., Zachwieja, J. J., Horswill, C. A., Murray, R., Anderson, S. A. and Eichner, E. R., 2005. Sweat and sodium losses in NCAA football players: a precursor to heat cramps? *Int J Sport Nutr Exerc Metab.* 15, 641-652.
- 223.** Sucholeiki, R., 2005. Heatstroke. *Semin Neurol.* 25, 307-314.
- 224.** Sun, Y. and Leaman, D. W., 2005. Involvement of Noxa in cellular apoptotic responses to interferon, double-stranded RNA, and virus infection. *J Biol Chem.* 280, 15561-15568.
- 225.** Suntres, Z. E. and Lui, E. M., 2006a. Prooxidative effect of copper--metallothionein in the acute cytotoxicity of hydrogen peroxide in Ehrlich ascites tumour cells. *Toxicology.* 217, 155-168.
- 226.** Suntres, Z. E. and Lui, E. M., 2006b. Antioxidant effect of zinc and zinc-metallothionein in the acute cytotoxicity of hydrogen peroxide in Ehrlich ascites tumour cells. *Chem Biol Interact.* 162, 11-23.
- 227.** Szabo, C., Day, B. J. and Salzman, A. L., 1996. Evaluation of the relative contribution of nitric oxide and peroxynitrite to the suppression of mitochondrial respiration in immunostimulated macrophages using a manganese mesoporphyrin superoxide dismutase mimetic and peroxynitrite scavenger. *FEBS Lett.* 381, 82-86.
- 228.** Tabakman, R., Jiang, H., Levine, R. A., Kohen, R. and Lazarovici, P., 2004. Apoptotic characteristics of cell death and the neuroprotective effect of homocarnosine on pheochromocytoma PC12 cells exposed to ischemia. *J Neurosci Res.* 75, 499-507.
- 229.** Takahashi, H., Hashimoto, Y., Aoki, N., Kinouchi, M., Ishida-Yamamoto, A. and Iizuka, H., 2000. Copper, zinc-superoxide dismutase protects from ultraviolet B-induced apoptosis of SV40-transformed human keratinocytes: the protection is associated with the increased levels of antioxidant enzymes. *J Dermatol Sci.* 23, 12-21.
- 230.** Takahashi, N., Kikuchi, S., Dai, Y., Kobayashi, K., Fukuoka, T. and Noguchi, K., 2003. Expression of auxiliary beta subunits of sodium channels in primary afferent neurons and the effect of nerve injury. *Neuroscience.* 121, 441-450.

- 231.** Takahashi, T., Min, Z., Uchida, I., Arita, M., Watanabe, Y., Koi, M. and Hemmi, H., 2005. Hypersensitivity in DNA mismatch repair-deficient colon carcinoma cells to DNA polymerase reaction inhibitors. *Cancer Lett.* 220, 85-93.
- 232.** Tanabe, M., Sasai, N., Nagata, K., Liu, X. D., Liu, P. C., Thiele, D. J. and Nakai, A., 1999. The mammalian HSF4 gene generates both an activator and a repressor of heat shock genes by alternative splicing. *J Biol Chem.* 274, 27845-27856.
- 233.** Terasawa, K., Minami, M. and Minami, Y., 2005. Constantly updated knowledge of Hsp90. *J Biochem (Tokyo).* 137, 443-447.
- 234.** Thannickal, V. J. and Fanburg, B. L., 2000. Reactive oxygen species in cell signaling. *Am J Physiol Lung Cell Mol Physiol.* 279, L1005-1028.
- 235.** Tonkiss, J. and Calderwood, S. K., 2005. Regulation of heat shock gene transcription in neuronal cells. *Int J Hyperthermia.* 21, 433-444.
- 236.** Trinklein, N. D., Chen, W. C., Kingston, R. E. and Myers, R. M., 2004b. Transcriptional regulation and binding of heat shock factor 1 and heat shock factor 2 to 32 human heat shock genes during thermal stress and differentiation. *Cell Stress Chaperones.* 9, 21-28.
- 237.** Trinklein, N. D., Murray, J. I., Hartman, S. J., Botstein, D. and Myers, R. M., 2004a. The role of heat shock transcription factor 1 in the genome-wide regulation of the mammalian heat shock response. *Mol Biol Cell.* 15, 1254-1261.
- 238.** Troy, C. M. and Shelanski, M. L., 1994. Down-regulation of copper/zinc superoxide dismutase causes apoptotic death in PC12 neuronal cells. *Proc Natl Acad Sci U S A.* 91, 6384-6387.
- 239.** Tsong, T. Y. and Su, Z. D., 1999. Biological effects of electric shock and heat denaturation and oxidation of molecules, membranes, and cellular functions. *Ann N Y Acad Sci.* 888, 211-232.
- 240.** Vandesompele, J., De Preter, K., Pattyn, F., Poppe, B., Van Roy, N., De Paepe, A. and Speleman, F., 2002. Accurate normalization of real-time quantitative RT-PCR data by geometric averaging of multiple internal control genes. *Genome Biol.* 3 (7), Research 0034.1-0034.11.
- 241.** Venturini, G., Colasanti, M., Fioravanti, E., Bianchini, A. and Ascenzi, P., 1999. Direct effect of temperature on the catalytic activity of nitric oxide synthases types I, II, and III. *Nitric Oxide.* 3, 375-382.

242. Verbeke, P., Fonager, J., Clark, B. F. and Rattan, S. I., 2001. Heat shock response and ageing: mechanisms and applications. *Cell Biol Int.* 25, 845-857.
243. Vogel, P., Dux, E. and Wiessner, C., 1997. Effect of heat shock on neuronal cultures: importance of protein synthesis and HSP72 induction for induced tolerance and survival. *Metab Brain Dis.* 12, 203-217.
244. Vujanac, M., Fenaroli, A. and Zimarino, V., 2005. Constitutive nuclear import and stress-regulated nucleocytoplasmic shuttling of mammalian heat-shock factor 1. *Traffic.* 6, 214-229.
245. Wang, C., Wang, M. W., Tashiro, S., Onodera, S. and Ikejima, T., 2005. IL-1 beta acts in synergy with endogenous IL-1 beta in A375-S2 human melanoma cell apoptosis through mitochondrial pathway. *J Korean Med Sci.* 20, 555-561.
246. Wegele, H., Muller, L. and Buchner, J., 2004. Hsp70 and Hsp90--a relay team for protein folding. *Rev Physiol Biochem Pharmacol.* 151, 1-44.
247. Wen, L., 2000. Effect of Primer Purity on the Banding Patterns of Differential Display Polymerase Chain Reaction. *Journal of Biomolecular Techniques.* 11, 87-91.
248. Wennborg, A., Classon, M., Klein, G. and von Gabain, A., 1995. Downregulation of c-myc expression after heat shock in human B-cell lines is independent of 5' mRNA sequences. *Biol Chem Hoppe Seyler.* 376, 671-680.
249. Wexler, R. K., 2002. Evaluation and treatment of heat-related illnesses. *Am Fam Physician.* 65, 2307-2314.
250. White, M. G., Emery, M., Nonner, D. and Barrett, J. N., 2003. Caspase activation contributes to delayed death of heat-stressed striatal neurons. *J Neurochem.* 87, 958-968.
251. Willcox, J. K., Ash, S. L. and Catignani, G. L., 2004. Antioxidants and prevention of chronic disease. *Crit Rev Food Sci Nutr.* 44, 275-295.
252. Xiao, N., Callaway, C. W., Lipinski, C. A., Hicks, S. D. and DeFranco, D. B., 1999. Geldanamycin provides posttreatment protection against glutamate-induced oxidative toxicity in a mouse hippocampal cell line. *J Neurochem.* 72, 95-101.

253. Xiong, Y., Shie, F. S., Zhang, J., Lee, C. P. and Ho, Y. S., 2005. Prevention of mitochondrial dysfunction in post-traumatic mouse brain by superoxide dismutase. *J Neurochem.* 95, 732-744.
254. Yan, Y. E., Zhao, Y. Q., Wang, H. and Fan, M., 2006. Pathophysiological factors underlying heatstroke. *Med Hypotheses.* 67, 609-617.
255. Yang, C. Y. and Lin, M. T., 2002. Oxidative stress in rats with heat stroke-induced cerebral ischemia. *Stroke.* 33, 790-794.
256. Yang, H., Li, Y., Guan, G. H. and Li, X. Y., 2004. [Transcriptional differences between a heterokaryon and its segregants of *Fusarium oxysporum* f. sp. *vasinfectum*]. *Yi Chuan Xue Bao.* 31, 166-170.
257. Yang, P. M., Chiu, S. J. and Lin, L. Y., 2005. Differential effects of salen and manganese-salen complex (EUK-8) on the regulation of cellular cadmium uptake and toxicity. *Toxicol Sci.* 85, 551-559.
258. Yeo, T. P., 2004. Heat stroke: a comprehensive review. *AACN Clin Issues.* 15, 280-293.
259. Yoo, C. G., Lee, S., Lee, C. T., Kim, Y. W., Han, S. K. and Shim, Y. S., 2000. Anti-inflammatory effect of heat shock protein induction is related to stabilization of I kappa B alpha through preventing I kappa B kinase activation in respiratory epithelial cells. *J Immunol.* 164, 5416-5423.
260. Yoo, H. Y., Chang, M. S. and Rho, H. M., 1999. The activation of the rat copper/zinc superoxide dismutase gene by hydrogen peroxide through the hydrogen peroxide-responsive element and by paraquat and heat shock through the same heat shock element. *J Biol Chem.* 274, 23887-23892.
261. Zelko, I. N., Mariani, T. J. and Folz, R. J., 2002. Superoxide dismutase multigene family: a comparison of the CuZn-SOD (SOD1), Mn-SOD (SOD2), and EC-SOD (SOD3) gene structures, evolution, and expression. *Free Radic Biol Med.* 33, 337-349.
262. Zhang, H. J., Doctrow, S. R., Oberley, L. W. and Kregel, K. C., 2006a. Chronic antioxidant enzyme mimetic treatment differentially modulates hyperthermia-induced liver HSP70 expression with aging. *J Appl Physiol.* 100, 1385-1391.
263. Zhang, H. J., Doctrow, S. R., Xu, L., Oberley, L. W., Beecher, B., Morrison, J., Oberley, T. D. and Kregel, K. C., 2004. Redox modulation of the liver with chronic antioxidant enzyme mimetic treatment prevents age-related oxidative damage associated with environmental stress. *FASEB J.* 18, 1547-1549.

- 264.** Zhang, H. J., Drake, V. J., Morrison, J. P., Oberley, L. W. and Kregel, K. C., 2002. Selected contribution: Differential expression of stress-related genes with aging and hyperthermia. *J Appl Physiol.* 92, 1762-1769.
- 265.** Zhang, H. J., Xu, L., Drake, V. J., Xie, L., Oberley, L. W. and Kregel, K. C., 2003. Heat-induced liver injury in old rats is associated with exaggerated oxidative stress and altered transcription factor activation. *FASEB J.* 17, 2293-2295.
- 266.** Zhang, Y., Qu, D., Morris, E. J., O'Hare, M. J., Callaghan, S. M., Slack, R. S., Geller, H. M. and Park, D. S., 2006b. The Chk1/Cdc25A pathway as activators of the cell cycle in neuronal death induced by camptothecin. *J Neurosci.* 26, 8819-8828.
- 267.** Zhao, Q. L., Fujiwara, Y. and Kondo, T., 2006. Mechanism of cell death induction by nitroxide and hyperthermia. *Free Radic Biol Med.* 40, 1131-1143.
- 268.** Zuker, M., 2003. Mfold web server for nucleic acid folding and hybridization prediction. *Nucleic Acids Res.* 31, 3406-3415.
- 269.** Zuo, L., Christofi, F. L., Wright, V. P., Liu, C. Y., Merola, A. J., Berliner, L. J. and Clanton, T. L., 2000. Intra- and extracellular measurement of reactive oxygen species produced during heat stress in diaphragm muscle. *Am J Physiol Cell Physiol.* 279, C1058-1066.